

Fluorescent 7-Azaindole *N*-linked 1,2,3-triazole: Synthesis and Study of Antimicrobial, Molecular Docking, ADME and DFT Properties

Kanika Sharma,^a Ram Kumar Tittal,^{a,*} Kashmiri Lal,^b Ramling S. Mathpati,^a Ghule Vikas D.^a

^aDepartment of Chemistry, National Institute of Technology, Kurukshetra, Haryana 136119, India.

E-mail: rkittaliitd@mail.nitkr.ac.in

^bDepartment of Chemistry, GJUS&T, Hisar, Haryana 125001, India.

Table of Content:

S. No.	Contents	Page No.
1	Table of Contents	S-1
2	X-Ray Crystallography Experimental Section	S-2
3	Table SI-1. Crystal data and structure refinement parameters for 4f .	S-2
4	Figure SI-1. Unit cell showing two molecular units in the asymmetric unit of compound 4f .	S-3
5	Figure SI-2. Absorbance spectrum of 7-AI (1), 7-AI-linked alkyne (2), and 1,2,3-triazoles (4a-i)	S-3
6	Table SI-2. Docking results of 1,2,3- triazole hybrids 4a-q , docked in the active sites of DNA 14 α -demethylase lanosterol enzyme (PDB ID 1EA1).	S-4
7	Figure SI-3. 2D and 3D interacting mode of 4a-4q docked in the active site of lanosterol 14- α -demethylase.	S-5 to S-10
8	Table SI-3. Physicochemical data for Drug Likeness based on the Lipinski rule (SAR)	S-11
9	Table SI-4 Bioactivity score by Molinspiration Cheminformatics software	S-11
10	Computational study (general)	S-12
11	Table SI-5. Calculated FMOs, energy gap, chemical potential, chemical hardness, and electrophilicity index (eV), B3LYP/6-311G(d,p).	S-12
12	Figure SI-4. Highest occupied and lowest unoccupied molecular orbitals (HOMO and LUMO) distribution at the ground state of molecules 2 , and 4a-4q .	S-13 to S-17
13	General procedure for the synthesis of 7-azaindole <i>N</i> -linked alkyne (2)	S-17
14	General procedure for the synthesis of 7-azaindole <i>N</i> -linked aryl 1,2,3-triazoles (4a-4q).	S-18
15	Spectroscopic data of compound (2)	S-18
16	Spectroscopic data of compound (4a-4q)	S-18 to S-24
17	References	S-24
18	Physical spectra of compounds 2 and 4a-4q (¹ H-NMR, ¹³ C-NMR and HRMS)	S-25 to S-59

X-Ray Crystallography Experimental Section:

A block-shaped clear whiteish yellow color single crystals were carefully picked under a polarizing microscope and pasted to a very fine glass fiber with the help of cyanoacrylate (superglue) adhesive. The single-crystal X-ray diffraction data were collected with Bruker APEX-II CCD diffractometer with monochromatic Mo $K\alpha$ radiation ($\lambda = 0.71073 \text{ \AA}$) at 296 (2) K by using ω and ϕ scan. The X-ray generator was operated at 50 kV and 20 mA. The data were reduced by using APEX3, the SAINTPLUS⁵ program was used for diffraction profiles integration, and absorption correction (multiscan) was done by the SADABS program.¹ The structure was solved and refined by the full-matrix least square method on F^2 using the SHELXL 2018/3 program,² present in the WinGx package of programs (version 1.63.04a).³ All the hydrogen positions were initially located in the different Fourier maps, and for the final refinement, the hydrogen atoms were placed in geometrically ideal positions and refined in the riding mode. The final refinement comprised the atomic positions of all the atoms, isotropic thermal parameters for all the hydrogen atoms, and anisotropic thermal parameters for all the non-hydrogen atoms. Please refer following **Table SI-1** for a detailed explanation of the crystal

Table SI-1. Crystal data and structure refinement parameters for **4f**.

Compound	4f
Empirical formula	C ₁₇ H ₁₄ N ₅ Br ₁
Formula weight	368.240
Crystal system	Triclinic
Space group	<i>P</i> -1 (2)
<i>a</i> (Å)	5.5829 (2)
<i>b</i> (Å)	8.3646 (4)
<i>c</i> (Å)	16.4765 (8)
α (°)	80.4360 (10)
β (°)	87.5270 (10)
γ (°)	85.7270 (10)
<i>V</i> (Å ³)	756.26 (6)
<i>Z</i>	2
<i>D</i> (calc/gcm ⁻³)	1.617
μ (mm ⁻¹)	2.725
λ (Mo $K\alpha$ /Å)	0.71073
<i>F</i> ₀₀₀	372.00
θ_{\min} and θ_{\max}	2.585° and 28.317°
Measured reflections	12363
Independent reflections	3740
Reflections with $I > 2\sigma(I)$	3469
R _{int}	0.0343
R[F ² > 2σ(F ²)]	0.0263
wR(F ²)	0.0655

$$R_1 = \frac{\sum ||F_0| - |F_c||}{\sum |F_0|}; wR2 = \left\{ \frac{\sum [w(F_0^2 - F_c^2)^2]}{\sum [w(F_0^2)^2]} \right\}^{1/2}.$$

$$w = 1/[\sigma^2(F_0^2) + (aP)^2 + bP], P = [\max.(F_0^2, 0) + 2(F_c^2)]/3.$$

structure solution and final refinements for the structures. The crystallographic data for compound **4f** can be found in CCDC No: **2192737** free of charge from The Cambridge Crystallographic Data Centre (CCDC) via www.ccdc.cam.ac.uk/data_request/cif.

The X-ray single-crystal structure investigation revealed that compound **4f** was shaped in a triclinic crystal system. Compound **4f** crystallizes in triclinic cells with space group *P-1*. The resultant structure of compound **4f** contains two molecular units in the asymmetric unit and is represented in **Figure SI-1**. In the crystal structure, one can find two molecular structures anti-parallel to each other similar to the mirror image with respect to the 1,2,3-triazole unit in the middle. No hydrogen bonding interactions were found in the present compound.

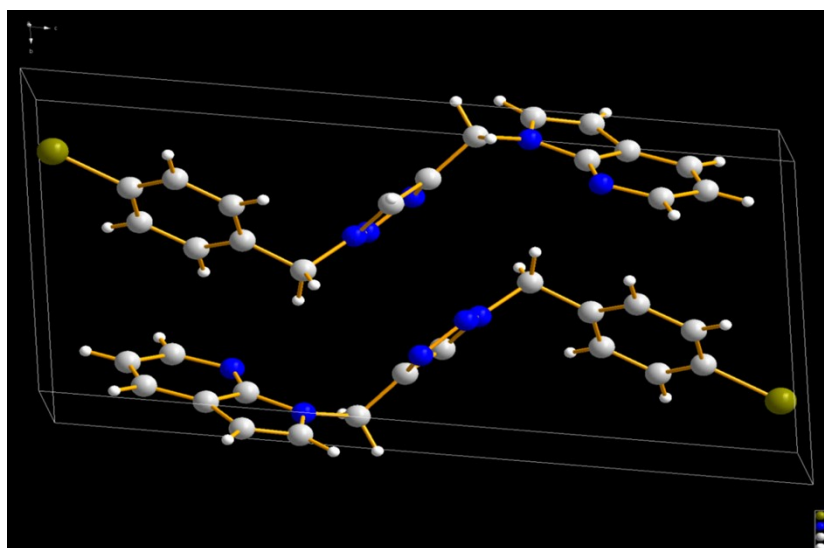


Figure SI-1. Unit cell showing two molecular units in the asymmetric unit of compound **4f**.

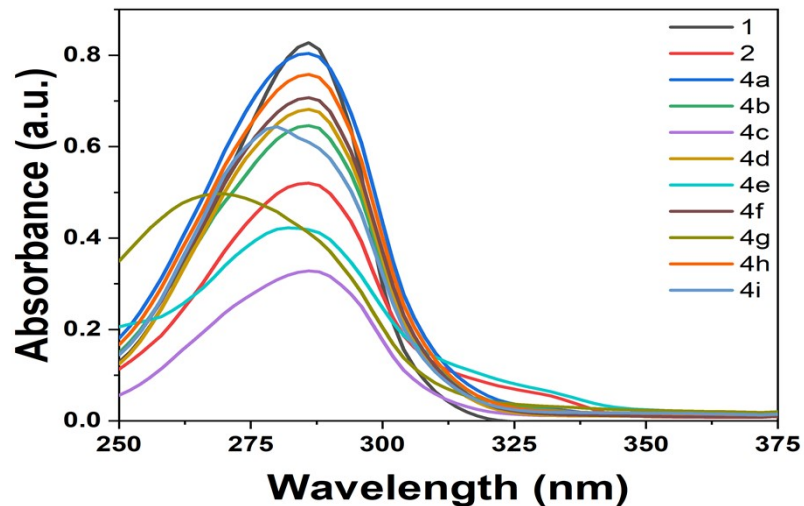
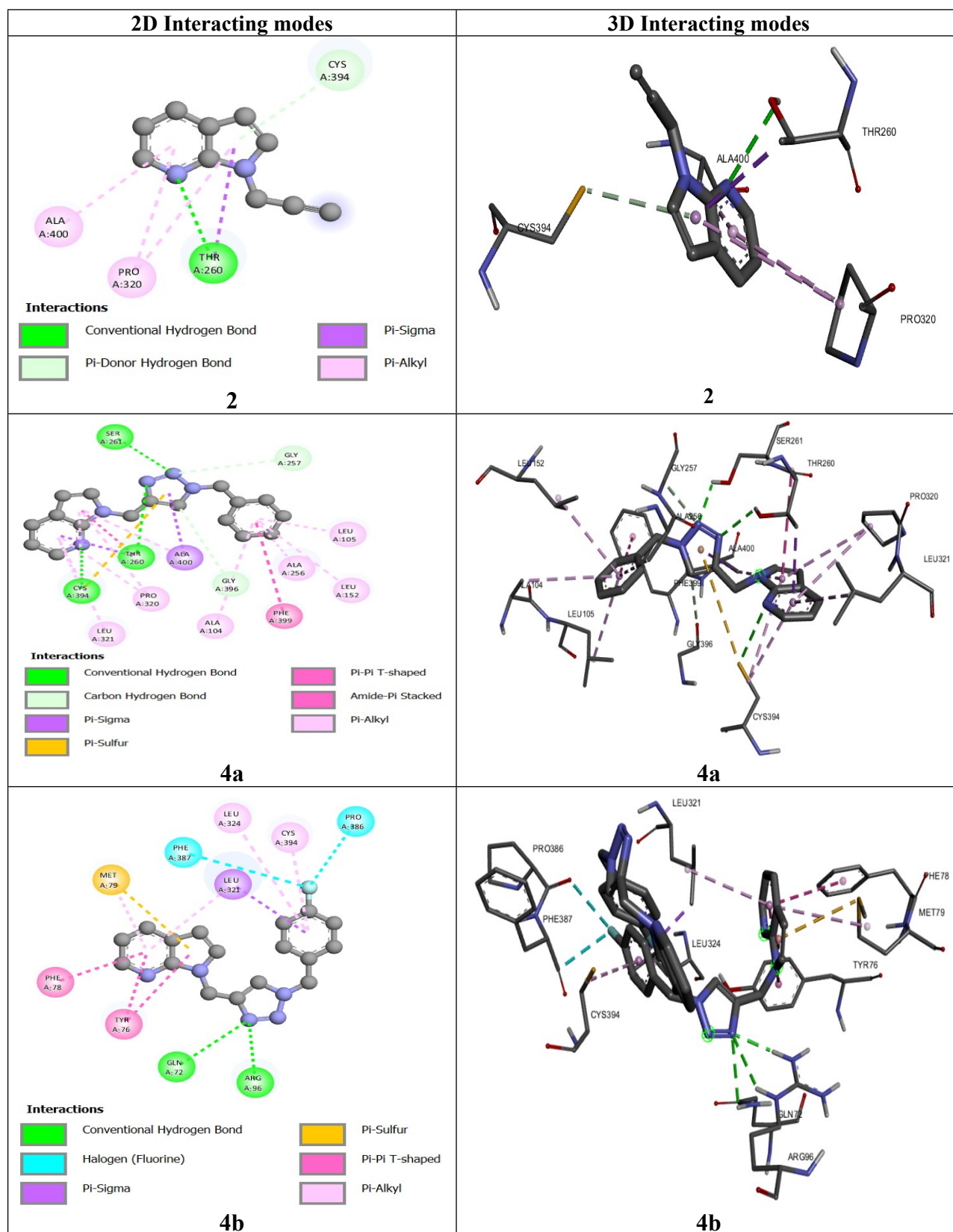
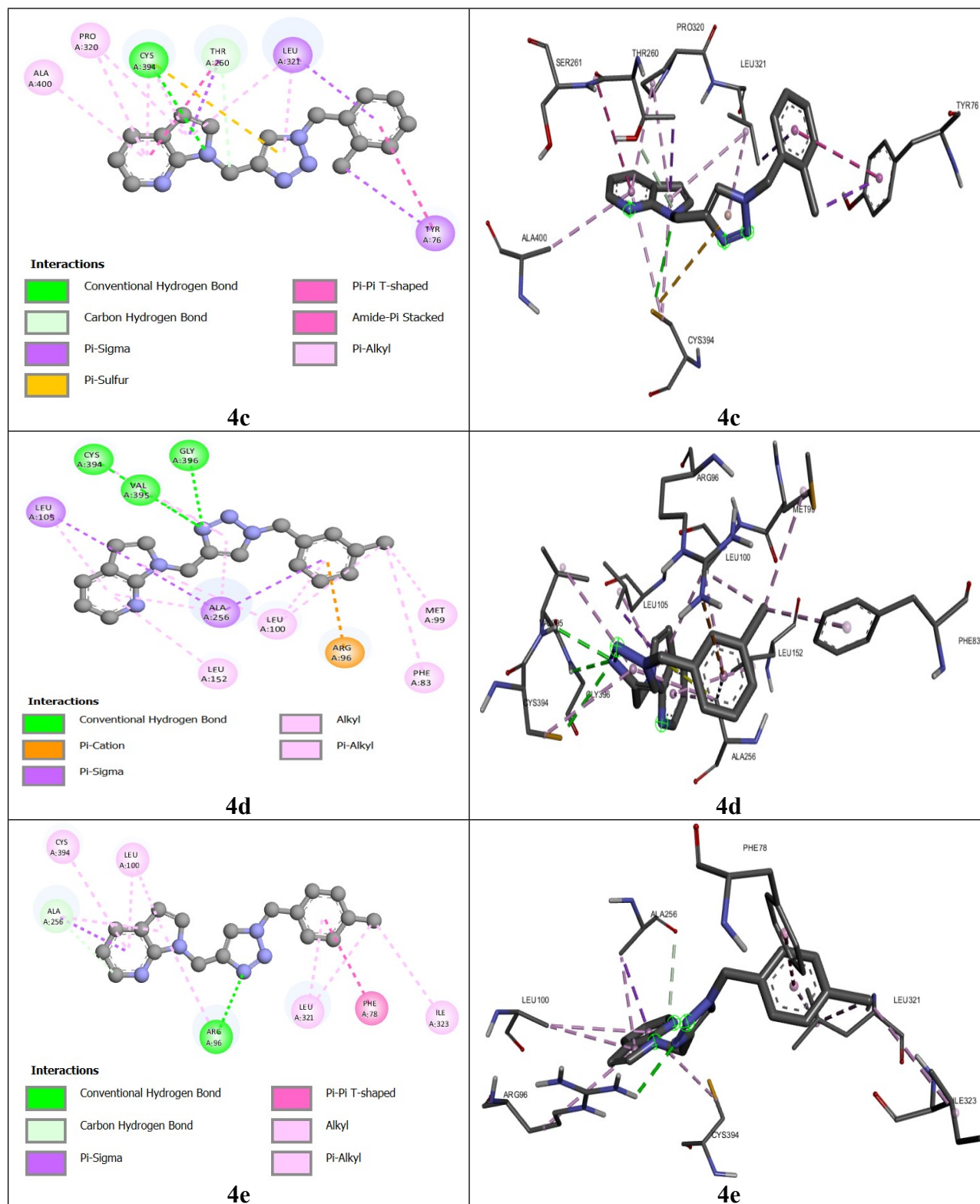


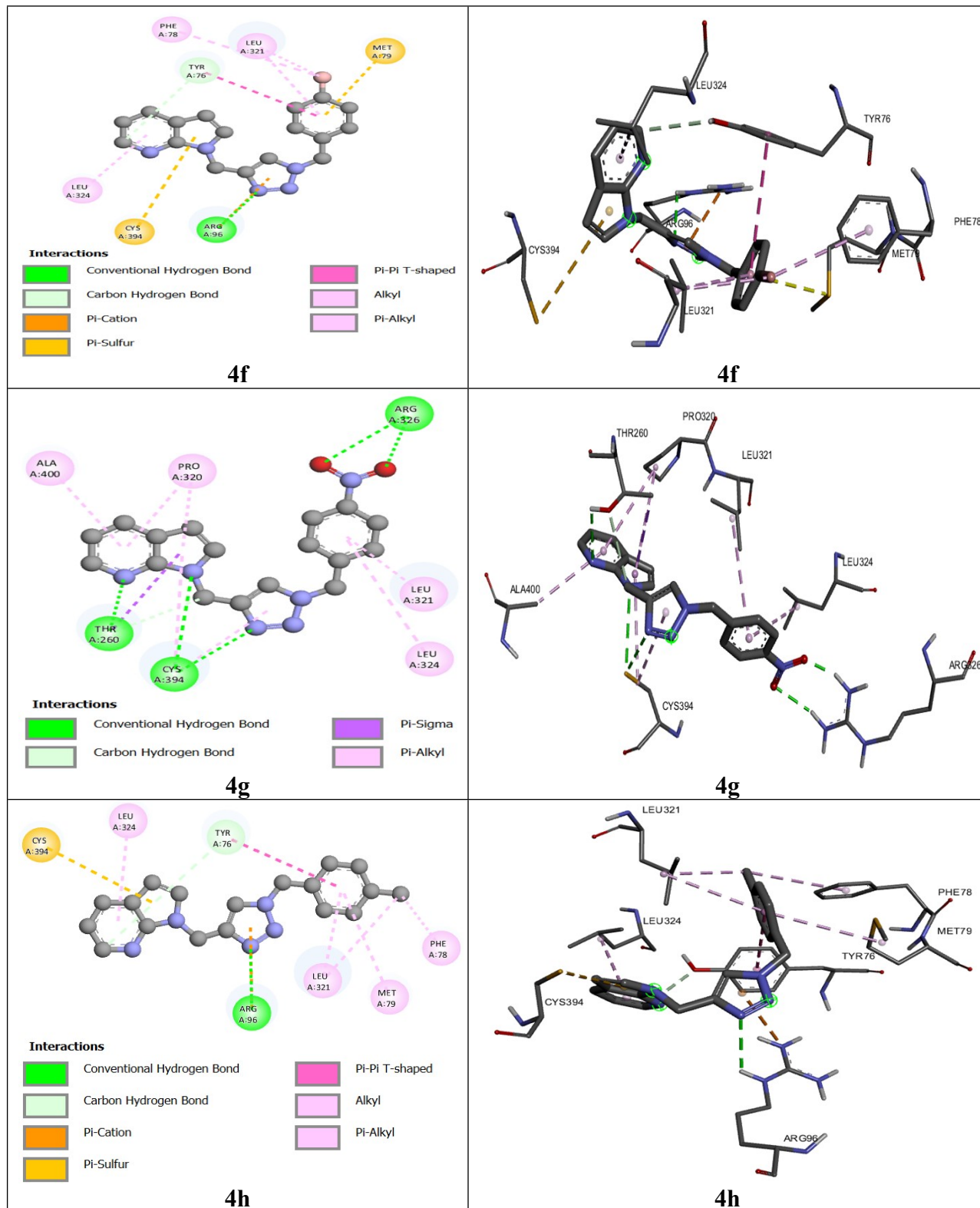
Figure SI-2. Absorbance spectrum of 7-AI (**1**), 7-AI-linked alkyne (**2**), and 1,2,3-triazoles (**4a-i**)

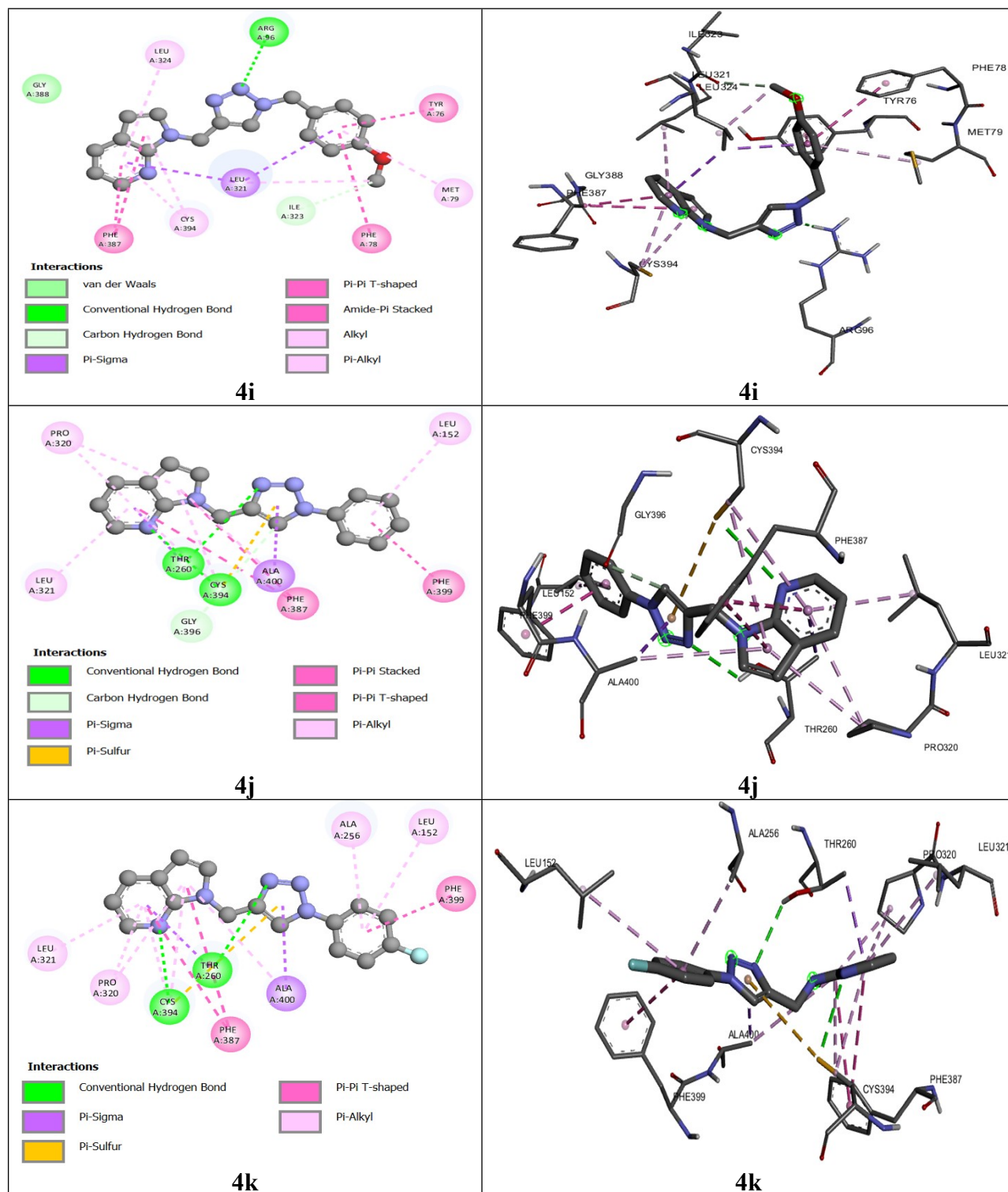
Table SI-2. Docking results of synthesized 1,2,3- triazole hybrids **4a-q**, docked in the active sites of DNA 14 α -demethylase lanosterol enzyme (PDB ID 1EA1).

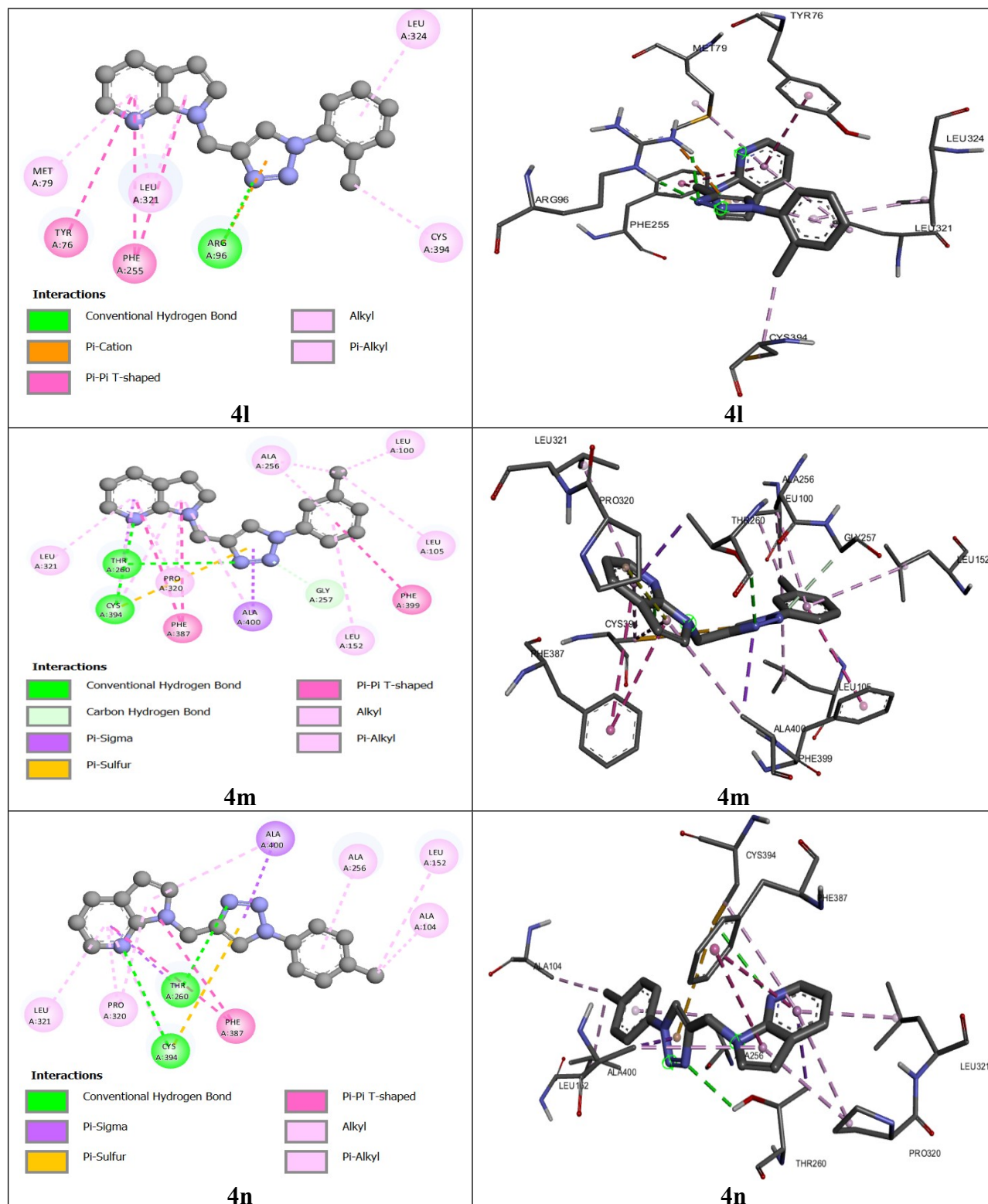
S. No.	Comp.	n, R	H-bond interactions with bond length	Other Interactions	B.E. (kcal mol ⁻¹)
1	2	-	THR260(2.93)	CYS394, PRO320, ALA400	-6.11
2	4a	1, H	THR260(2.74), SER261(2.48), CYS394(3.57)	GLY257 GLY396, ALA400, PHE399, PRO320, ALA104, LEU105, LEU152, ALA256, LEU321	-8.75
3	4b	1, 4-F	GLN72(3.09), ARG96(2.84), ARG96(2.23)	PRO386, PHE387, LEU321, MET79, TYR76, PHE78, LEU324, CYS394	-9.02
4	4c	1, 2-Cl	CYS394(3.72)	THR260, LEU321, TYR76, SER261, PRO320, LEU321	-8.65
5	4d	1, 3-Cl	CYS394(3.78), VAL395(2.948), GLY396(2.945)	ARG96, LEU105, ALA256, ALA256, LEU100, MET99, PHE83	-8.81
6	4e	1,4-Cl	ARG96(2.69)	ALA256, ALA256, PHE78, LEU321, ILE323, LEU100	-9.05
7	4f	1, 4-Br	ARG96(2.46)	TYR76, MET79, CYS394, TYR76, LEU321, PHE78	-8.76
8	4g	1, 4-NO ₂	THR260(2.87), ARG326(1.85), ARG326 (2.43), CYS394(3.48), CYS394(3.63)	PRO320, ALA400, LEU321, LEU32	-8.74
9	4h	1, 4-Me	ARG96(2.77)	TYR76, CYS394, LEU321, PHE78, MET79, LEU324	-9.28
10	4i	1,4-OMe	ARG96(2.25)	ILE323, LEU321, TYR76, PHE78, PHE387, GLY388, CYS394, MET79, LEU324	-8.38
11	4j	0, H	THR260(2.72), CYS394(3.76)	GLY396, ALA400,PHE399, PHE387, PRO320,LEU152, LEU321	-9.09
12	4k	0, 4-F	THR260(2.96), CYS394(3.60)	ALA400, PHE387, PHE399, PRO320, LEU152, ALA256, LEU321	-9.21
13	4l	0, 2-Cl	ARG96(2.55), ARG96(2.39)	TYR76, PHE255, CYS394, LEU321, MET79, LEU324	-8.55
14	4m	0, 3-Cl	THR260(2.84), CYS394(3.65)	GLY257, ALA400, PHE387, PHE399,LEU100, ALA256, LEU105,PRO320, LEU152, LEU321	-9.17
15	4n	0, 4-Cl	THR260(2.77), CYS394(3.66)	ALA400, PHE387, ALA104, LEU152, PRO320, ALA256, LEU321	-8.79
16	4o	0, 4-Br	ARG96(2.36), ARG96(1.91)	LEU321, CYS394, TYR76, VAL434, PHE78, HIS259, LEU100, ALA256	-8.74
17	4p	0, 4-NO ₂	ARG96 (1.92), HIS259 (2.79)	VAL434, GLN72, LEU321, TYR76, PHE387, GLY388, LEU324, CYS394	-8.51
18	4q	0,4-OMe	ARG95(2.85), HIS392(2.27), CYS3949(3.69)	ARG391, THR260, PHE387, VAL395, PRO320, LEU321, ALA400, ARG96	-8.44











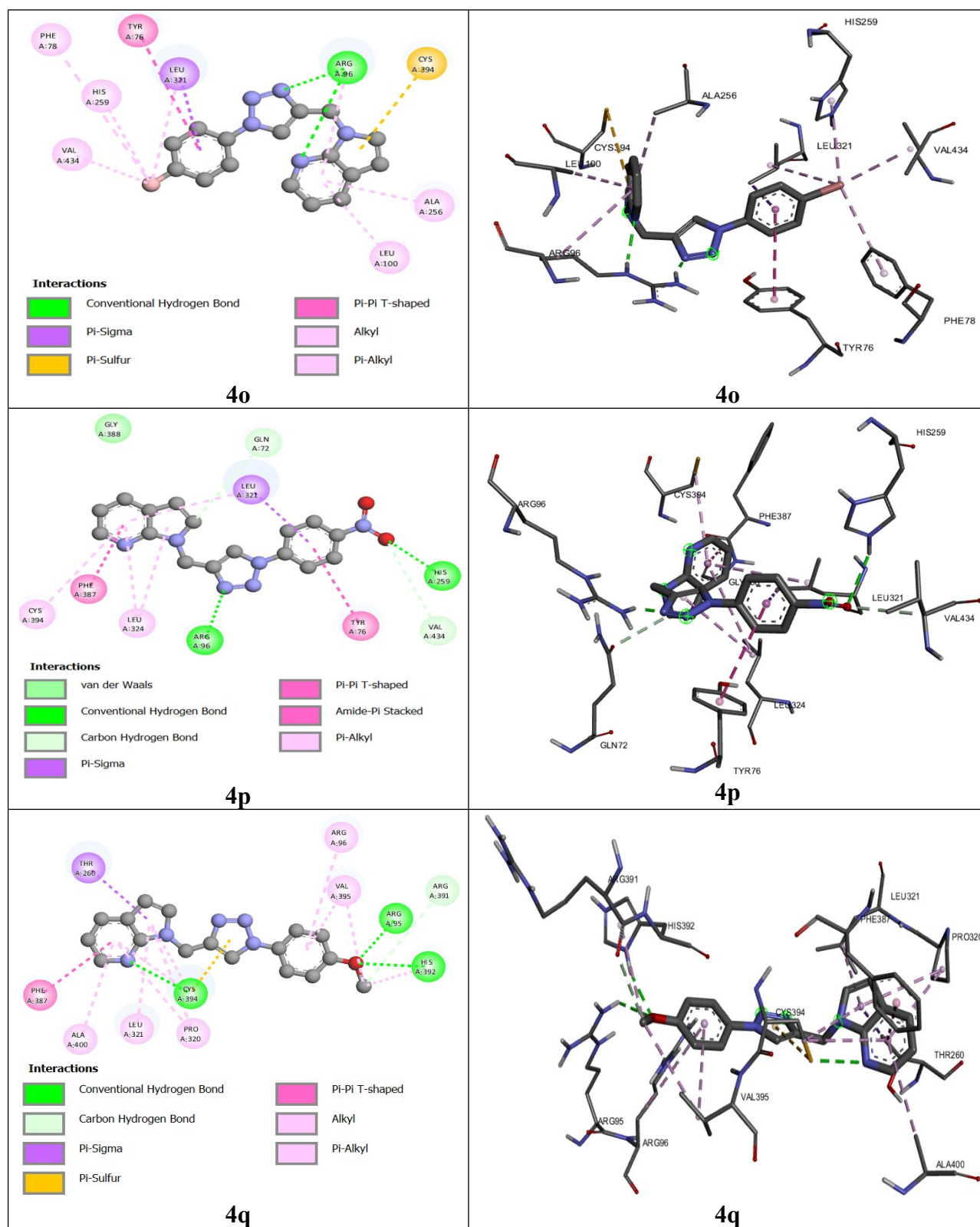


Figure SI-3. 2D and 3D interacting mode of **4a-4q** docked in the active site of lanosterol 14- α -demethylase.

Table SI-3. Physicochemical data for Drug Likeness based on the Lipinski rule (SAR)

Comp. Rule	%Abs ^a	miLogP ^b <5	TPSA ^c	N _{atoms} ^d	MW ^e <500	N _{ON} ^f <10	N _{OHNH} ^g <5	N _{viol} ^h	N _{rotb} ⁱ <10	Vol ^j
2	102.84	1.49	17.83	12	156.19	2	0	0	1	148.31
4a	92.25	2.67	48.54	22	289.34	5	0	0	4	262.72
4b	92.25	2.84	48.54	23	307.33	5	0	0	4	267.65
4c	92.25	3.03	48.54	23	323.79	5	0	0	4	276.26
4d	92.25	3.33	48.54	23	323.79	5	0	0	4	276.26
4e	92.25	3.35	48.54	23	323.79	5	0	0	4	276.26
4f	92.25	3.48	48.54	23	368.24	5	0	0	4	280.61
4g	76.44	2.68	94.37	25	334.34	8	0	0	5	286.06
4h	92.25	3.12	48.54	23	303.37	5	0	0	4	279.28
4i	89.06	2.73	57.78	24	319.37	6	0	0	5	288.27
4j	92.25	2.35	48.54	21	275.31	5	0	0	3	245.92
4k	92.25	2.52	48.54	22	293.31	5	0	0	3	250.85
4l	92.25	3.19	48.54	22	309.76	5	0	0	3	259.45
4m	92.25	3.22	48.54	22	309.76	5	0	0	3	259.45
4n	92.25	3.03	48.54	22	309.76	5	0	0	3	259.45
4o	92.25	3.16	48.54	22	354.21	5	0	0	3	263.81
4p	76.44	2.31	94.37	24	320.31	8	0	0	4	269.25
4q	89.06	2.41	57.78	23	305.34	6	0	0	4	271.46

^aAbsorption; ^boctanol-water partition coefficient, calculated by methodology developed by Molinspiration; ^cpolar surface area; ^dnumber of non-hydrogen atoms; ^emolecular weight; ^fnumber of hydrogen-bond acceptor (O and N atoms); ^gnumber of hydrogen-bond donors (OH and NH atoms); ^hnumber of “Rule of five” violations; ⁱnumber of rotatable bonds; ^jmolecular volume

Table SI-4 Bioactivity score by Molinspiration Cheminformatics software

S. No.	Compound	GPCR ^a	ICM ^b	KI ^c	NRL ^d	PI ^e	EI ^f
1.	2	-0.21	-0.17	-0.39	-0.88	-0.94	0.11
2.	4a	0.25	0.06	0.39	-0.18	-0.06	0.25
3.	4b	0.26	0.04	0.42	-0.13	-0.06	0.22
4.	4c	0.22	0.04	0.33	-0.18	-0.15	0.14
5.	4d	0.25	0.06	0.35	-0.18	-0.08	0.20
6.	4e	0.24	0.05	0.37	-0.17	-0.08	0.20
7.	4f	0.14	-0.02	0.34	-0.27	-0.16	0.16
8.	4g	0.07	-0.01	0.21	-0.24	-0.15	0.10
9.	4h	0.20	-0.02	0.34	-0.18	-0.10	0.17
10.	4i	0.19	-0.03	0.33	-0.15	-0.07	0.17
11.	4j	0.29	0.12	0.41	-0.14	-0.13	0.28
12.	4k	0.31	0.09	0.45	-0.08	-0.12	0.25
13.	4l	0.43	0.18	0.49	-0.14	-0.17	0.19
14.	4m	0.28	0.08	0.36	-0.13	-0.19	0.20
15.	4n	0.30	0.10	0.39	-0.13	-0.14	0.23
16.	4o	0.19	0.02	0.36	-0.23	-0.22	0.18
17.	4p	0.13	0.03	0.24	-0.19	-0.20	0.12
18.	4q	0.25	0.01	0.36	-0.10	-0.13	0.20

^aG-protein coupled receptor; ^bion channel modulator; ^ckinase inhibitor; ^dnuclear receptor ligand; ^eprotease inhibitor; ^fenzyme inhibitor

Computational Study:

The frontier orbitals of the chemical compounds are very significant parameters in drug design and in recognizing their reactivity.^{4,6} A molecule with a higher value of highest occupied molecular orbital (HOMO) can give electrons to suitable acceptor molecules with low energy and empty molecular orbitals. Predicted frontier orbital energies, chemical potential (μ), chemical hardness (η), and electrophilicity index (ω) are presented in the **Table SI-3**. The values of μ , η , and ω were obtained by using the highest occupied molecular orbital (HOMO) and the lowest unoccupied molecular orbital (LUMO) energies according to Koopmans' theorem and Parr approximation,⁷ expressed as:

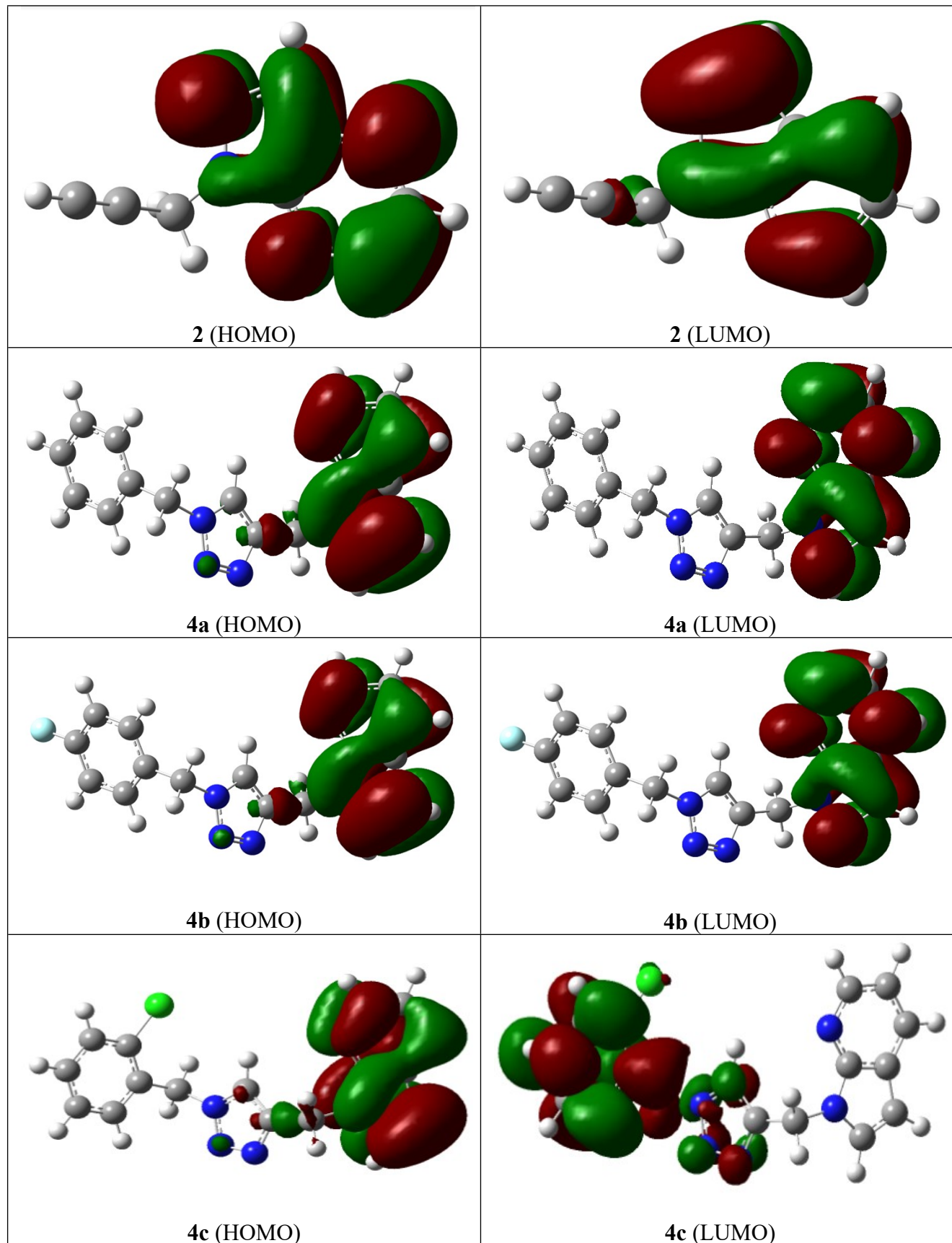
$$(1)$$

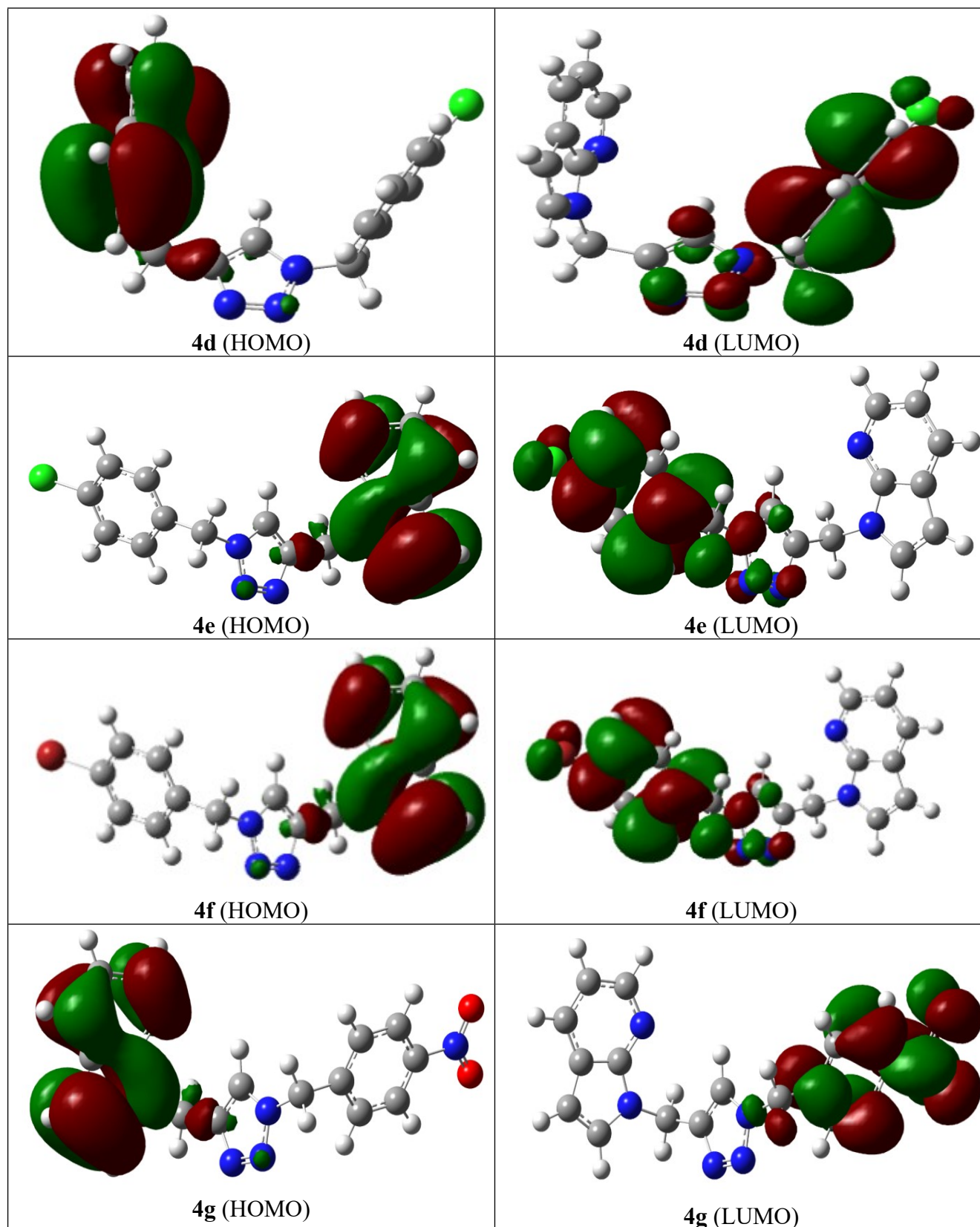
$$(2)$$

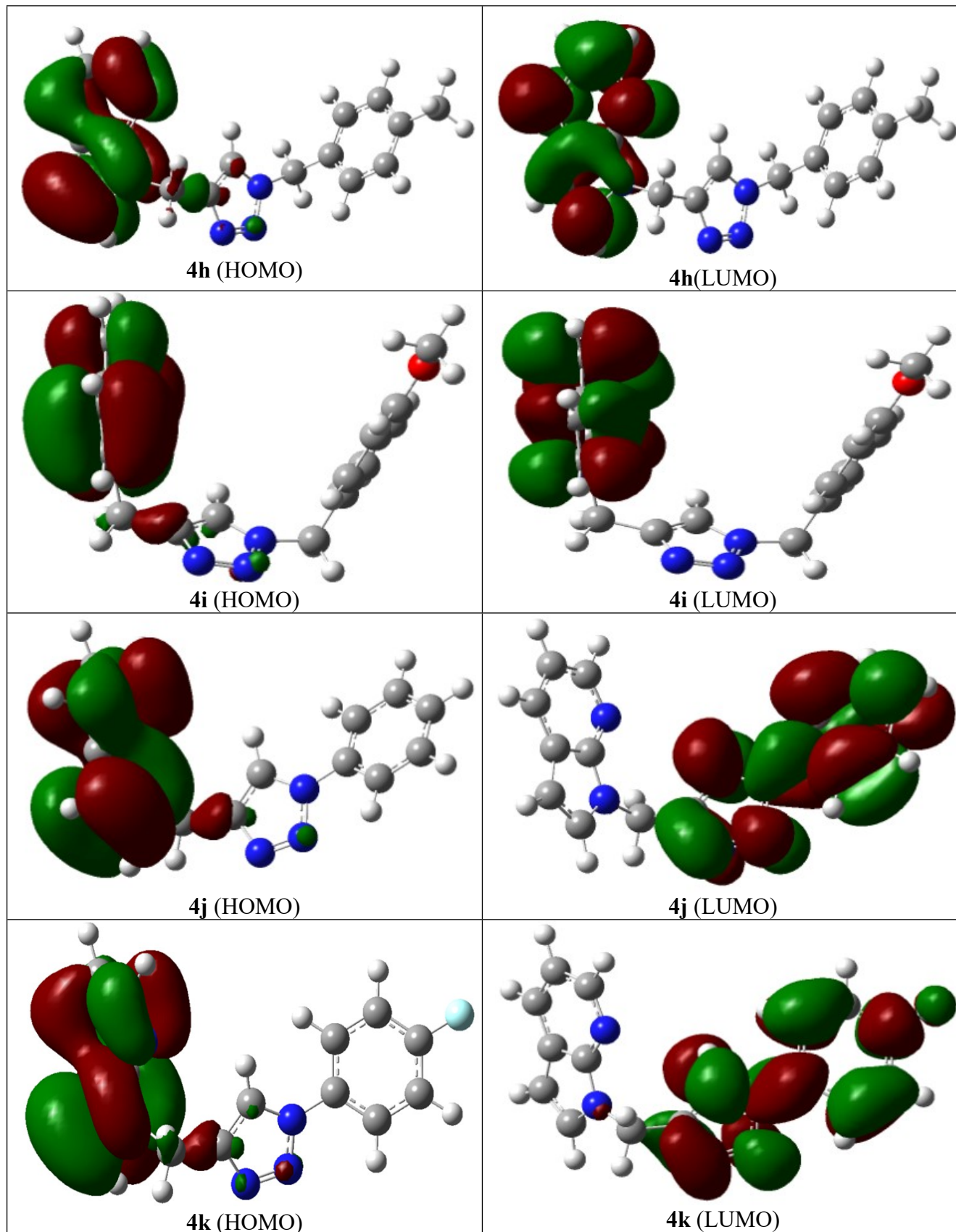
$$(3)$$

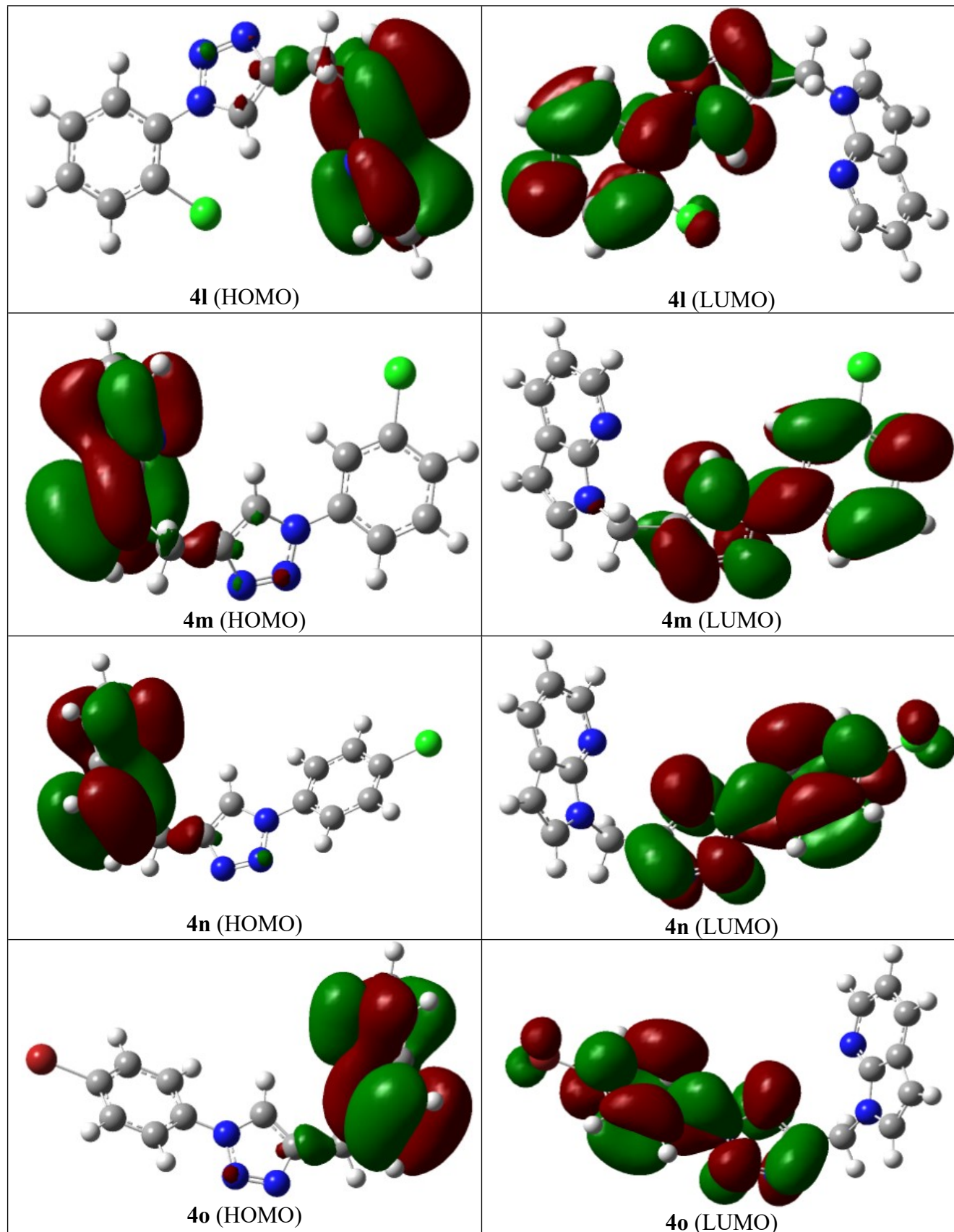
Table SI-5. Calculated FMOs, energy gap, chemical potential, chemical hardness, and electrophilicity index in eV at the B3LYP/6-311G(d,p) level of theory.

S. No.	Compound	E_{HOMO}	E_{LUMO}	$E_{\text{LUMO-HOMO}}$	μ	η	Softness	ω
					(eV)			
1.	2	-6.08	-0.98	5.11	-3.53	2.55	0.3921	2.44
2.	4a	-5.98	-0.95	5.03	-3.46	2.51	0.3984	2.39
3.	4b	-6.03	-1.00	5.03	-3.51	2.51	0.3984	2.45
4.	4c	-5.96	-1.15	4.81	-3.56	2.40	0.4167	2.63
5.	4d	-6.04	-1.06	4.98	-3.55	2.49	0.4016	2.53
6.	4e	-6.05	-1.08	4.97	-3.56	2.48	0.4032	2.56
7.	4f	-6.24	-0.80	5.44	-3.52	2.72	0.3676	2.28
8.	4g	-6.15	-2.80	3.35	-4.47	1.67	0.5988	5.97
9.	4h	-6.29	-1.12	5.17	-3.71	2.59	0.3861	2.66
10.	4i	-5.95	-0.91	5.03	-3.43	2.52	0.3968	2.34
11.	4j	-6.04	-1.31	4.73	-3.67	2.36	0.4237	2.85
12.	4k	-6.10	-1.34	4.76	-3.72	2.38	0.4201	2.90
13.	4l	-5.99	-1.42	4.57	-3.71	2.29	0.4366	3.00
14.	4m	-6.11	-1.59	4.52	-3.85	2.26	0.4424	3.28
15.	4n	-6.12	-1.57	4.55	-3.84	2.28	0.4385	3.25
16.	4o	-6.12	-1.58	4.54	-3.85	2.27	0.4405	3.26
17.	4p	-6.26	-2.91	3.35	-4.58	1.67	0.5988	6.27
18.	4q	-5.98	-1.02	4.96	-3.50	2.48	0.4032	2.47









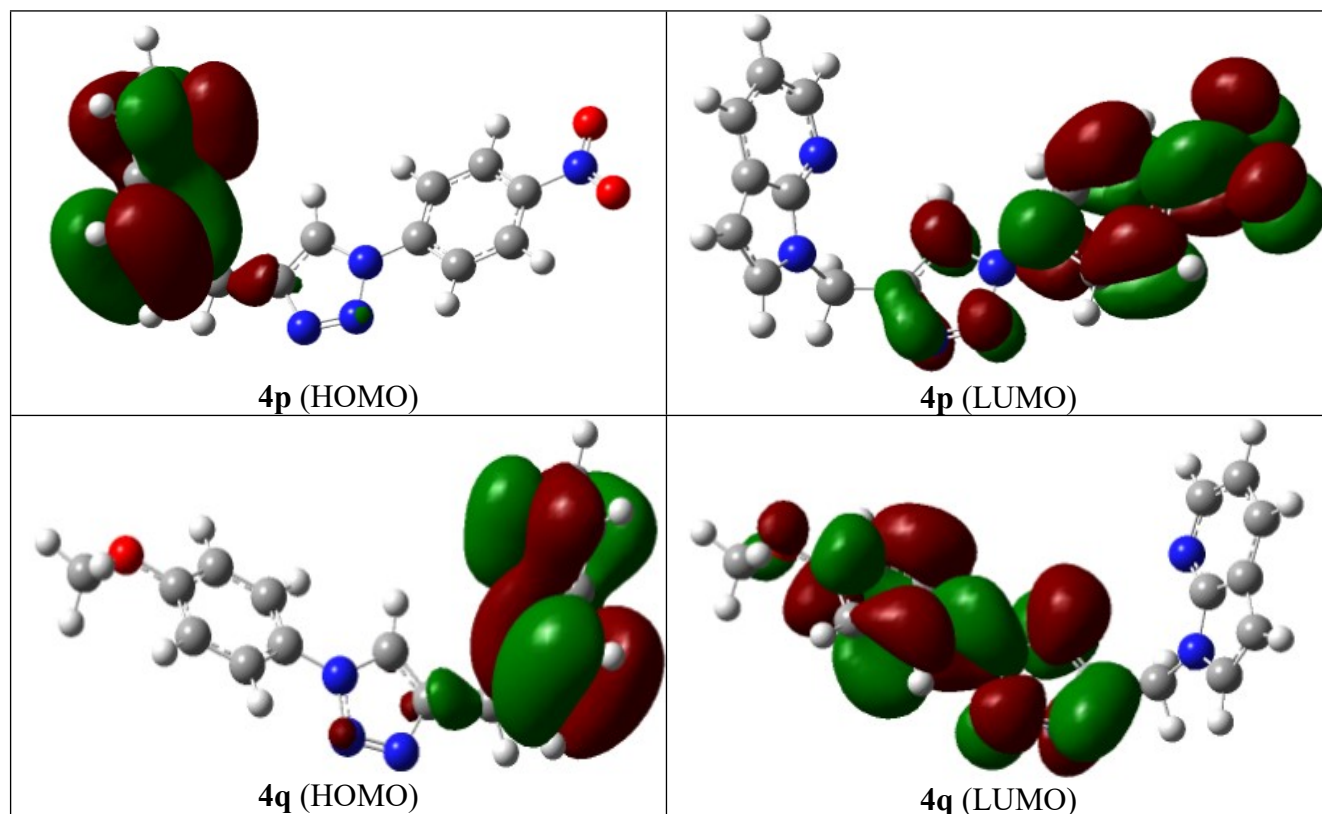


Figure SI-4. Highest occupied and lowest unoccupied molecular orbitals (HOMO and LUMO) distribution at the ground state of molecules **2**, and **4a-4q**.

Experimental

General procedure for the synthesis of 7-azaindole *N*-linked alkyne (**2**):

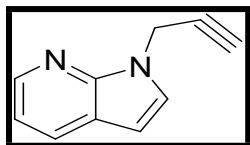
To a solution of 7-azaindole (1.0 g, 8.462 mmol) in DMF (5 mL) was added NaH (60% in oil, 304 mg, 12.693 mmol) in portion wise over 10 min at 0°C as per reported procedure.⁸ The reaction mixture was stirred for next half hour at same temperature. Propargyl bromide (1.510 mg, 12.693 mmol) was added drop-wise to the above resulting solution and stirred for 2-3 h at room temperature. After completion of the reaction, it was quenched with H₂O and extracted with EtOAc. The combined EtOAc layers were washed with brine solution, dried over Na₂SO₄ and concentrated under vacuum. The crude compound was purified by column chromatography on silica gel with EtOAc/hexane as eluent to give the pure desired compound 7-azaindole *N*-linked alkyne (**2**) i.e. 1-(prop-2-yn-1-yl)-1*H*-pyrrolo[2,3-*b*]pyridine.

General procedure for the synthesis of 7-azaindole *N*-linked aryl 1,2,3-triazoles (4a-4q):

7-Azaindole *N*-linked alkyne (**2**) (1mmol), benzyl halide (1mmol), and sodium azide (1.2 mmol) and the catalyst (0.1 mol% Cu) CuSO₄·5H₂O, sodium ascorbate were added to 10 mL of DMF:H₂O (4:1 v/v) taken in a round-bottom flask as per reported procedure.⁹ The reaction mixture was stirred at rt until TLC analysis shows that the reaction is complete. The reaction mixture was extracted with ethyl acetate and recrystallized. The solvent was evaporated in vacuum to get the desired triazoles (**4a-4q**) in good yield.

Spectroscopic data of compound(2):

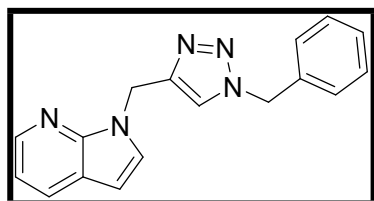
1-(prop-2-yn-1-yl)-1H-pyrrolo[2,3-b]pyridine (**2**)



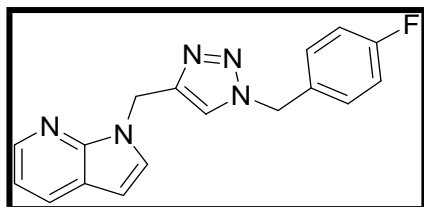
Appearance: brown liquid, Yield: 80%, FTIR (KBr, $\nu_{\max}/\text{cm}^{-1}$): 3292(s), 2121(m), 1508(s), 1305(s) cm^{-1} ; $R_f = 0.4$ (10% EtOAc/*n*-hexane); ¹H NMR (400 MHz, CDCl₃): δ 8.33 (dd, $J=4.8, 1.6\text{Hz}$, 1H), 7.90 (dd, $J=8.0, 1.6\text{Hz}$, 1H), 7.40 (d, $J=3.6\text{Hz}$, 1H), 7.07 (dd, $J=8.0, 4.8\text{Hz}$, 1H), 6.50 (d, $J=3.2\text{Hz}$, 1H), 5.09 (d, $J=2.8\text{Hz}$, 2H), 2.39 (t, $J=2.8\text{Hz}$, 1H); ¹³C NMR (100 MHz, CDCl₃): δ 147.15 (C), 143.08 (CH), 129.08 (C), 127.16 (CH), 120.85 (C), 116.21 (CH), 100.59 (CH), 78.27 (CH), 73.26 (CH), 33.68 (CH₂); ESI-MS [M+H]⁺: m/z cal. for C₁₀H₈N₂H⁺: 157.08, found 157.08.

Spectroscopic data of compounds (4a-q):

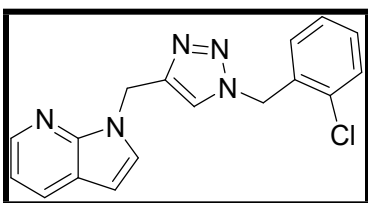
1-((1-benzyl-1H-1,2,3-triazol-4-yl) methyl)-1H-pyrrolo[2,3-b]pyridine (**4a**)



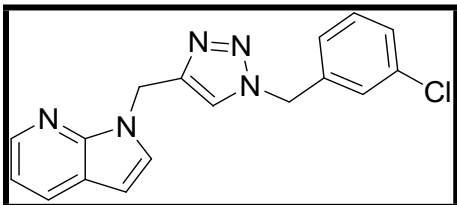
Appearance: Off white solid; yield: 97%; m.p: 56-58°C; FTIR (KBr, $\nu_{\max}/\text{cm}^{-1}$): 3119(m), 3063(m), 2933(m), 1508(s), 1305(s) cm^{-1} ; ¹H NMR (400 MHz, CDCl₃): δ 8.30 (dd, $J=1.6, 1.2\text{Hz}$, 1H), 7.90 (dd, $J=1.6, 1.2\text{Hz}$, 1H), 7.41 (s, 1H), 7.38-7.31 (m, 4H), 7.20 (dd, $J=3.2, 2\text{Hz}$, 2H), 7.06 (dd, $J=4.8, 4.4\text{Hz}$, 1H), 6.45 (d, $J=3.2\text{Hz}$, 1H), 5.57 (s, 2H), 5.43(s, 2H); ¹³C NMR (100 MHz, DMSO-d₆): δ 147.40 (C), 144.58 (CH), 143.05 (C), 136.58 (C), 129.41 (CH), 129.31 (CH), 129.18 (CH), 128.70 (CH), 128.53 (CH), 124.00 (CH), 120.60 (C), 116.38 (CH), 100.22 (CH), 53.33 (CH₂), 39.41 (CH₂); ESI-MS [M+H]⁺: m/z cal. for C₁₇H₁₅N₅H⁺ is 290.14, found 290.14.

1-((1-(4-fluorobenzyl)-1*H*-1,2,3-triazol-4-yl) methyl)-1*H*-pyrrolo [2,3-*b*]pyridine (**4b**)

Appearance: Creamish-green solid; yield: 87%, m.p: 50-52°C. FTIR (KBr, $\nu_{\max}/\text{cm}^{-1}$): 3117(m), 3070(s), 2935(m), 1510(s), 1303(s), 1221(m) cm^{-1} ; ^1H NMR (400 MHz, CDCl_3): δ 8.21 (d, $J=4\text{Hz}$, 1H), 7.80 (dd, $J=7.6, 1.2\text{Hz}$, 1H), 7.26 (d, $J=3.6\text{Hz}$, 1H), 7.13-7.08 (m, 2H), 6.99-6.89 (m, 3H), 6.36 (d, $J=3.6\text{Hz}$, 1H), 5.48 (s, 2H), 5.29 (s, 2H); ^{13}C NMR (100 MHz, CDCl_3): δ 163.96 (C), 161.49 (C), 147.06 (C) 144.88 (CH), 142.72 (C), 130.22 (CH), 130.19 (CH), 129.88 (CH), 129.81 (CH), 128.84 (CH), 127.91 (CH), 122.23 (CH), 120.59 (C), 116.08 (CH), 115.86 (CH), 100.14 (CH), 53.29 (CH_2), 39.40 (CH_2); ESI-MS $[\text{M}+\text{H}]^+$: m/z cal. for $\text{C}_{17}\text{H}_{14}\text{N}_5\text{FH}^+$ is 308.13, found 308.13.

1-((1-(2-chlorobenzyl)-1*H*-1,2,3-triazol-4-yl) methyl)-1*H*-pyrrolo[2,3-*b*]pyridine (**4c**)

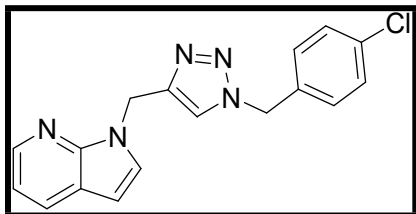
Appearance: Light orange solid; yield: 82.9%; m.p: 58-60°C; FTIR (KBr, $\nu_{\max}/\text{cm}^{-1}$): 3117(s), 3053(m), 2910(m), 1514(s), 1303(s), 727(s) cm^{-1} ; ^1H NMR (400 MHz, CDCl_3): δ 8.31 (dd, $J=4.8, 1.6\text{Hz}$, 1H), 7.90(dd, $J=7.6, 1.6\text{Hz}$, 1H), 7.53 (s, 1H), 7.40-7.36 (m, 2H), 7.31-7.19(m, 2H), 7.11(dd, $J=7.6, 2\text{Hz}$, 1H), 7.06 (dd, $J=7.6, 4.8\text{Hz}$, 1H), 6.45 (d, $J=3.6\text{ Hz}$, 1H), 5.59 (s, 2H), 5.57 (s, 2H); ^{13}C NMR (100 MHz, CDCl_3): δ 147.04 (C), 144.62 (CH), 142.66 (C), 133.37 (C), 132.23 (C), 130.17 (CH), 130.15 (CH), 129.84 (CH), 128.95 (CH), 127.99 (CH), 127.50 (CH), 122.79 (CH), 120.69 (C), 115.86 (CH), 100.20 (CH), 51.34 (CH_2), 39.44 (CH_2); ESI-MS $[\text{M}+\text{H}]^+$: m/z cal. for $\text{C}_{17}\text{H}_{14}\text{N}_5\text{ClH}^+$ is 324.10, found 324.10.

1-((1-(3-chlorobenzyl)-1*H*-1,2,3-triazol-4-yl) methyl)-1*H*-pyrrolo[2,3-*b*]pyridine (**4d**)

Appearance: Creamish-orange solid; yield: 92%; m.p: 52-54°C; FTIR (KBr, $\nu_{\max}/\text{cm}^{-1}$): 3142(m), 3095(m), 2945(m), 1508(s), 1307(s), 723(s) cm^{-1} ; ^1H NMR (400 MHz, DMSO-d_6): δ 8.27 (dd, $J=4.8, 1.2\text{Hz}$, 1H), 8.10(s, 1H), 7.99-7.95 (dd, $J=7.6, 1.6\text{Hz}$, 1H), 7.60 (d, $J=3.6\text{Hz}$, 1H), 7.40-7.21 (m, 4H), 7.10 (dd, $J=7.6, 4.4\text{Hz}$, 1H), 6.50 (d, $J=3.6\text{Hz}$, 1H), 5.58-5.54 (m, 4H); ^{13}C NMR (100 MHz, DMSO-d_6): δ 147.42 (C), 144.71 (CH), 143.08 (C), 138.97 (C), 133.96 (C), 131.29 (CH), 129.46 (CH), 129.22(CH), 128.73 (CH),

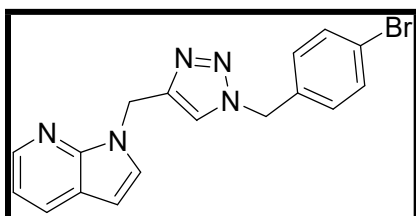
128.46 (CH), 127.28 (CH), 124.22 (CH), 120.64 (C), 116.42 (CH), 100.26 (CH), 52.57 (CH₂), 39.46 (CH₂); ESI-MS [M+H]⁺: m/z cal. for C₁₇H₁₄N₅ClH⁺ is 324.10, found 324.10.

1-((1-(4-chlorobenzyl)-1*H*-1,2,3-triazol-4-yl) methyl)-1*H*-pyrrolo[2,3-*b*]pyridine (**4e**)



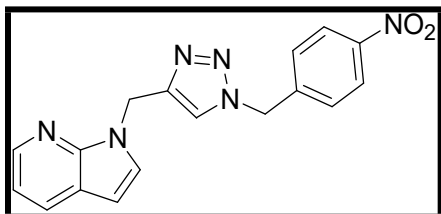
Appearance: Brown solid; yield: 89.44%; m.p: 88-90°C; FTIR (KBr, $\nu_{\max}/\text{cm}^{-1}$): 3117(m), 3053(m), 2968(m), 1514(s), 1303(s), 771(s) cm^{-1} ; ¹H NMR (400 MHz, DMSO-*d*₆): δ 8.26 (d, *J*=4Hz, 1H), 8.08(s, 1H), 7.97 (dd, *J*=7.6, 1.6Hz, 1H), 7.60 (d, *J*=3.6Hz, 1H), 7.44-7.40 (m, 4H), 7.33-7.28 (m, 2H), 7.10 (dd, *J*=8.0, 4.8Hz, 1H), 6.50 (d, *J*=3.2Hz, 1H), 5.55 (d, *J*=1.2Hz, 4H); ¹³C NMR (100 MHz, DMSO-*d*₆): δ 147.41 (C), 144.69 (CH), 143.08 (C), 135.59 (C), 133.47 (C), 130.53 (CH), 129.44 (CH), 129.34 (CH), 129.22 (CH), 124.10 (CH), 120.64 (C), 116.43 (CH), 100.26 (CH), 52.55 (CH₂), 39.43 (CH₂); ESI-MS [M+H]⁺: m/z cal. for C₁₇H₁₄N₅Cl⁺ is 324.10, found 324.10.

1-((1-(4-bromobenzyl)-1*H*-1,2,3-triazol-4-yl) methyl)-1*H*-pyrrolo[2,3-*b*]pyridine (**4f**)



Appearance: Muddy-yellow solid; yield: 87%; m.p: 86-90°C; FTIR (KBr, $\nu_{\max}/\text{cm}^{-1}$): 3117(m), 3063(m), 2945(m), 1512(s), 1305(s), 688(s) cm^{-1} ; ¹H NMR (400 MHz, CDCl₃): δ 8.33 (s, 1H), 7.90 (d, *J* = 4Hz, 1H), 7.44 (d, *J*=8.4Hz, 3H), 7.35 (d, *J*=3.6Hz, 1H), 7.06 (d, *J*=8.4Hz, 3H), 6.46 (d, *J* = 3.6Hz, 1H), 5.57 (s, 2H), 5.36 (s, 2H); ¹³C NMR (100 MHz, CDCl₃): δ 147.22 (C), 145.44 (CH), 142.83 (C), 133.51 (C), 132.33 (C), 129.75 (CH), 129.03 (CH), 128.11 (CH), 123.01 (CH), 122.65 (CH), 120.89 (C), 116.14 (CH), 100.37 (CH), 53.57 (CH₂), 39.64 (CH₂); ESI-MS [M+H]⁺: m/z cal. for C₁₇H₁₄N₅BrH⁺ is 368.05, found 368.05.

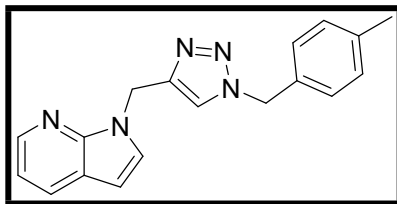
1-((1-(4-nitrobenzyl)-1*H*-1,2,3-triazol-4-yl) methyl)-1*H*-pyrrolo[2,3-*b*]pyridine (**4g**)



Appearance: Yellow solid; yield: 80.8%; m.p: 95-96°C; FTIR (KBr, $\nu_{\max}/\text{cm}^{-1}$): 3157(m), 3086(m), 2945(m), 1526(m), 1510(s), 1309(s), 348(m) cm^{-1} ; ¹H NMR (400 MHz, CDCl₃): δ 8.30 (dd, *J* = 4.8, 1.2Hz, 1H), 8.18 (dd, *J*=2.4, 2.0Hz, 2H), 7.90 (dd, *J*=7.6, 1.6Hz, 1H), 7.5 (s, 1H), 7.37-7.32 (m, 3H), 7.07 (dd, *J* = 8, 4.8Hz, 1H), 6.45 (d, *J*=3.6Hz, 1H), 5.60 (s, 2H), 5.54 (s, 2H); ¹³C NMR (100 MHz, CDCl₃): δ 148.02 (C), 147.07 (C), 145.39 (CH), 142.79 (C), 141.36 (C), 129.01 (CH), 128.54 (CH), 127.98 (CH), 124.23 (CH),

122.71 (CH), 120.71 (C), 115.97 (CH), 100.31 (CH), 53.05 (CH₂), 39.55 (CH₂); ESI-MS [M+H]⁺ : m/z cal. for C₁₇H₁₄N₆O₂H⁺ is 335.13, found 335.12.

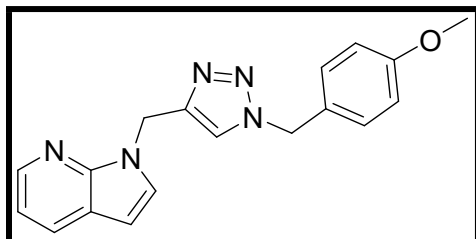
1-((1-(4-methylbenzyl)-1*H*-1,2,3-triazol-4-yl) methyl)-1*H*-pyrrolo[2,3-*b*]pyridine (**4h**)



Appearance: Muddy-brown; yield: 92%; m.p: 76-78°C; FTIR (KBr, $\nu_{\max}/\text{cm}^{-1}$): 3117(m), 3053(m), 2901(m), 1514(s), 1317(s) cm^{-1} ; ¹H NMR (400 MHz, DMSO-*d*₆): δ 8.26 (s, 1H), 8.02 (s, 1H), 7.96(d, *J*=7.6Hz, 1H), 7.58 (d, *J*=3.6Hz, 1H), 7.20-7.07(m, 5H), 6.49 (d, *J*=3.6Hz, 1H), 5.52 (s, 2H), 5.47(s, 2H),

2.25(s, 3H); ¹³C NMR (100 MHz, DMSO-*d*₆): δ 147.39 (C), 144.66 (CH), 143.66 (C), 138.08 (C), 133.59 (C), 129.87 (CH), 129.44 (CH), 129.21 (CH), 128.62 (CH), 123.87 (CH), 120.64 (C), 116.42 (CH), 100.24 (CH), 53.16 (CH₂), 39.41 (CH₂), 21.30 (CH₃); ESI-MS [M+H]⁺: m/z cal. for C₁₈H₁₇N₅H⁺ is 304.16, found 304.15.

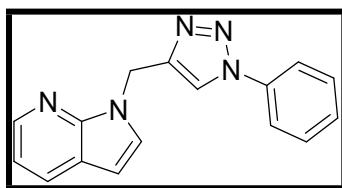
1-((1-(4-methoxybenzyl)-1*H*-1,2,3-triazol-4-yl) methyl)-1*H*-pyrrolo[2,3-*b*]pyridine (**4i**)



Appearance: Reddish-brown solid, yield: 77.5%, m.p: 60-62°C. FT IR (KBr, $\nu_{\max}/\text{cm}^{-1}$): 3111(m), 3057(m), 2955(m), 1514(s), 1303(s), 1252(m) cm^{-1} ; ¹H NMR (400 MHz, DMSO-*d*₆): δ 8.26 (s, 1H), 8.01 (s, 1H), 7.97 (dd, *J*=8.0, 0.8Hz, 1H), 7.58 (d, *J*=3.6Hz, 1H), 7.24-7.28 (m, 2H),

7.10 (dd, *J*= 8.0, 4.8Hz, 1H), 6.92-6.88 (m, 2H), 6.49 (d, *J*=3.2Hz, 1H), 5.52 (s, 2H), 5.44 (s, 2H), 3.71 (s, 3H); ¹³C NMR (100 MHz, DMSO-*d*₆): δ 159.14 (C), 146.78 (C), 142.48 (CH), 129.68(C), 129.67(C), 128.87 (CH), 128.66 (CH), 127.90 (CH), 123.11 (CH), 120.08 (C), 115.86 (CH), 114.12 (CH), 99.68 (CH), 55.14 (CH₂), 52.34 (CH₃), 38.84 (CH₂); ESI-MS [M+H]⁺: m/z cal. for C₁₈H₁₇N₅OH⁺ is 320.15, found 320.15.

1-((1-phenyl-1*H*-1,2,3-triazol-4-yl) methyl)-1*H*-pyrrolo[2,3-*b*]pyridine (**4j**)

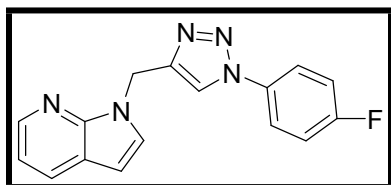


Appearance: Colourless crystalline solid; yield: 84%; m.p: 72-74°C; FTIR (KBr, $\nu_{\max}/\text{cm}^{-1}$): 3144(m), 3051(m), 2941(m), 1506(s), 1300(s) cm^{-1} ; ¹H NMR (400 MHz, CDCl₃): δ 8.35 (dd, *J*= 4.8, 1.6Hz, 1H), 7.89-7.94 (m, 2H), 7.67-7.61 (m, 2H), 7.50-7.35(m, 4H),

7.08(m, 1H), 6.48 (d, *J*=3.6Hz ,1H), 5.68 (s, 2H); ¹³C NMR (100 MHz, CDCl₃): δ 147.08 (C), 142.75 (CH), 136.87 (C), 129.63 (C), 129.05 (CH), 128.74 (CH), 128.05 (C), 125.22 (CH),

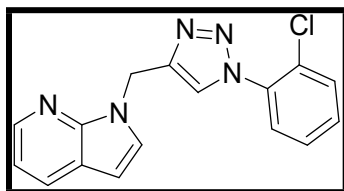
120.81 (CH), 120.50 (CH), 116.01 (CH), 115.59 (CH), 100.35 (CH), 39.54 (CH₂); ESI-MS [M+H]⁺: m/z cal. for C₁₆H₁₃N₅H⁺ is 276.12, found 276.12.

1-((1-(4-fluorophenyl)-1*H*-1,2,3-triazol-4-yl) methyl)-1*H*-pyrrolo[2,3-*b*]pyridine (**4k**)



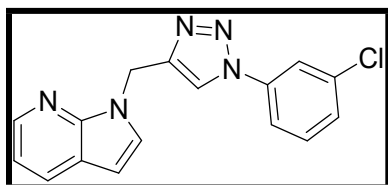
Appearance: Off white needles, yield: 84.5%, m.p: 76-78°C. FTIR (KBr, $\nu_{\max}/\text{cm}^{-1}$): 3125(m), 3074(m), 2937(m), 1514(s), 1305(s), 1227(m) cm^{-1} ; ¹H NMR (400 MHz, CDCl₃): δ 8.35 (dd, $J=4.8, 1.2\text{Hz}$, 1H), 7.94-7.87 (m, 2H), 7.58-7.65 (m, 2H), 7.42 (d, $J=3.6\text{Hz}$, 1H), 7.19-7.12 (m, 2H), 7.09 (dd, $J=7.6, 4.4\text{Hz}$, 1H), 6.49 (d, $J=3.6\text{Hz}$, 1H), 5.67 (s, 2H); ¹³C NMR (100 MHz, CDCl₃): δ 163.59 (C), 161.12 (C), 147.13 (CH), 145.30 (C), 142.89 (C), 133.14 (CH), 129.01 (CH), 127.99 (CH), 122.52 (CH), 122.44 (CH), 120.89 (C), 120.72 (CH), 116.72 (CH), 116.49 (CH), 116.00 (CH), 100.34(CH), 39.49 (CH₂); ESI-MS [M+H]⁺: m/z cal. for C₁₆H₁₂N₅FH⁺ is 294.11, found 294.11.

1-((1-(2-chlorophenyl)-1*H*-1,2,3-triazol-4-yl) methyl)-1*H*-pyrrolo[2,3-*b*]pyridine (**4l**)



Appearance: Off white solid, yield: 92%, m.p: 58-60°C. FTIR (KBr, $\nu_{\max}/\text{cm}^{-1}$): 3157(m), 3073(m), 2924(m), 1508(s), 1311(s), 768(s) cm^{-1} ; ¹H NMR (400 MHz, CDCl₃): δ 8.35-8.32 (m, 1H), 7.94(s, 1H), 7.93-7.89 (m, 1H), 7.56-7.50 (m, 2H), 7.46-7.34 (m, 3H), 7.07(dd, $J=4.8, 8.0\text{Hz}$, 1H), 6.49 (d, $J=3.6\text{Hz}$, 1H), 5.70 (s, 2H); ¹³C NMR (100 MHz, CDCl₃): δ 147.21 (C), 144.15 (CH), 142.85 (C), 134.71 (C), 130.70 (C), 130.66(CH), 128.91 (CH), 128.54 (CH), 127.78 (CH), 127.68 (CH), 124.63(CH), 120.68 (C), 115.93 (CH), 100.29(CH), 39.45 (CH₂); ESI-MS [M+H]⁺: m/z cal. for C₁₆H₁₂ClN₅H⁺ is 310.085, found 310.088.

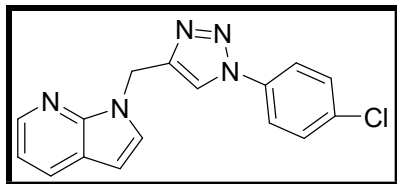
1-((1-(3-chlorophenyl)-1*H*-1,2,3-triazol-4-yl) methyl)-1*H*-pyrrolo[2,3-*b*]pyridine (**4m**)



Appearance: Light brown solid, yield: 84.66%, m.p: 52-54°C. FTIR (KBr, $\nu_{\max}/\text{cm}^{-1}$): 3124(m), 3086(m), 3057(m), 1510(s), 1315(s), 727(s) cm^{-1} ; ¹H NMR (400 MHz, CDCl₃): δ 8.39 (s, 1H), 7.93 (d, $J=7.2\text{Hz}$, 2H), 7.70 (d, $J=1.6\text{Hz}$, 1H), 7.57-7.52 (m, 1H), 7.42-7.33 (m, 3H), 7.11 (d, $J=3.2\text{Hz}$, 1H), 6.50 (d, $J=1.2\text{Hz}$, 1H), 5.68 (s, 2H); ¹³C NMR (100 MHz, CDCl₃): δ 147.27 (C), 143.01 (CH), 142.94 (C), 137.89 (C), 135.64 (C), 130.89 (CH), 129.18 (CH), 128.96 (CH), 128.13 (CH), 120.89 (C), 120.54 (CH), 118.60 (CH), 116.44

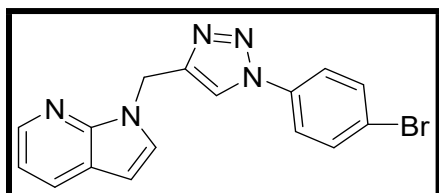
(CH), 116.31 (CH), 100.61 (CH), 39.71 (CH₂); ESI-MS [M+H]⁺: m/z cal. for C₁₆H₁₂N₅ClH⁺ is 310.085, found 310.085.

1-((1-(4-chlorophenyl)-1*H*-1,2,3-triazol-4-yl) methyl)-1*H*-pyrrolo[2,3-*b*]pyridine (**4n**)



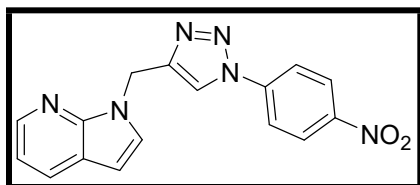
Appearance: Off white needles; yield: 83.8%; m.p: 86-88°C; FTIR (KBr, $\nu_{\max}/\text{cm}^{-1}$): 3128(m), 3057(m), 2941(m), 1508(s), 1305(s), 1508(s), 1305(s), 717(s) cm^{-1} ; ¹H NMR (400 MHz, CDCl₃): δ 8.35 (dd, $J=4.8, 1.6\text{Hz}$, 1H), 7.95-7.89 (m, 2H), 7.62-7.57 (m, 2H), 7.47-7.40 (m, 3H), 7.09 (dd, $J=8, 4.8\text{ Hz}$, 1H), 6.49 (d, $J=3.6\text{Hz}$, 1H), 5.68 (s, 2H); ¹³C NMR (100 MHz, CDCl₃): δ 147.22 (C), 145.44 (CH), 142.83 (C), 133.51 (C), 132.33 (C), 129.75 (CH), 129.03 (CH), 128.11 (CH), 123.01 (C), 120.89 (CH), 116.14 (CH), 100.37(CH), 53.57 (CH), 39.64 (CH₂); ESI-MS [M+H]⁺: m/z cal. for C₁₆H₁₂N₅ClH⁺ is 310.085, found 310.089.

1-((1-(4-bromophenyl)-1*H*-1,2,3-triazol-4-yl) methyl)-1*H*-pyrrolo[2,3-*b*]pyridine(**4o**)



Appearance: Off white needles; yield: 84%; m.p: 96-98°C; FTIR (KBr, $\nu_{\max}/\text{cm}^{-1}$): 3136(m), 3097(m), 3040(m), 2940(m), 1508(s), 1305(s), 685(s) cm^{-1} ; ¹H NMR (400 MHz, CDCl₃): δ 8.28 (dd, $J=4.8, 1.2\text{Hz}$, 1H), 7.87-7.81 (m, 2H), 7.55-7.50 (m, 2H), 7.49-7.44 (m, 2H), 7.34 (d, $J=3.6\text{ Hz}$, 1H), 7.02 (dd, $J=7.6, 4.8\text{ Hz}$, 1H), 6.42 (d, $J=3.6\text{Hz}$, 1H), 5.60 (s, 2H); ¹³C NMR (100 MHz, CDCl₃): δ 147.16 (C), 145.50 (CH), 142.93 (C), 135.83 (C), 132.81 (C), 129.03 (CH), 127.97 (CH), 122.42 (CH), 121.88 (CH), 120.74 (C), 120.56 (CH), 116.05 (CH), 100.40 (CH), 39.52 (CH); ESI-MS [M+H]⁺: m/z cal. for C₁₆H₁₂N₅BrH⁺ is 354.035, found 354.041.

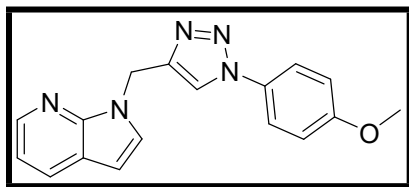
1-((1-(4-nitrophenyl)-1*H*-1,2,3-triazol-4-yl) methyl)-1*H*-pyrrolo[2,3-*b*]pyridine (**4p**)



Appearance: Off white solid; yield: 83%; m.p: 196-198°C; FTIR (KBr, $\nu_{\max}/\text{cm}^{-1}$): 3127(m), 3074(m), 2930(m), 1506(s), 1529(s), 1344(s), 1313(s) cm^{-1} ; ¹H NMR (400 MHz, CDCl₃): δ 8.50-8.25 (m, 3H), 8.05 (s, 1H), 7.91 (dd, $J=9.2, 16.8\text{Hz}$, 3H), 7.42 (d, $J=3.6\text{Hz}$, 1H), 7.11 (dd, $J=4.4, 8\text{Hz}$, 1H), 6.51 (d, $J=3.2\text{Hz}$, 1H), 5.70 (s, 2H); ¹³C NMR (100 MHz, CDCl₃): δ 147.23 (C), 147.17 (C), 146.16 (C), 143.02 (CH), 141.01 (C), 129.15

(CH), 127.96 (CH), 125.46 (CH), 120.81 (CH), 120.64 (C), 120.48 (CH), 116.16 (CH), 100.57 (CH), 39.52 (CH₂); ESI-MS [M+H]⁺: m/z cal. for C₁₆H₁₂N₆O₂H⁺ is 321.11, found 321.11.

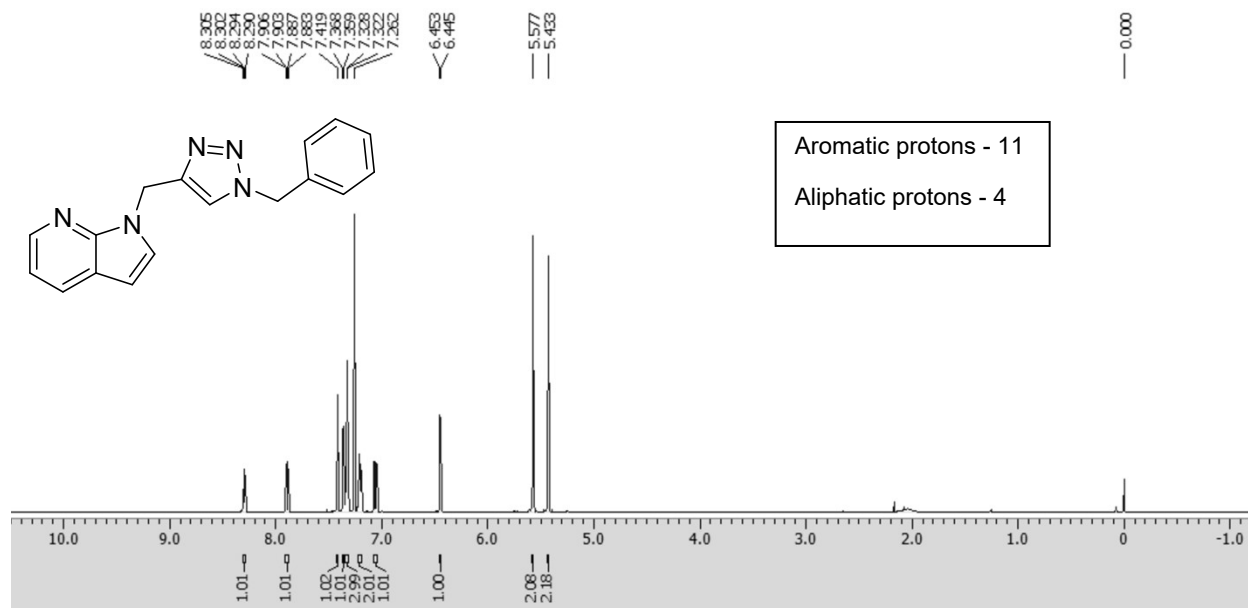
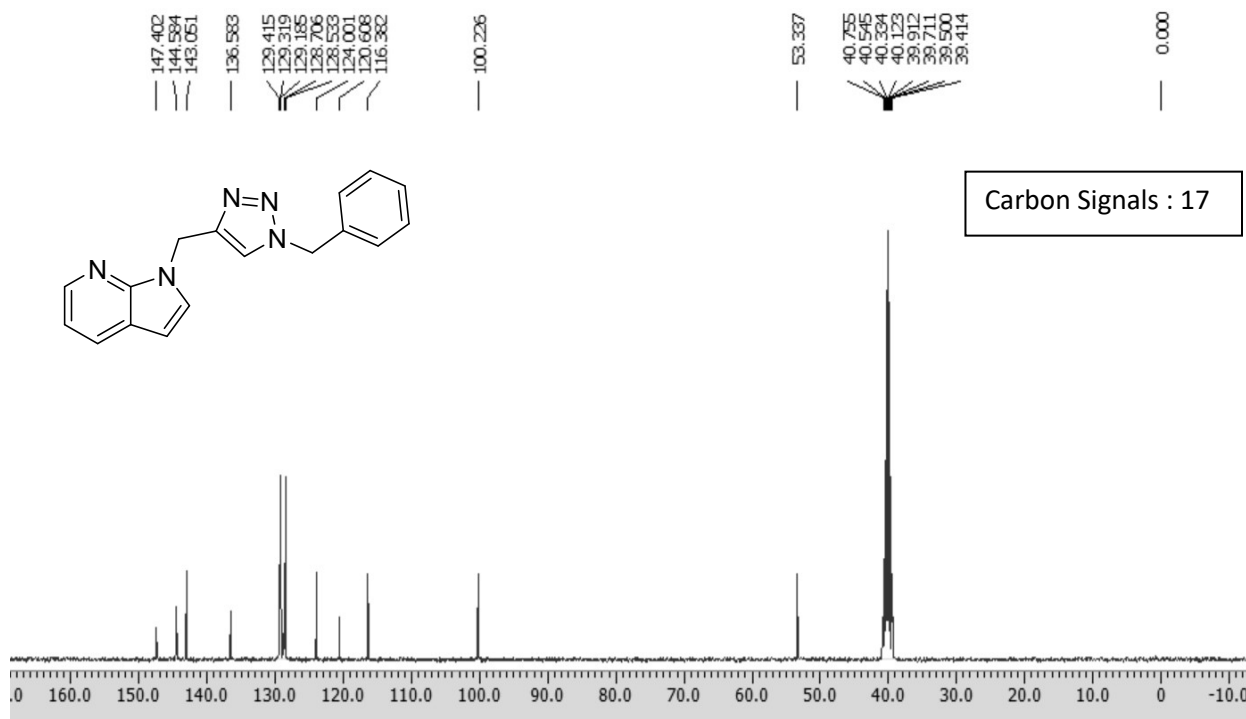
1-((1-(4-methoxyphenyl)-1*H*-1,2,3-triazol-4-yl) methyl)-1*H*-pyrrolo[2,3-*b*]pyridine (**4q**)



Appearance: Grey solid, Yield: 79%, m.p: 72-74°C. FTIR (KBr, $\nu_{\max}/\text{cm}^{-1}$): 3136(m), 3088(m), 2935(m), 2835(m), 1519(s), 1305(s), 1248(s) cm^{-1} ; ¹H NMR (400 MHz, CDCl₃): δ 8.39 (s, 1H), 7.94 (d, $J=7.6\text{Hz}$, 1H), 7.88 (s, 1H), 7.57-7.52 (m, 2H), 7.44 (d, $J=3.2\text{Hz}$, 1H), 7.11 (s, 1H), 6.99-6.94 (m, 2H), 5.69 (s, 2H), 3.38 (s, 3H); ¹³C NMR (100 MHz, CDCl₃): δ 159.92 (C), 147.21 (C), 142.49 (CH), 130.68 (C), 130.60 (C), 129.14 (CH), 128.33 (CH), 128.25 (CH), 122.34 (CH), 121.23 (C), 116.15 (CH), 114.83 (CH), 100.52 (CH), 55.72 (CH₂), 39.79 (CH₃); ESI-MS [M+H]⁺: m/z cal. for C₁₇H₁₅N₅OH⁺ is 306.13, found 306.13.

References:

1. Krause, L., Herbst-Irmer, R., Sheldrick G.M. & Stalke D. *J. Appl. Cryst.* 2015, **48**, 3.
2. G. M. Sheldrick, *Acta Crystallogr C Struct Chem.* 2015, **71**, 3.
3. J. L. Farrugia, G. X. Win, *J. Appl. Crystallogr.*, 1999, **32**, 837.
4. L. H. Mendoza-Huizar, C. H. Rios-Reyes *J Mex Chem Soc* 2011, **55**, 142.
5. I. Piyanzina, B. Minisini, D. Tayurskii, J. F. Bardeau, *J Mol. Model.* 2015, **21**, 34.
6. M. Elango, R. Parthasarathi, V. Subramanian, U. Sarkar, P.K. Chattaraj, *J. Mol. Str. THEOCHEM* 2005, **723**, 43.
7. R. G. Parr, L. V. Szentpaly, S. Liu, *J. Am. Chem. Soc.* 1999, **121**, 1922.
8. P. K. Naikawadi, L. Mucherla, R. Dandela, M. Sambari, K.S. Kumar, *Adv. Synth. Catal* 2021, **363**, 3796.
9. L. Jing, X. W. Hao, F.A. Olotu, D. Kang, C.H. Chen, K.H. Lee, M. E. S. Solima, X. Liu, Y. Song, P. Zhan, *Eur. J. Med. Chem*, 2019, **183**, 111696.

Figure SI-7. $^1\text{H-NMR}$ (4a)Figure SI-8. $^{13}\text{C NMR}$ (4a)

Sample Name : KS_01
Test Name :
010622_KS_01 34 (0.592)

IITRPR

XEVO G2-XS QTOF

1: TOF MS ES+
2.57e7

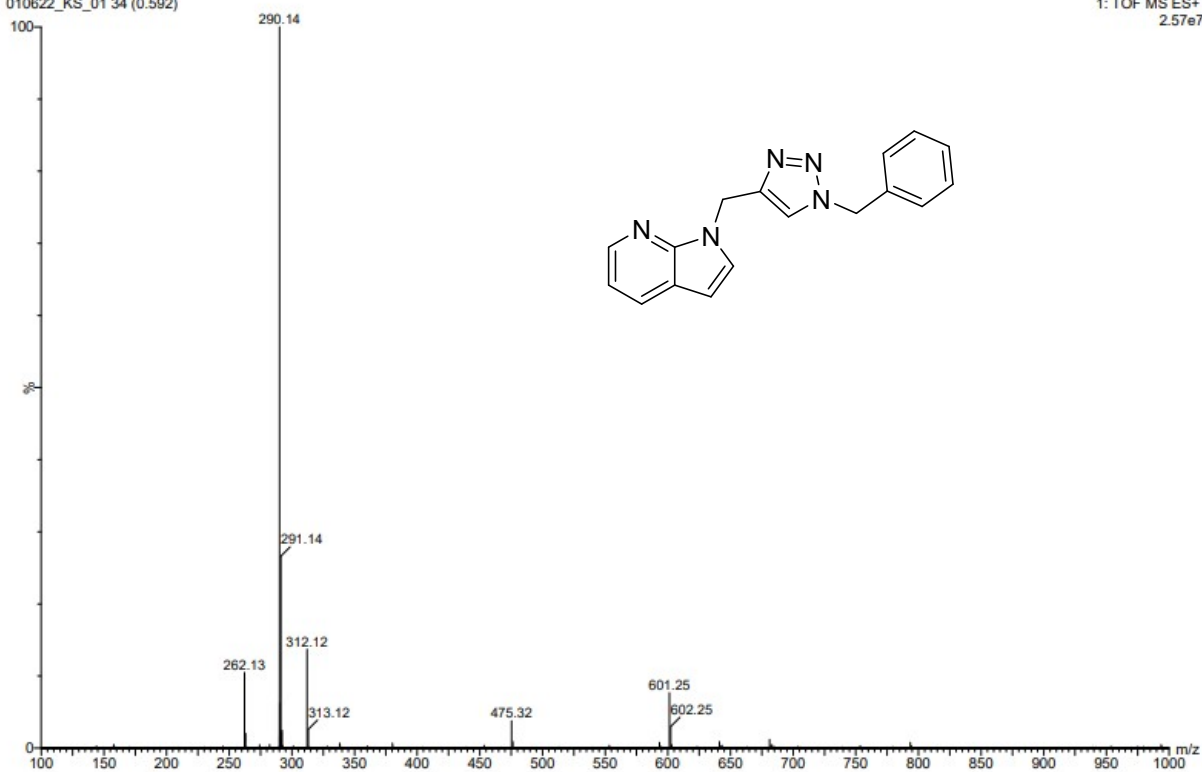
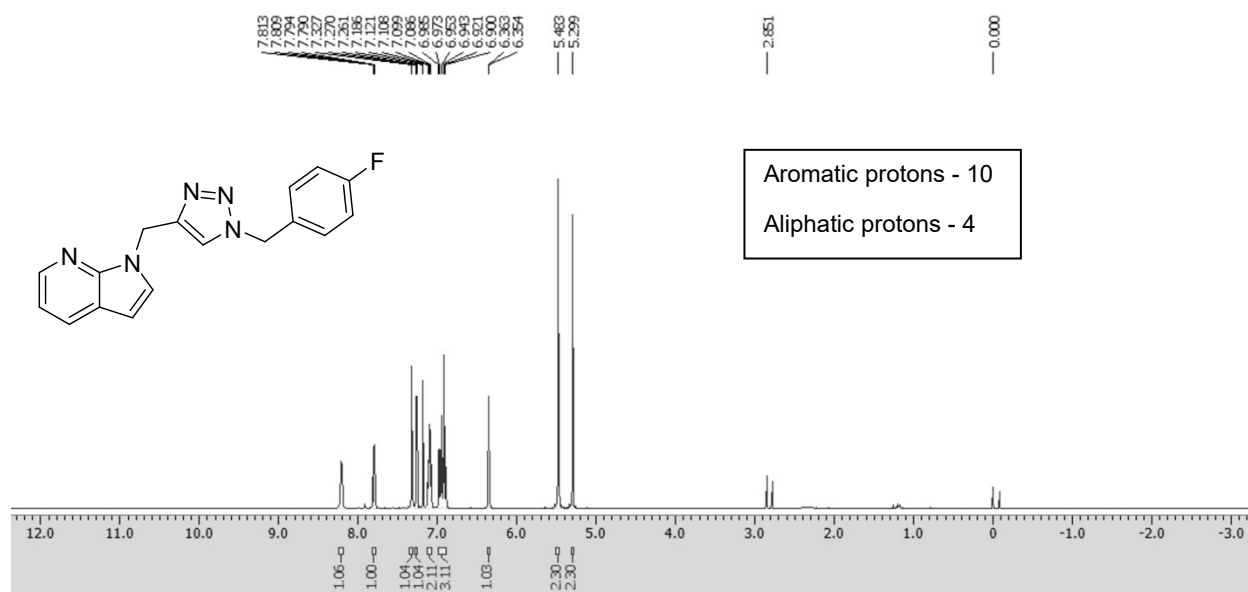
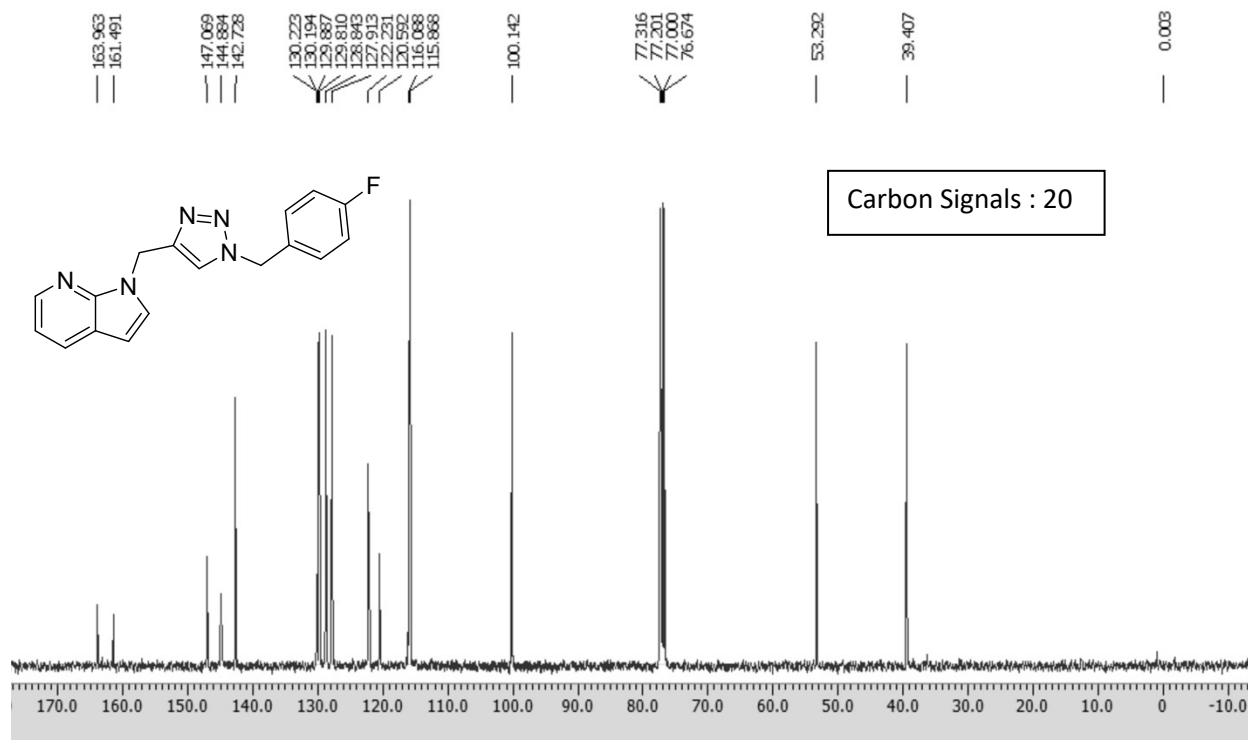


Figure SI-9. ESI-MS $[M+H]^+$: m/z for (4a) $C_{17}H_{15}N_5$: 290.14

Figure SI-10. ¹H-NMR (4b)Figure SI-11. ¹³C-NMR (4b)

Sample Name : KS_05
Test Name :
010622_KS_05 18 (0.321)

IITRPR

XEVO G2-XS QTOF

1: TOF MS ES+
2.05e8

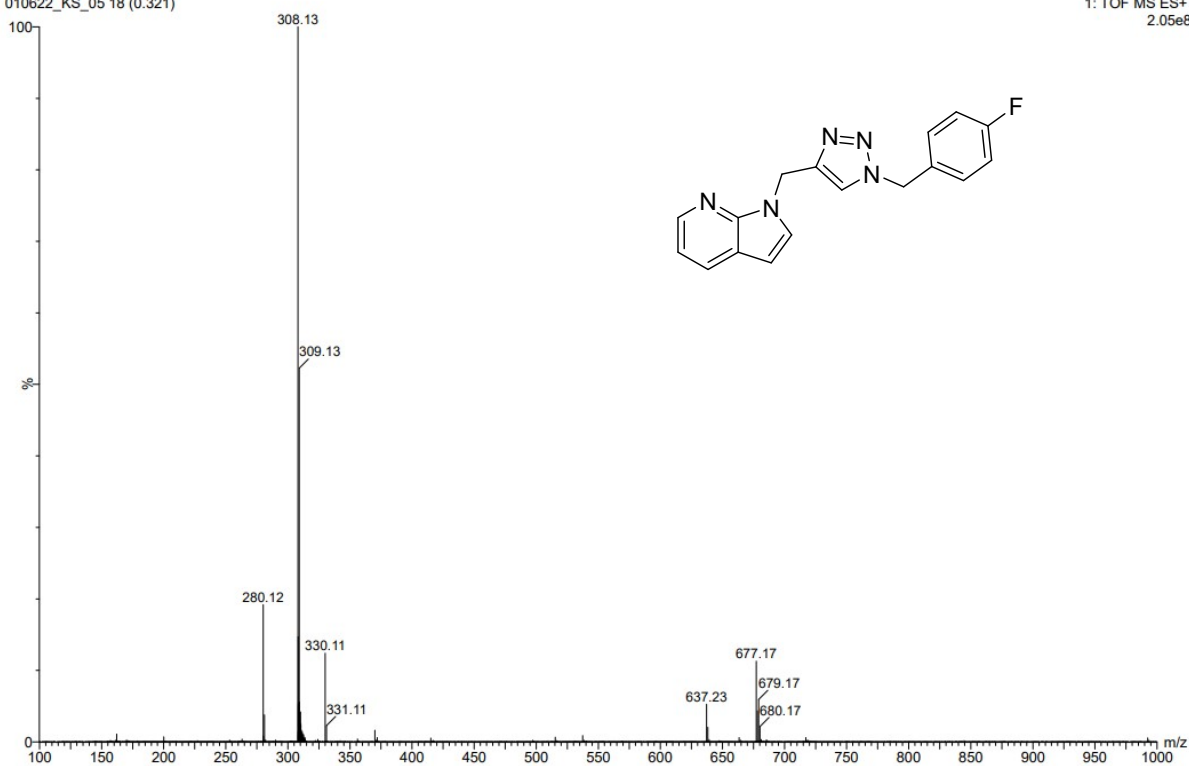
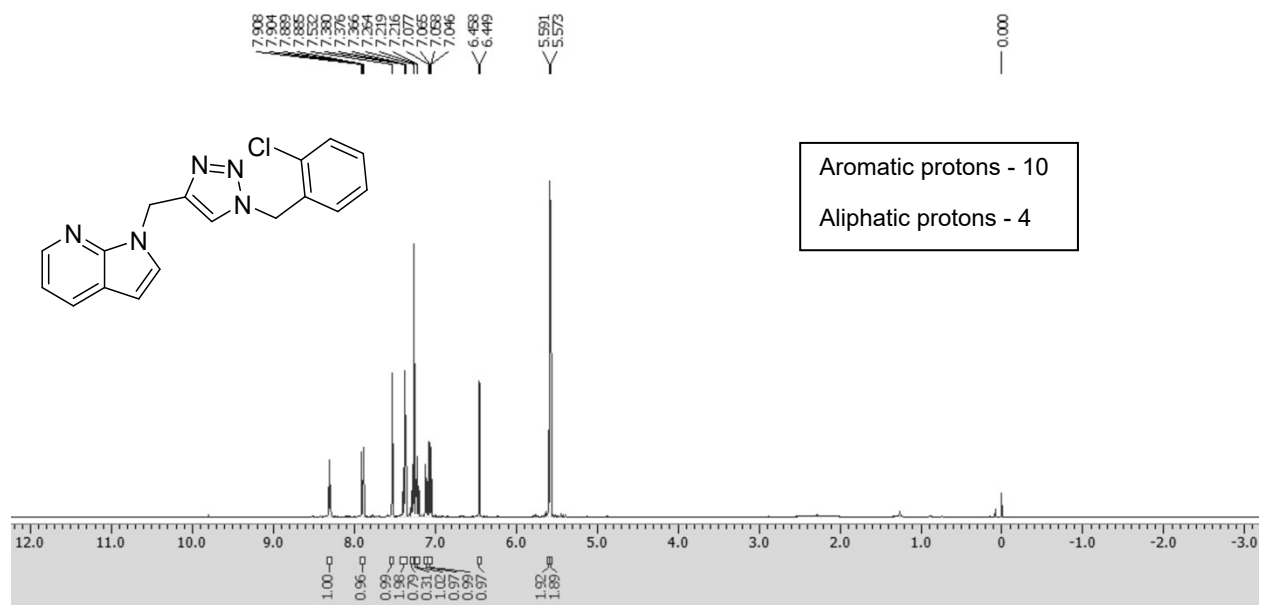
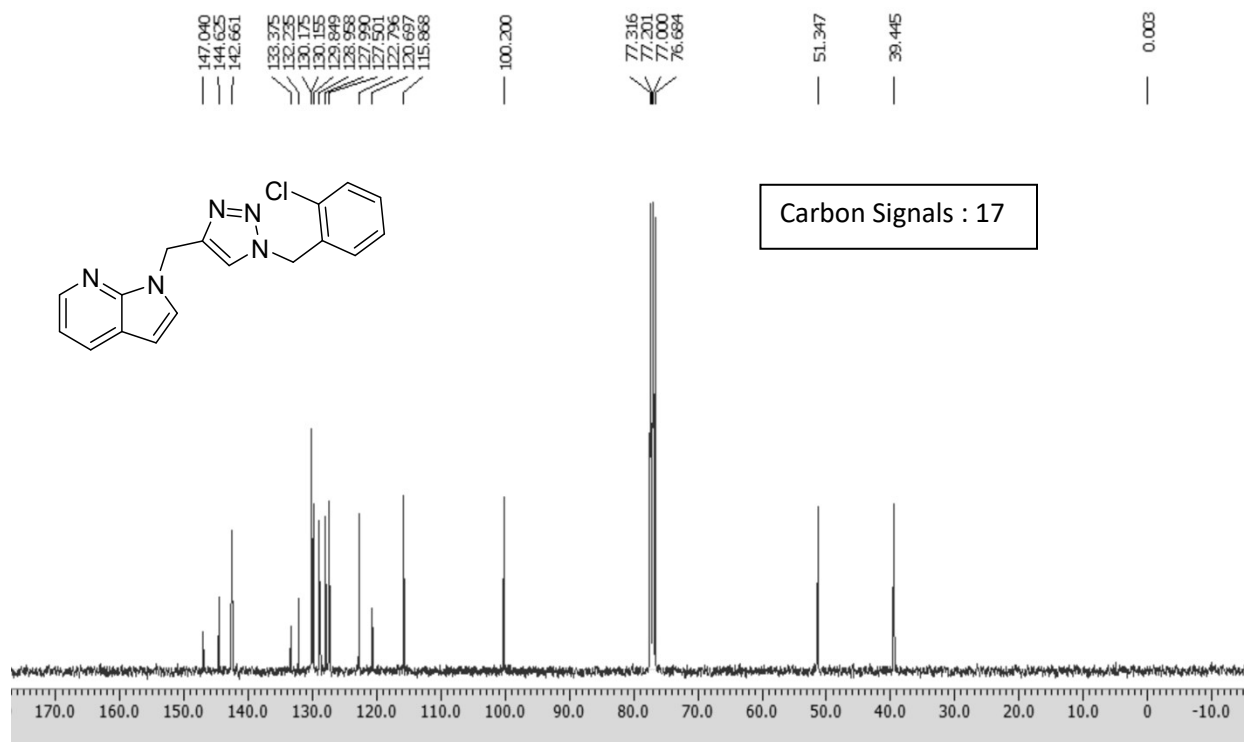


Figure SI-12. ESI-MS $[M+H]^+$: m/z for (4b) $C_{17}H_{14}N_3F$: 308.13

Figure SI-13. $^1\text{H-NMR}$ (4c)Figure SI-14. $^{13}\text{C-NMR}$ (4c)

Sample Name : KS_08
Test Name :
010622_KS_08 22 (0.389)

IITRPR

XEVO G2-XS QTOF

1: TOF MS ES+
2.39e8

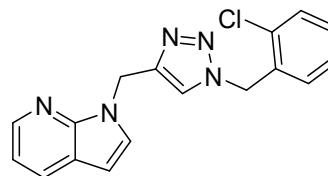
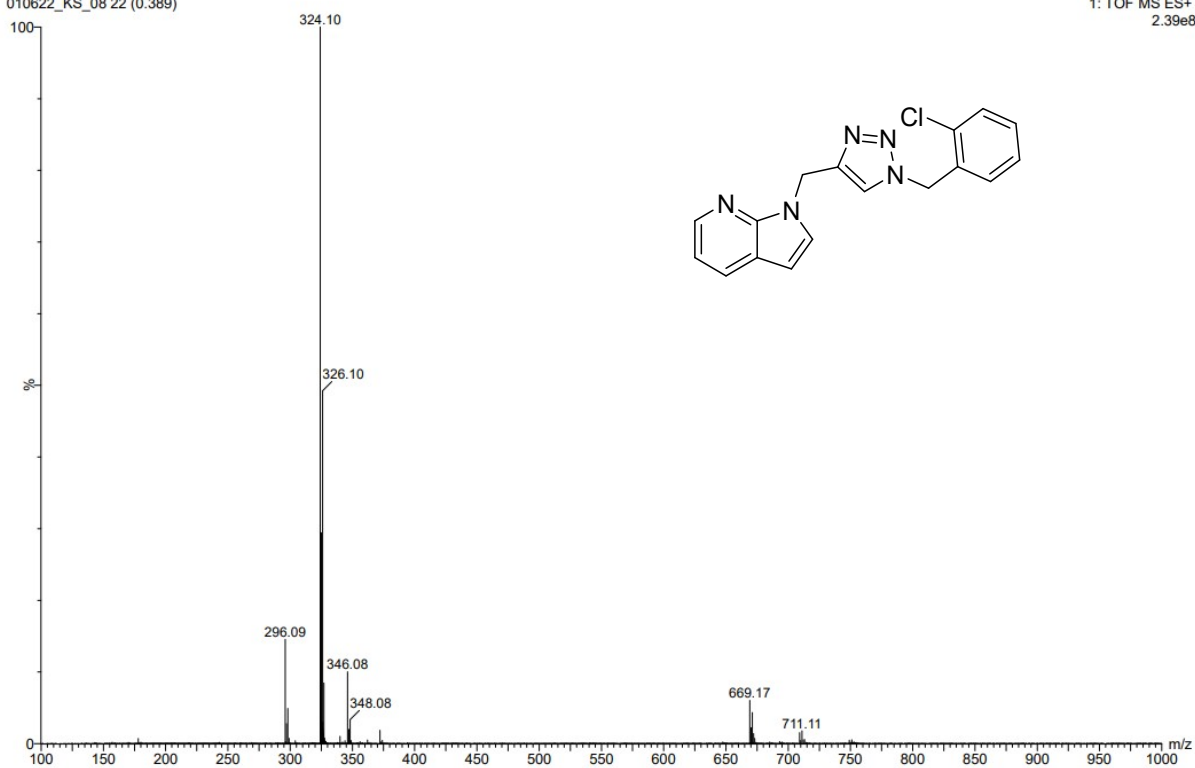


Figure SI-15. ESI-MS $[M+H]^+$: m/z for (**4c**) $C_{17}H_{14}N_5Cl$: 324.10

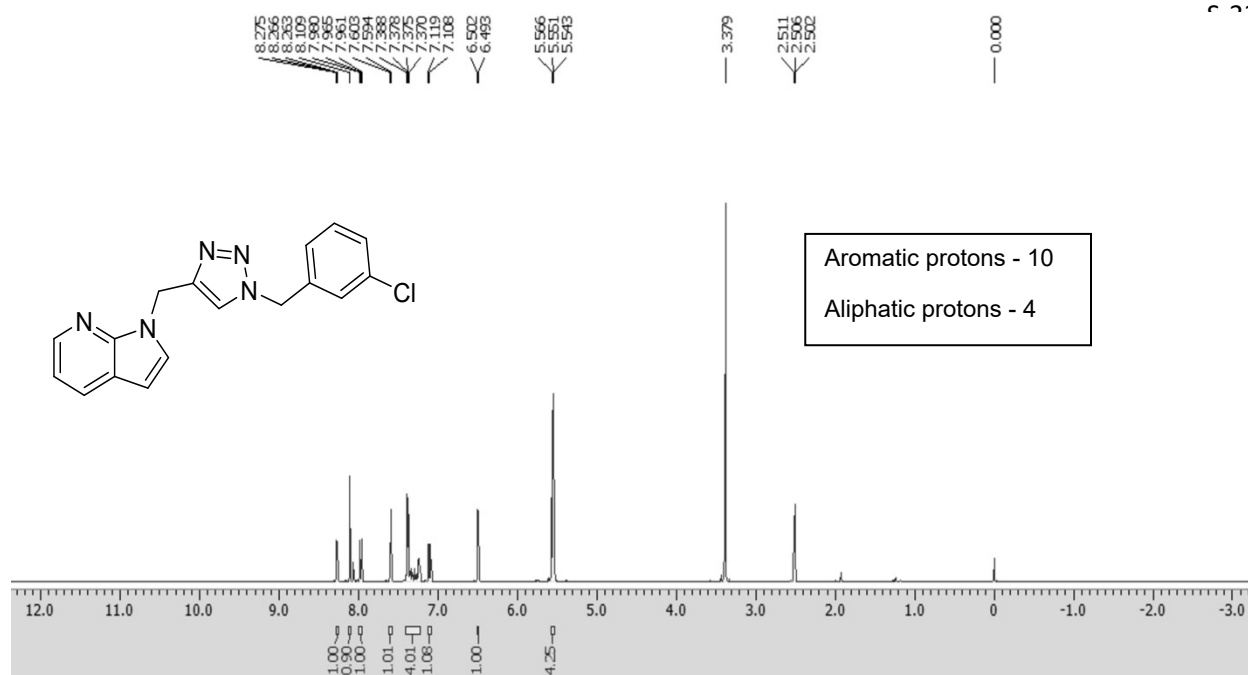


Figure SI-16. ¹H-NMR (4d)

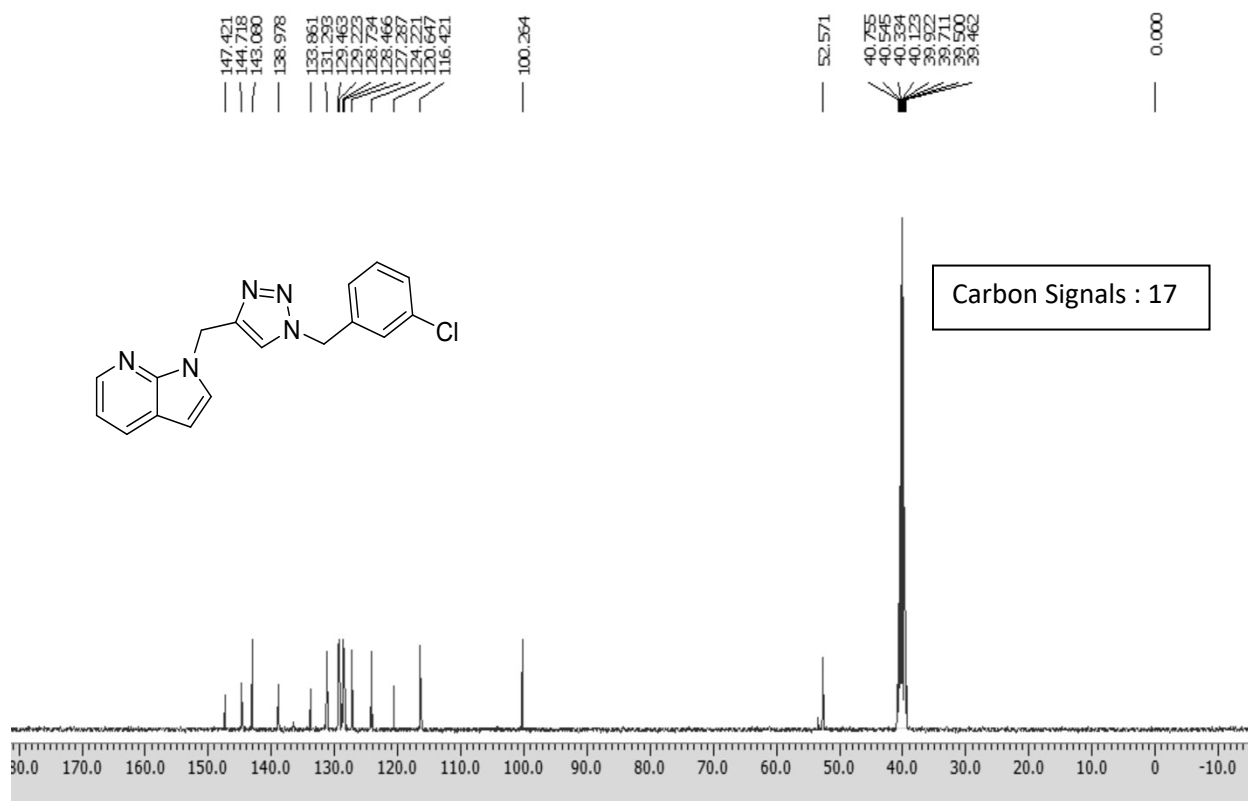


Figure SI-17. ¹³C-NMR (4d)

Sample Name : KS_09
Test Name :
010622_KS_09 28 (0.490)

IITRPR

XEVO G2-XS QTOF

1: TOF MS ES+
1.40e8

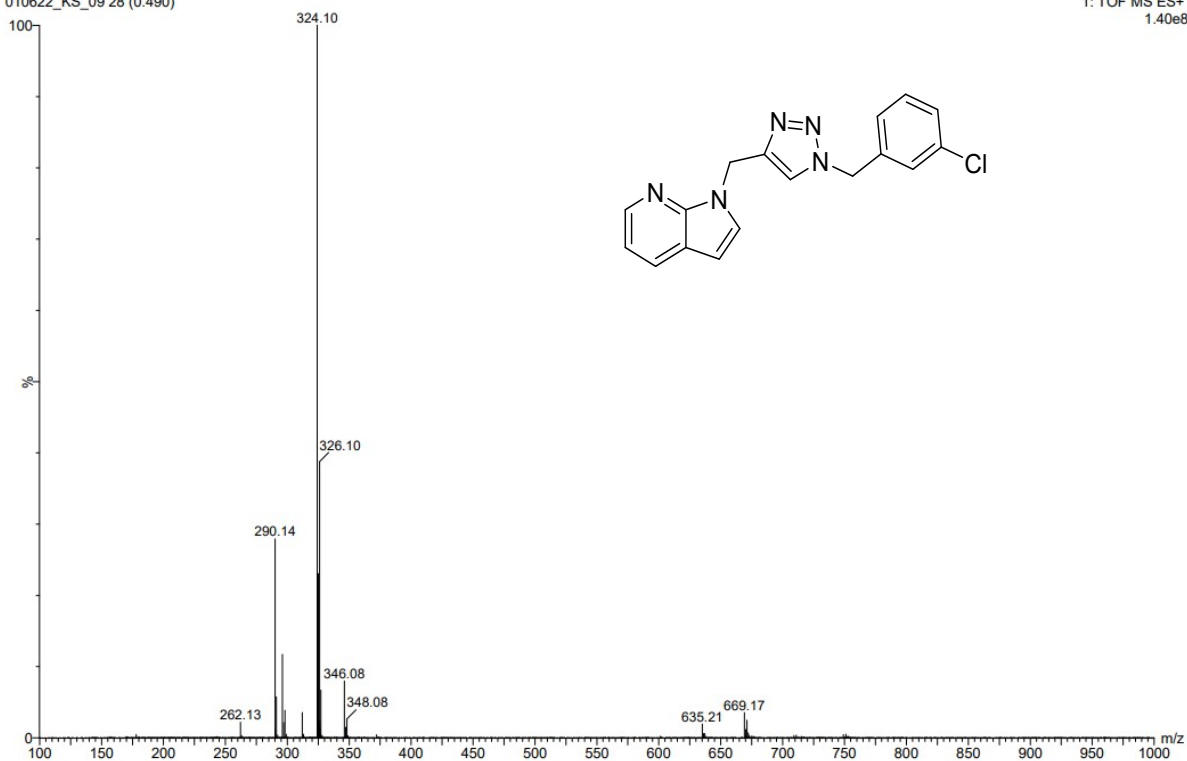
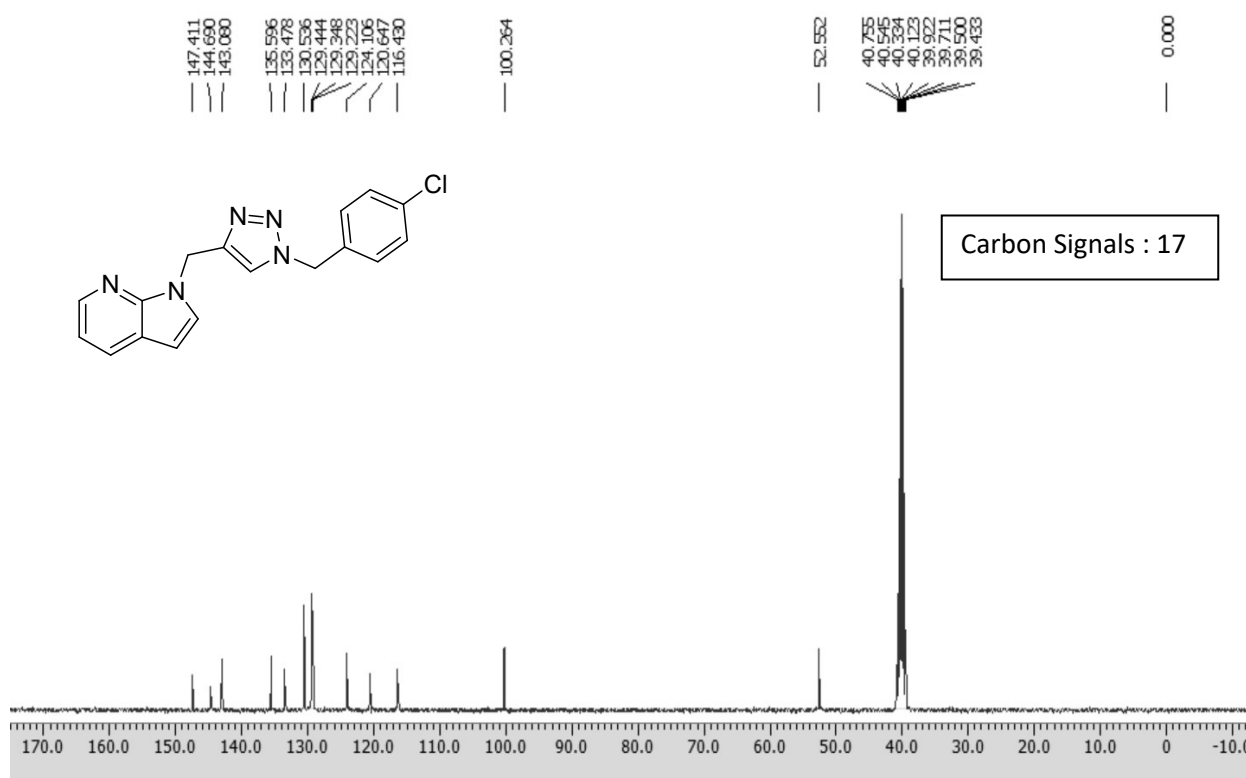
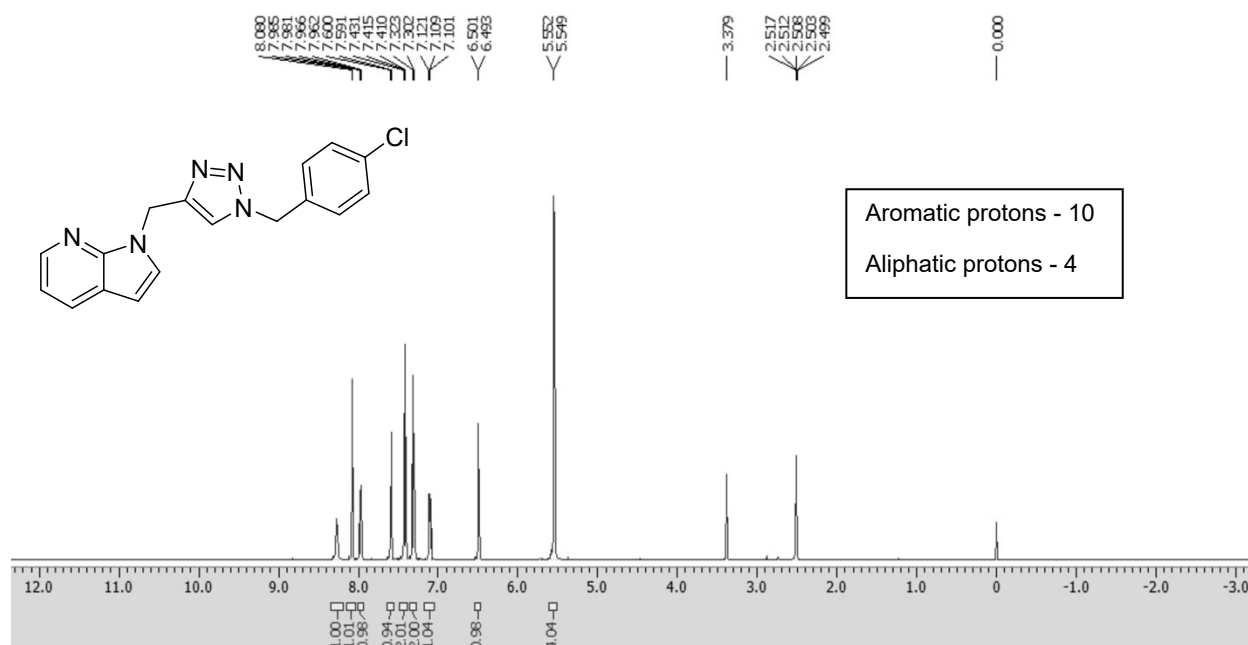


Figure SI-18. ESI-MS $[M+H]^+$: m/z for (**4d**) $C_{17}H_{14}N_5Cl$: 324.10



Sample Name : KS_04
Test Name :
010622_KS_04 20 (0.355)

IITRPR

XEVO G2-XS QTOF

1: TOF MS ES+
1.18e8

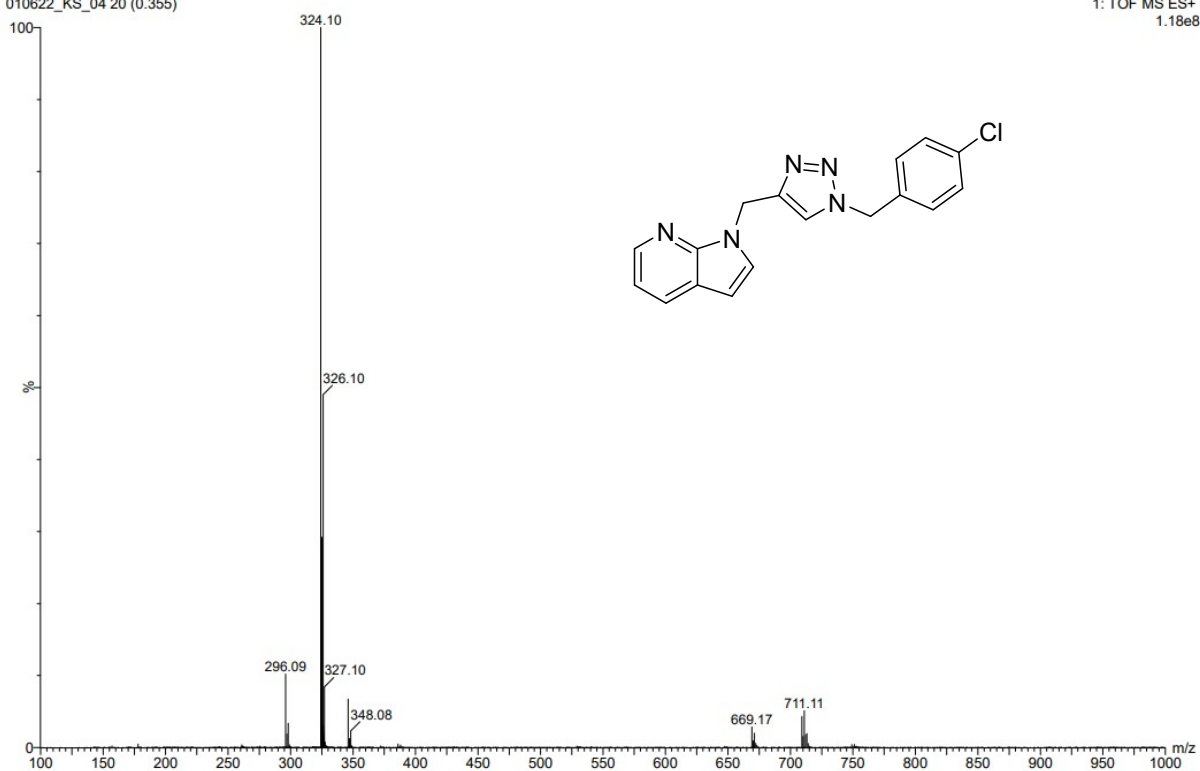
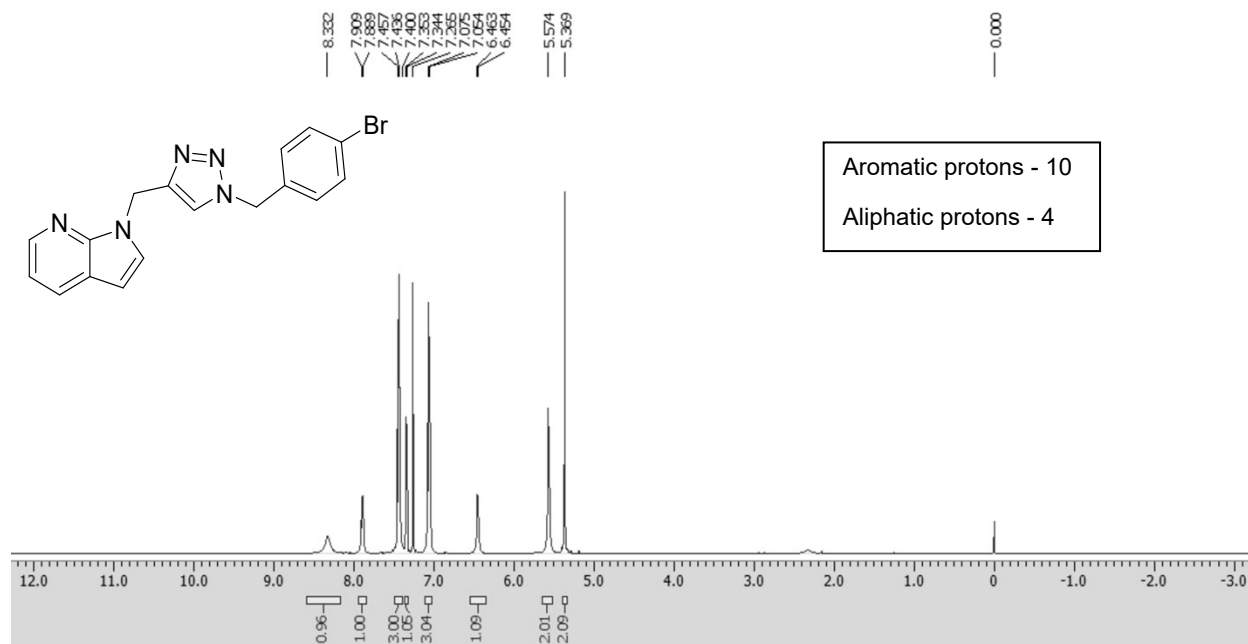
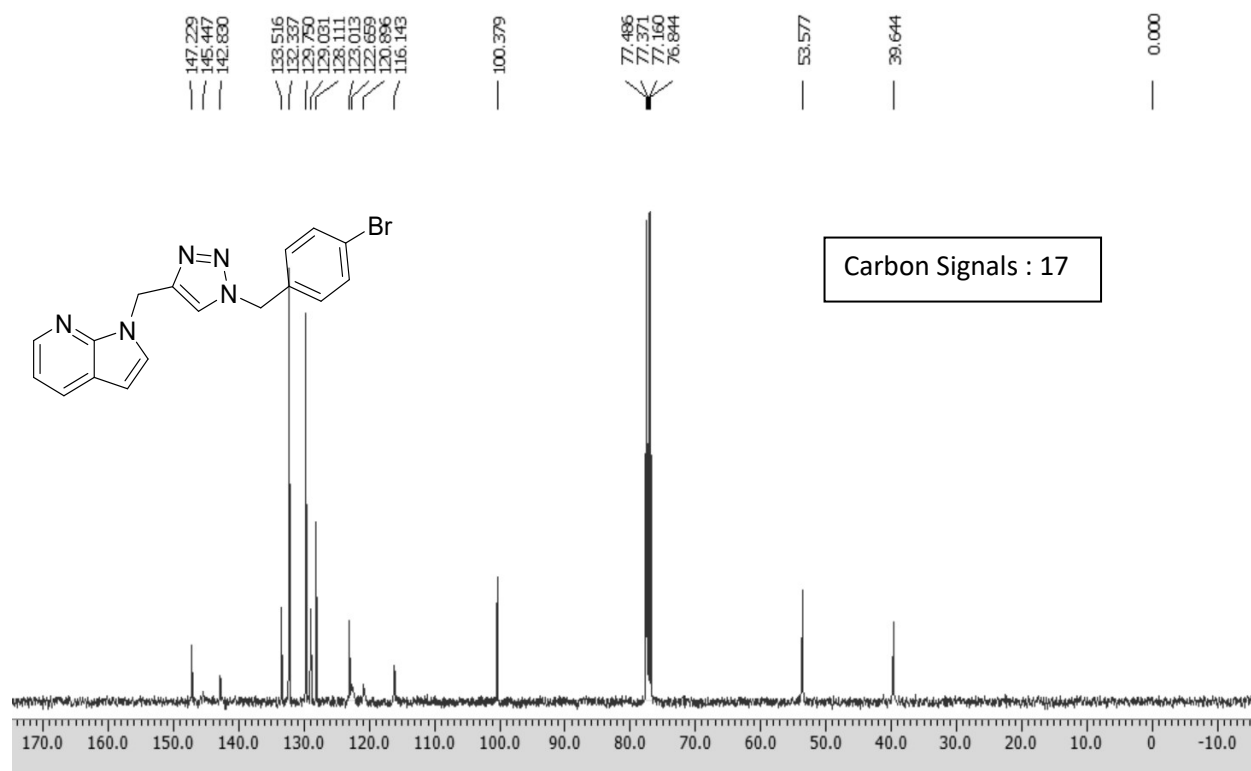


Figure SI-21. ESI-MS $[M+H]^+$: m/z for (4e) $C_{17}H_{14}N_5Cl$: 324.10

Figure SI-22. ¹H-NMR (4f)Figure SI-23. ¹³C-NMR (4f)

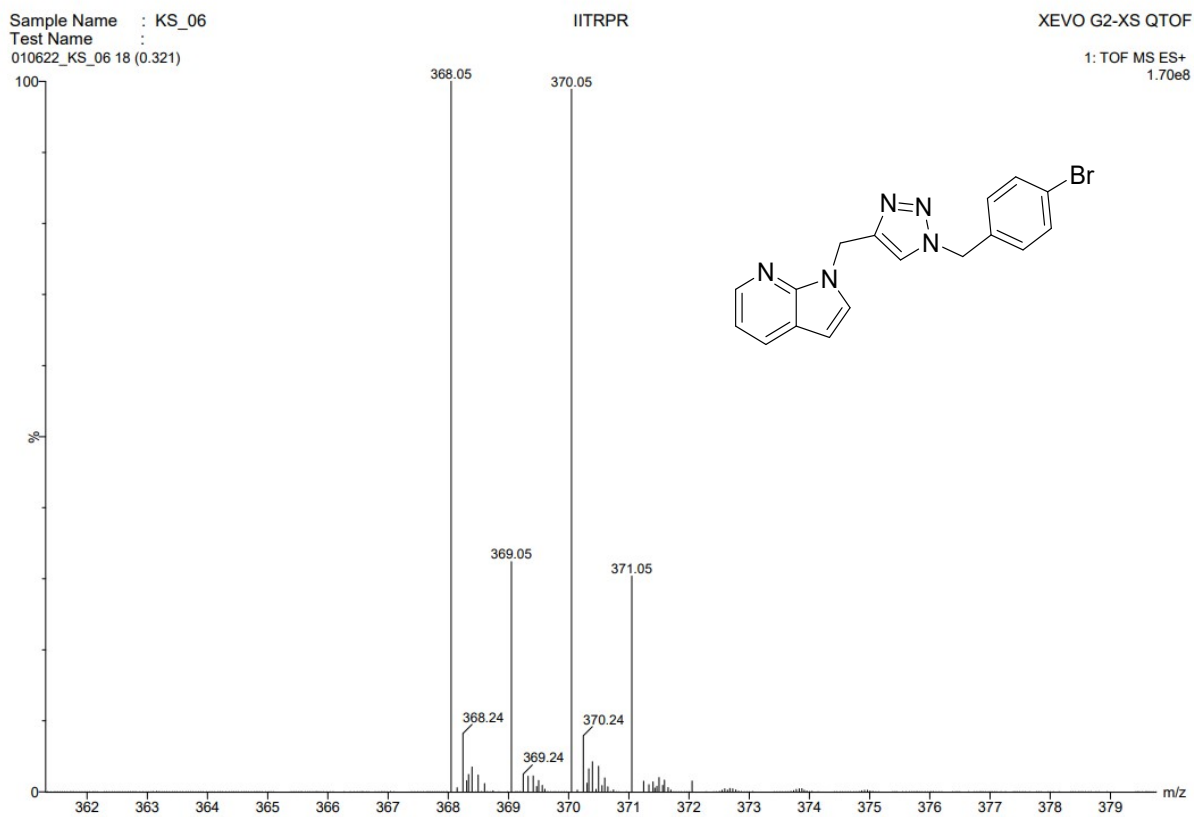


Figure SI-24. ESI-MS $[M+H]^+$: m/z for (**4f**) $C_{17}H_{14}N_5Br$: 368.05

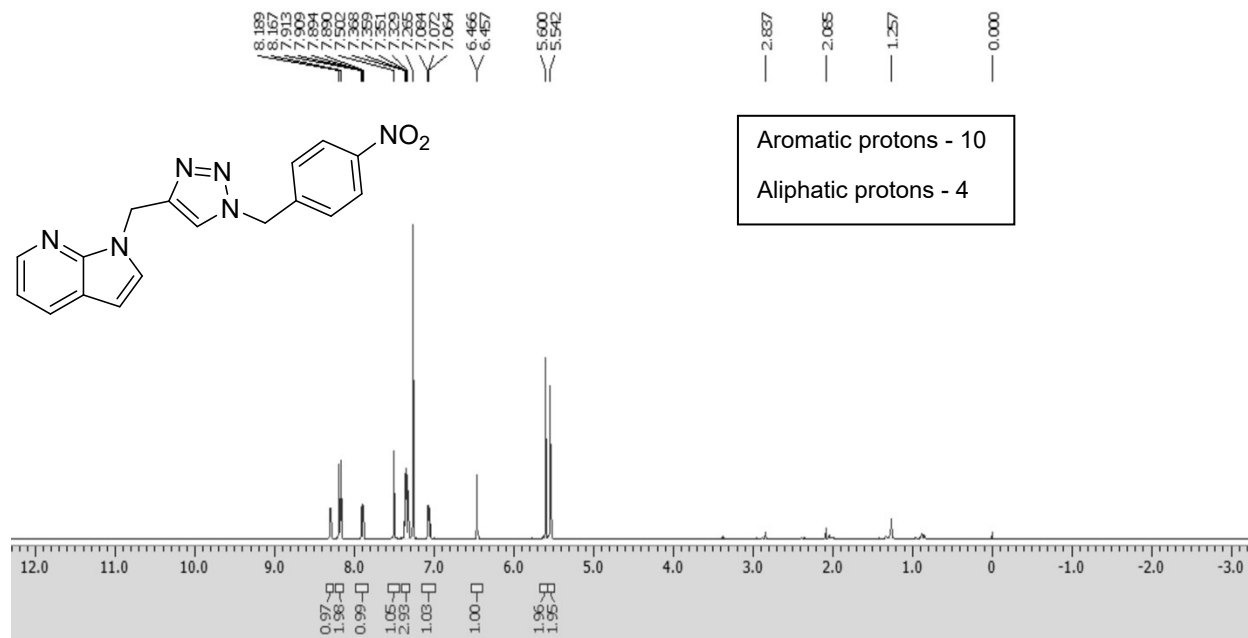


Figure SI-25. ¹H-NMR (4g)

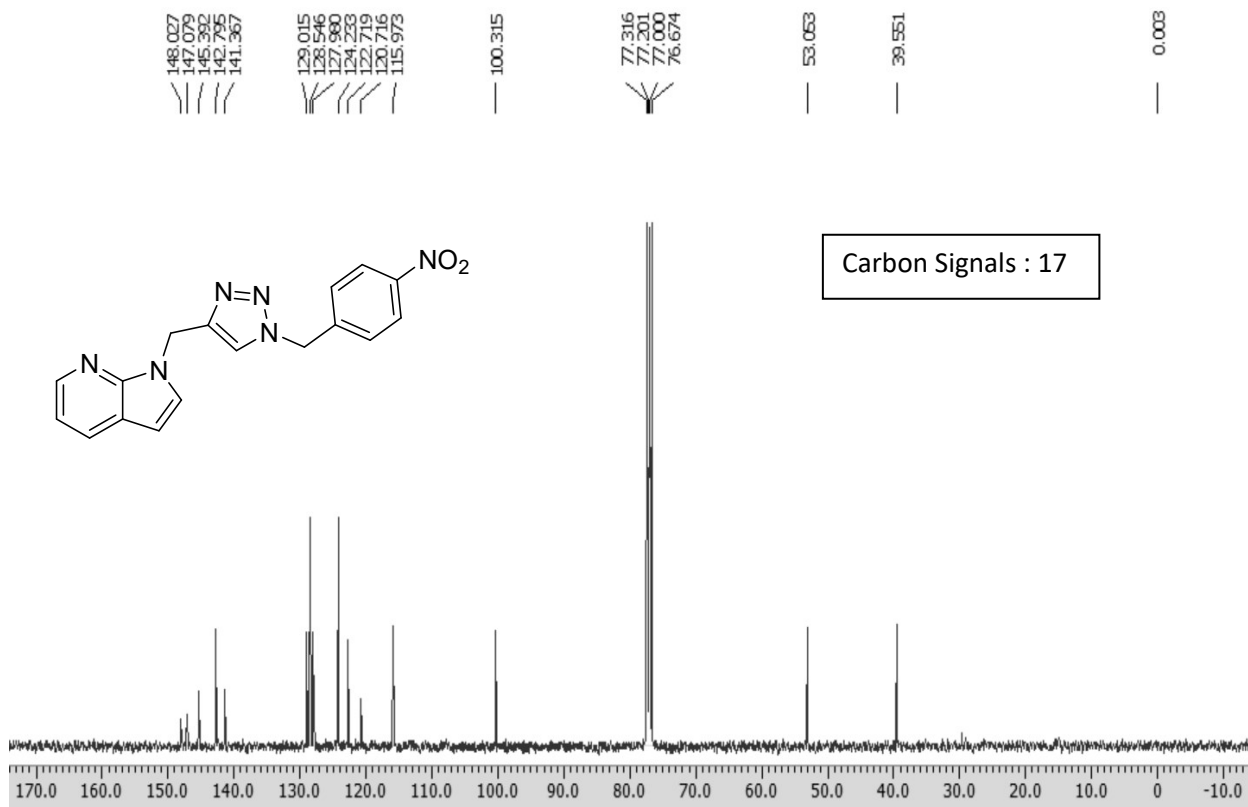


Figure SI-26. ¹³C-NMR (4g)

Sample Name : KS_03
Test Name :
010622_KS_03 15 (0.270)

IITRPR

XEVO G2-XS QTOF

1: TOF MS ES+
3.36e7

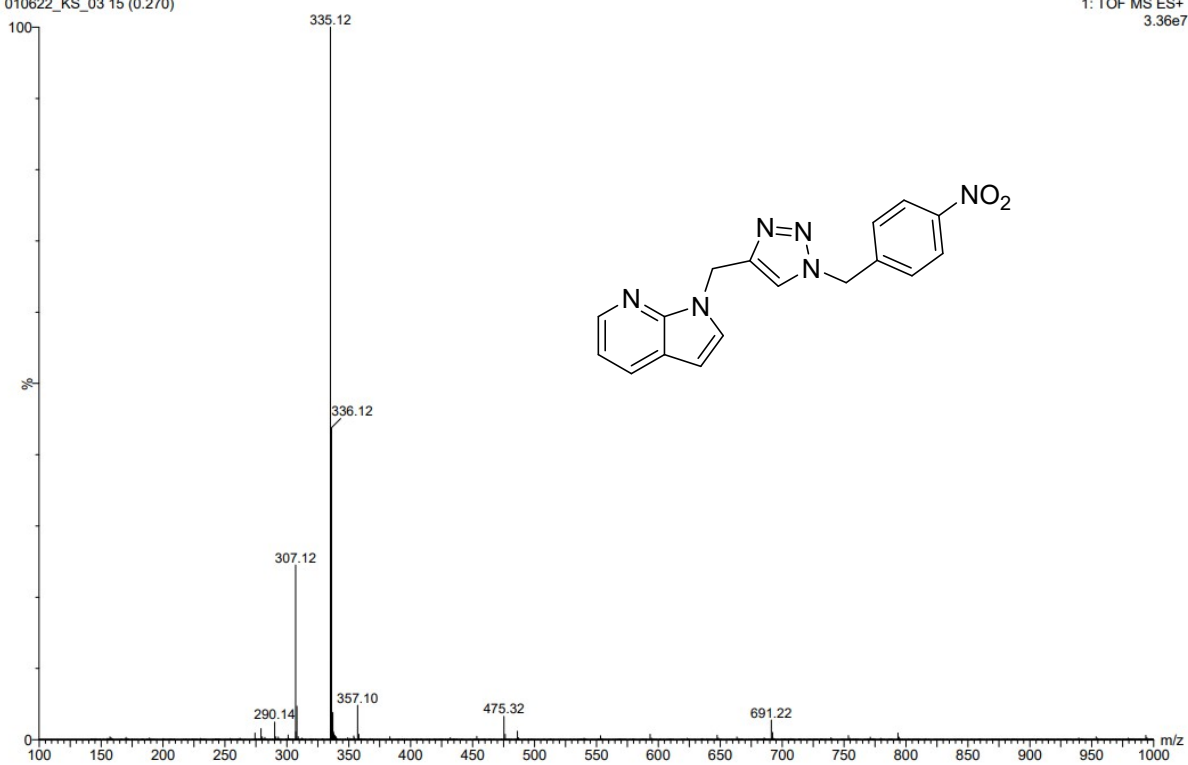


Figure SI-27. ESI-MS $[M+H]^+$: m/z for (**4g**) $C_{17}H_{14}N_6O_2$: 335.12

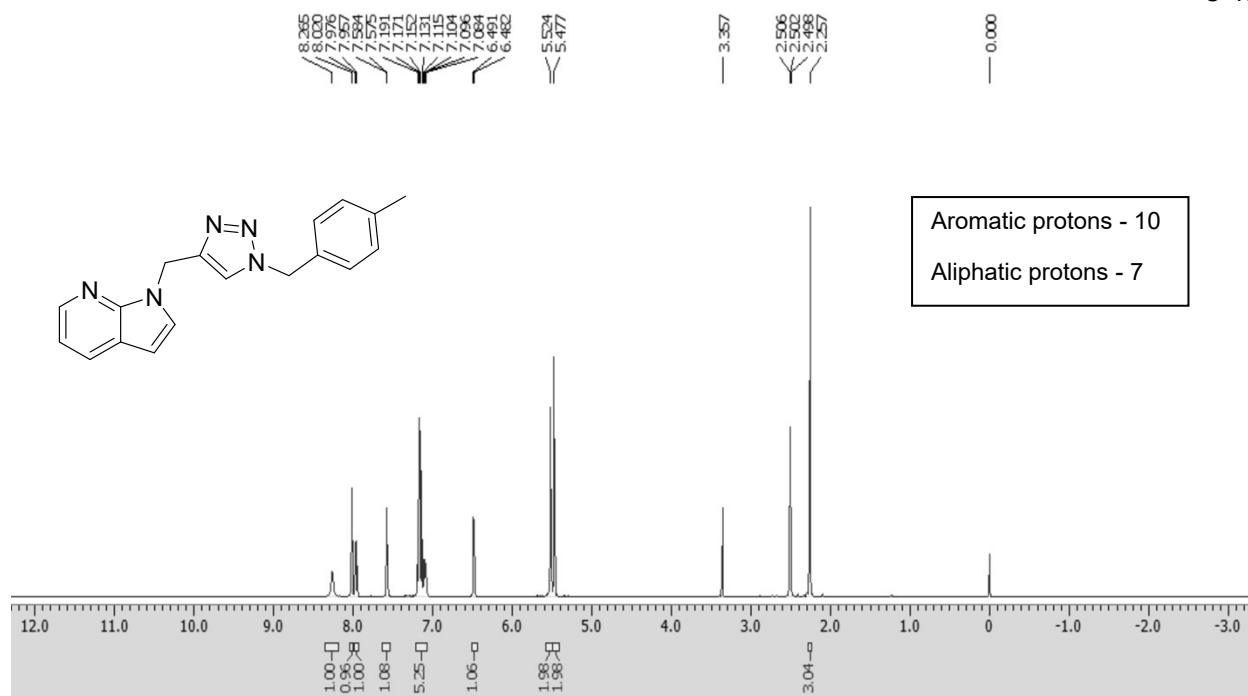


Figure SI-28. ¹H-NMR (4h)

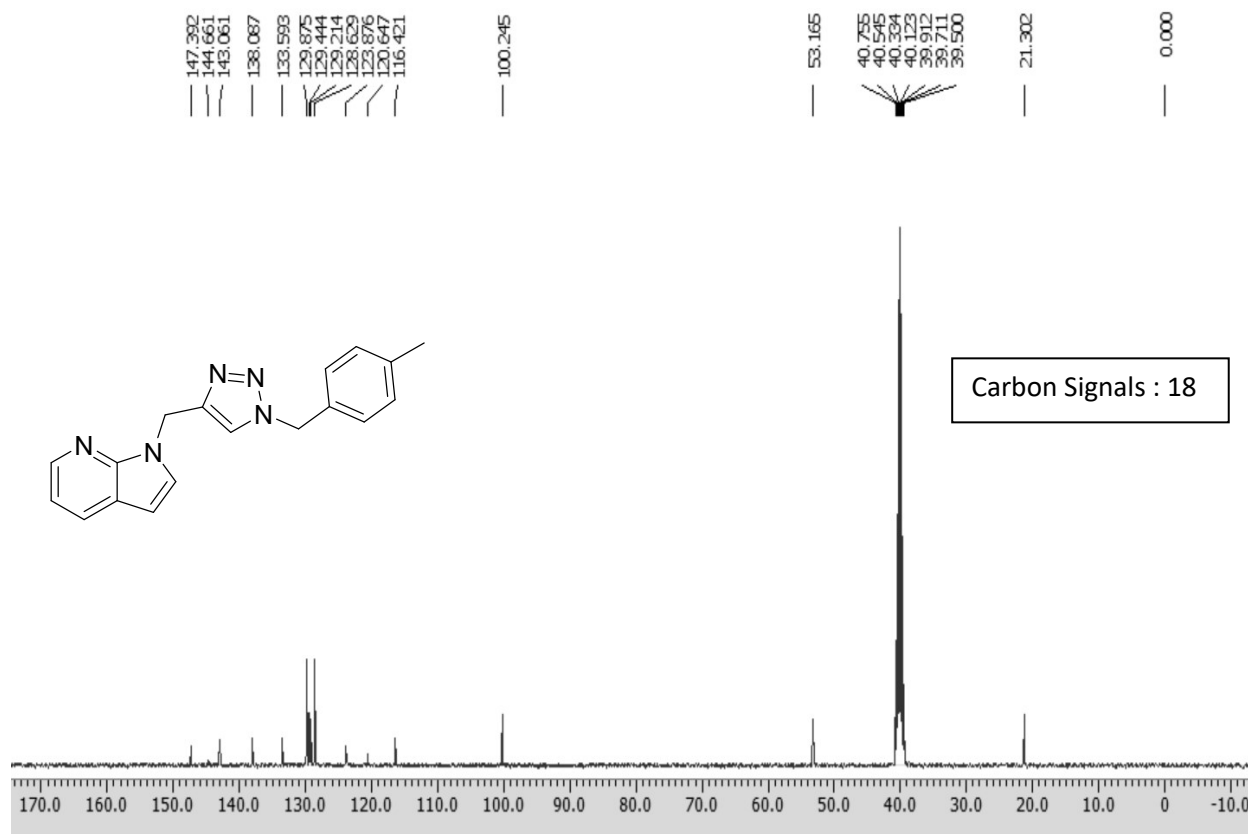


Figure SI-29. ¹³C-NMR (4h)

Sample Name : KS_07
Test Name :
010622_KS_07 27 (0.473)

IITRPR

XEVO G2-XS QTOF

1: TOF MS ES+
1.37e8

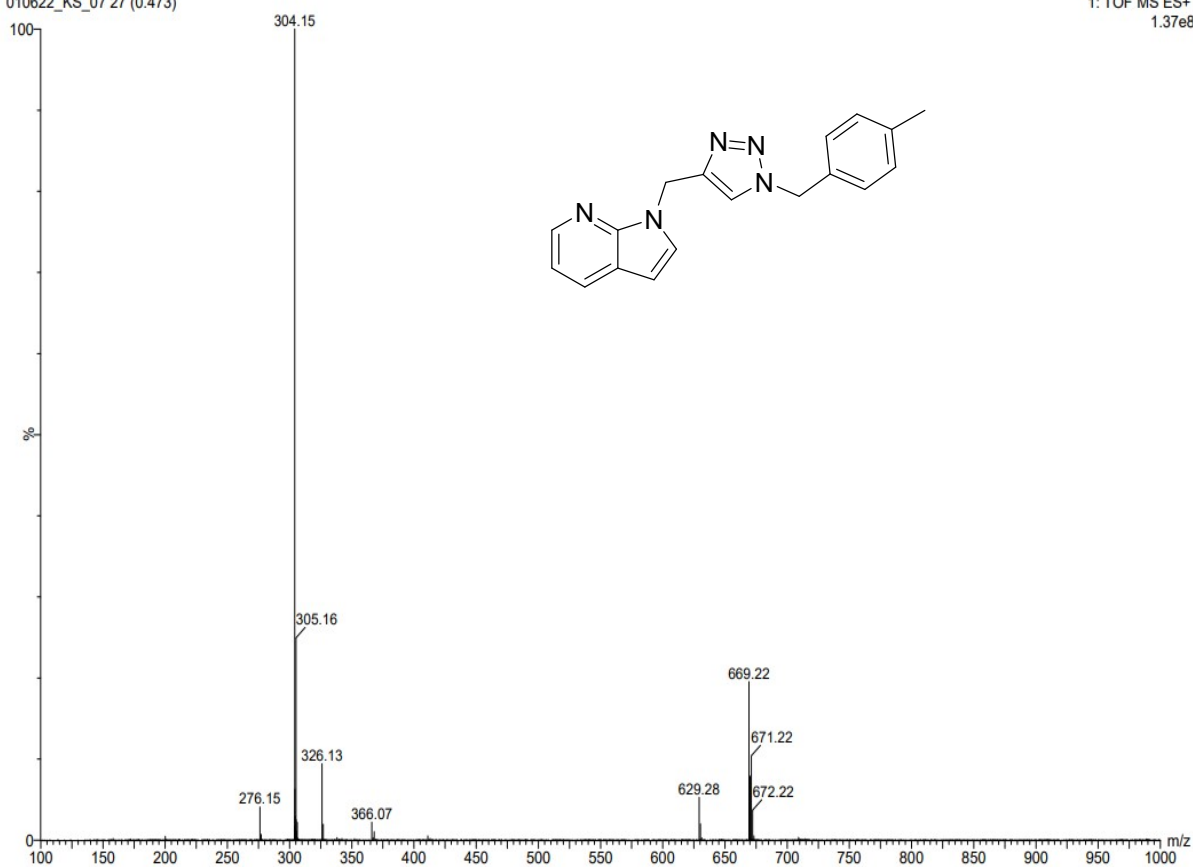
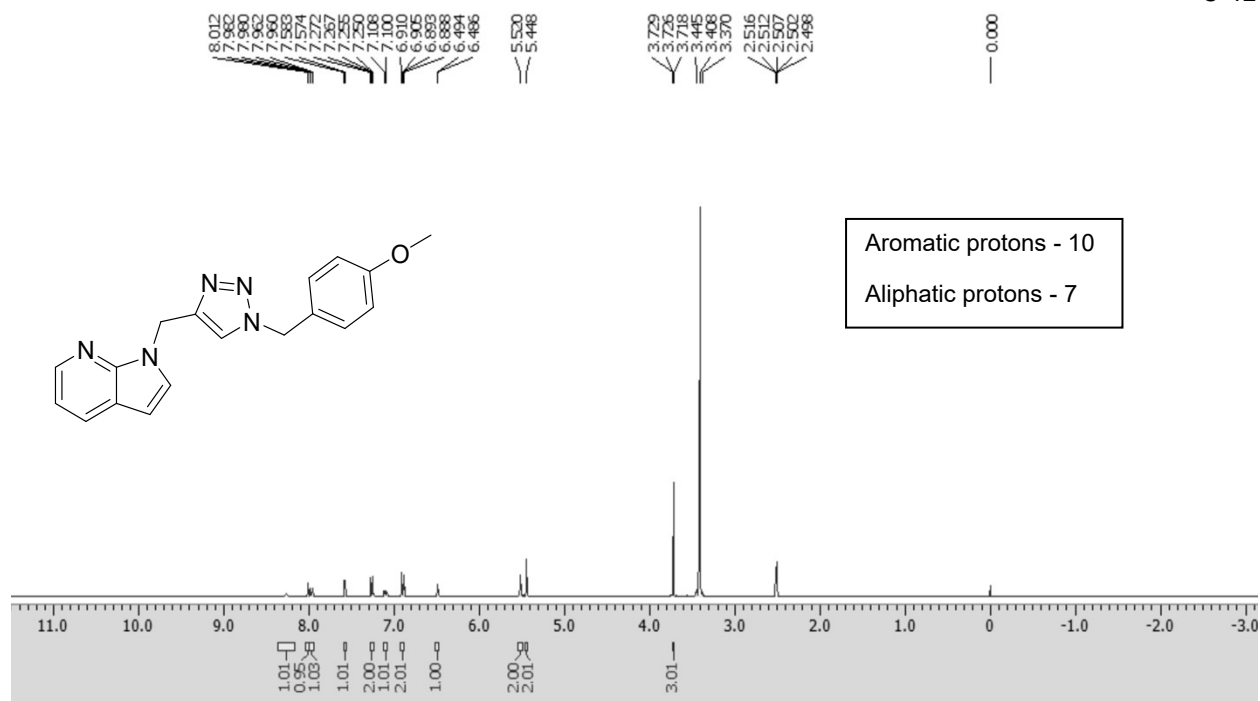
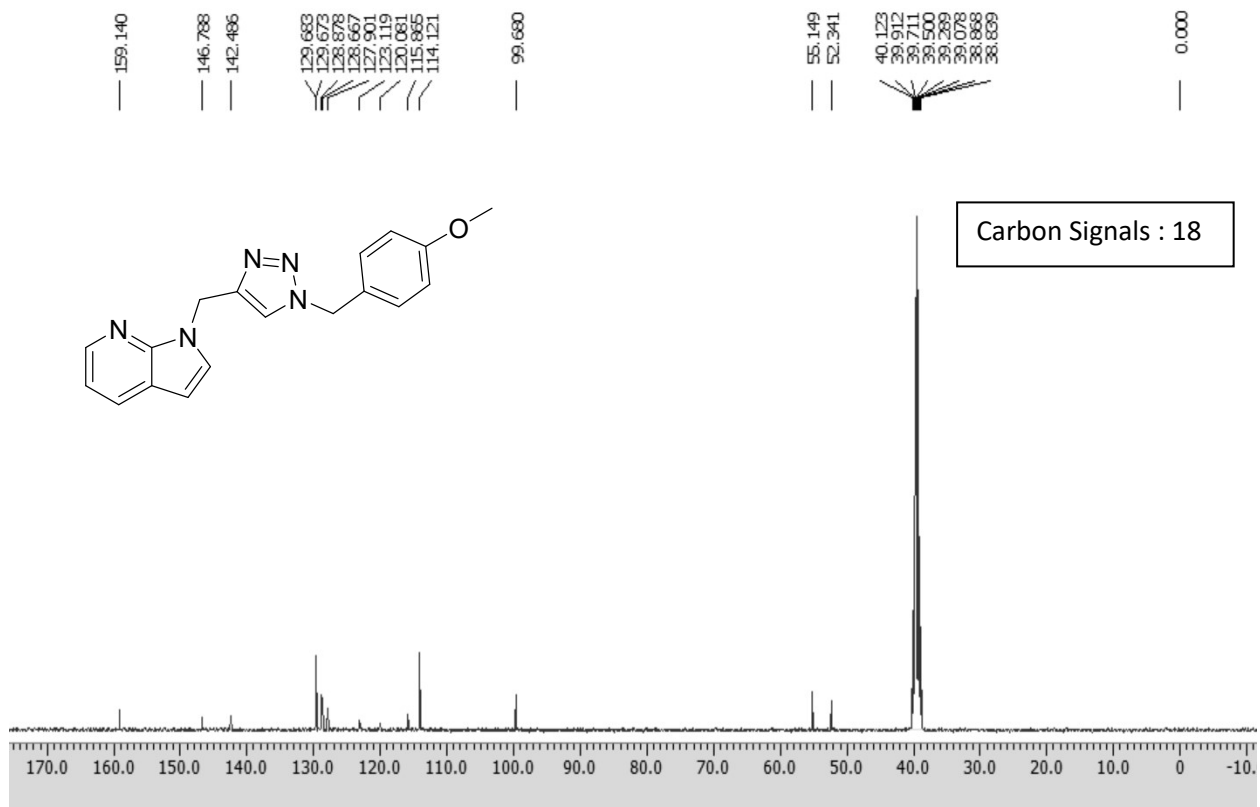


Figure SI-30. ESI-MS $[M+H]^+$: m/z for (4h) $C_{18}H_{17}N_5$: 304.15

Figure SI-31. ¹H-NMR (4i)Figure SI-32. ¹³C-NMR (4i)

Sample Name : KS_10
Test Name :
010622_KS_10 22 (0.389)

IITRPR

XEVO G2-XS QTOF

1: TOF MS ES+
1.58e8

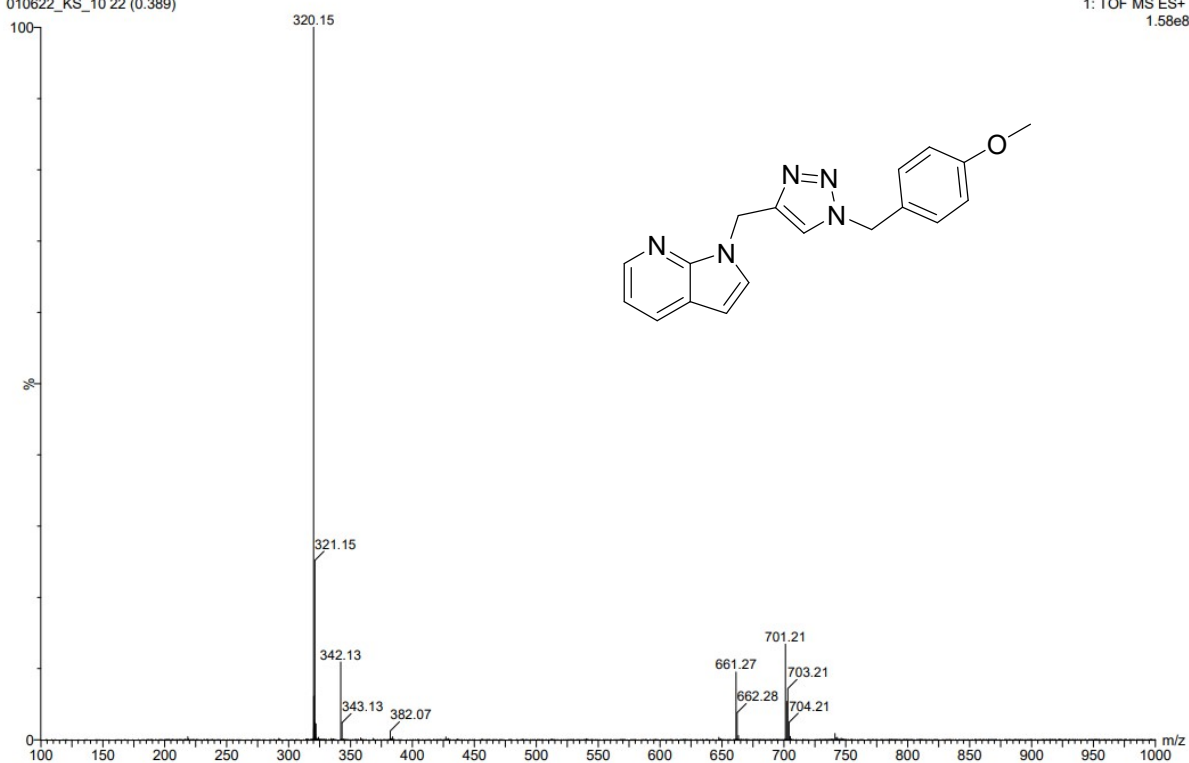


Figure SI-33. ESI-MS $[M+H]^+$: m/z for (4i) $C_{18}H_{17}N_5O$: 320.15

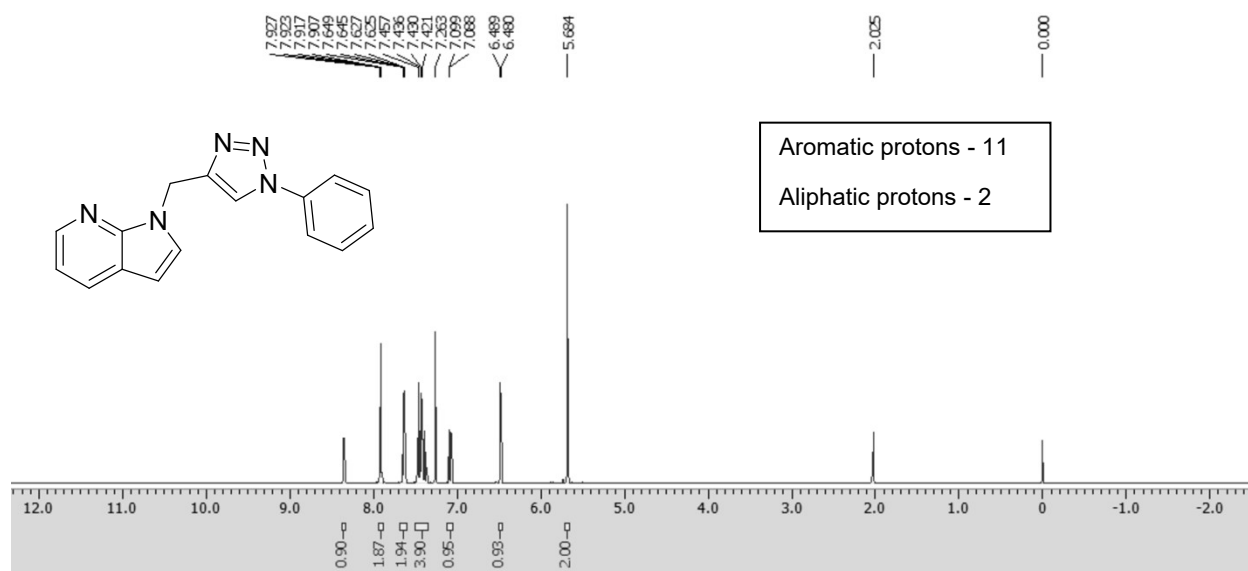


Figure SI-34. ¹H-NMR (4j)

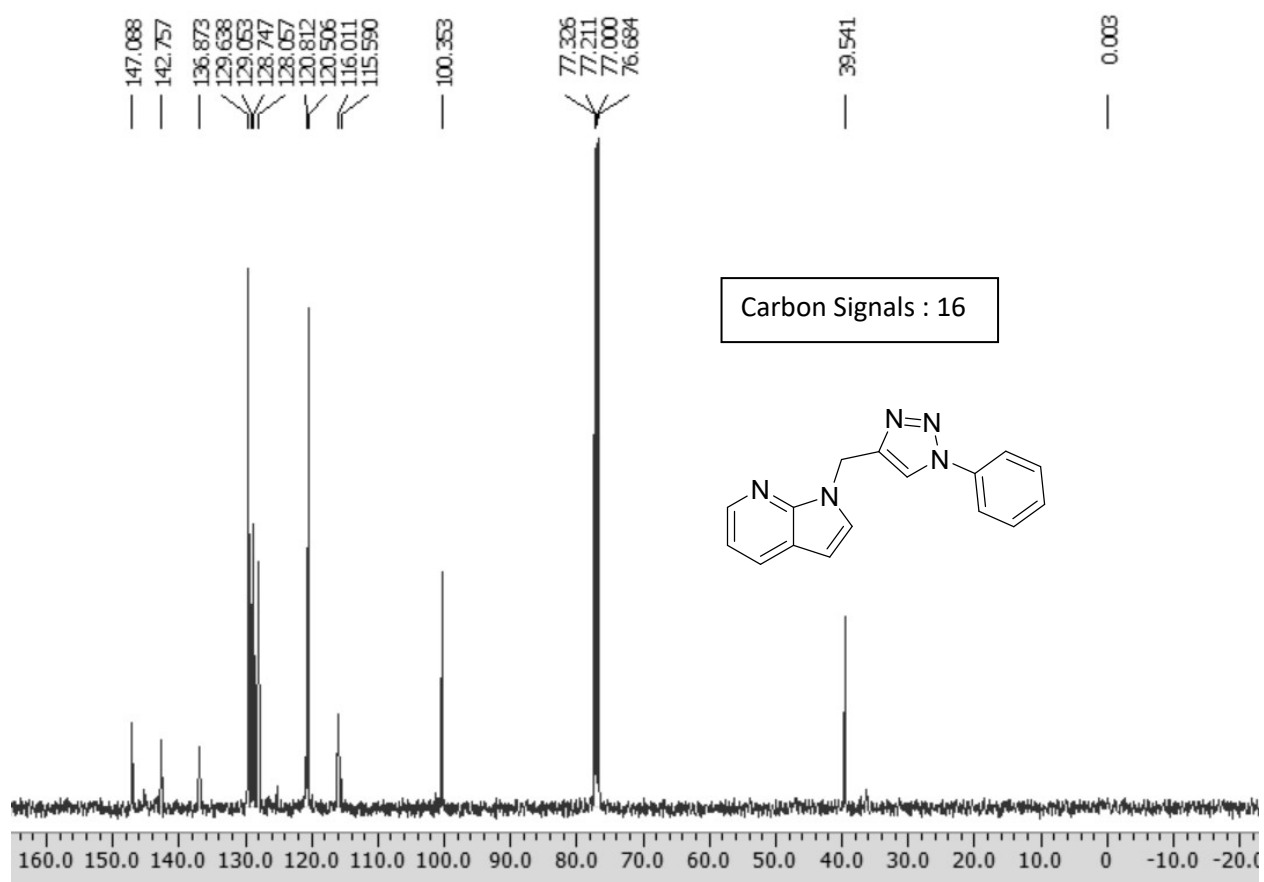


Figure SI-35. ¹³C-NMR (4j)

Sample Name : KS_12
Test Name :
010622_KS_12_14 (0.254)

IITRPR

XEVO G2-XS QTOF

1: TOF MS ES+
5.03e7

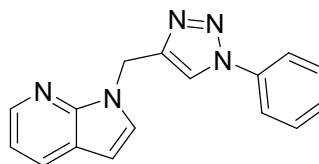
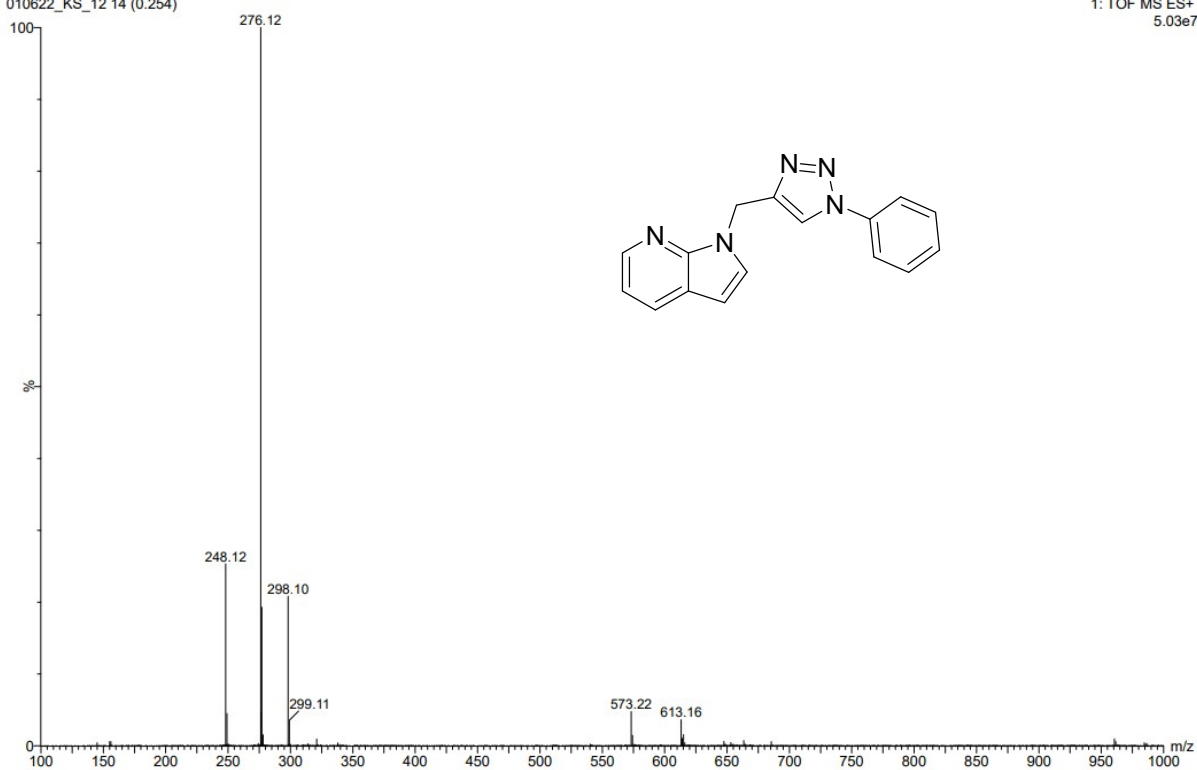
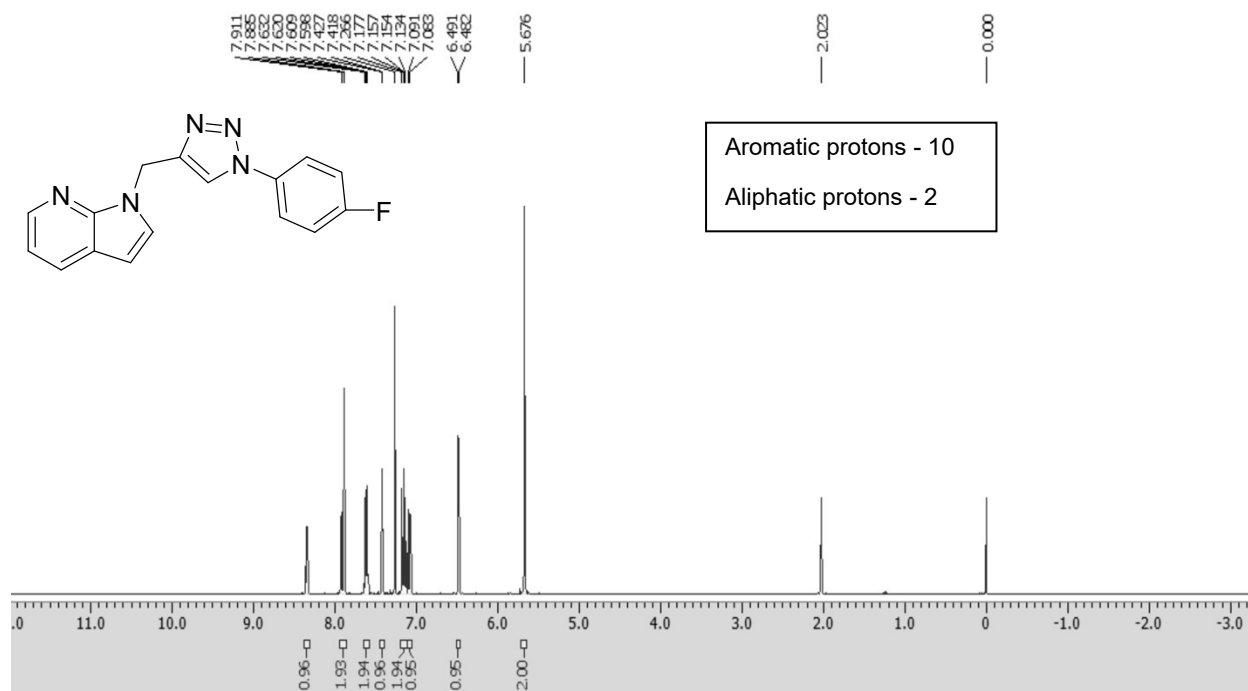
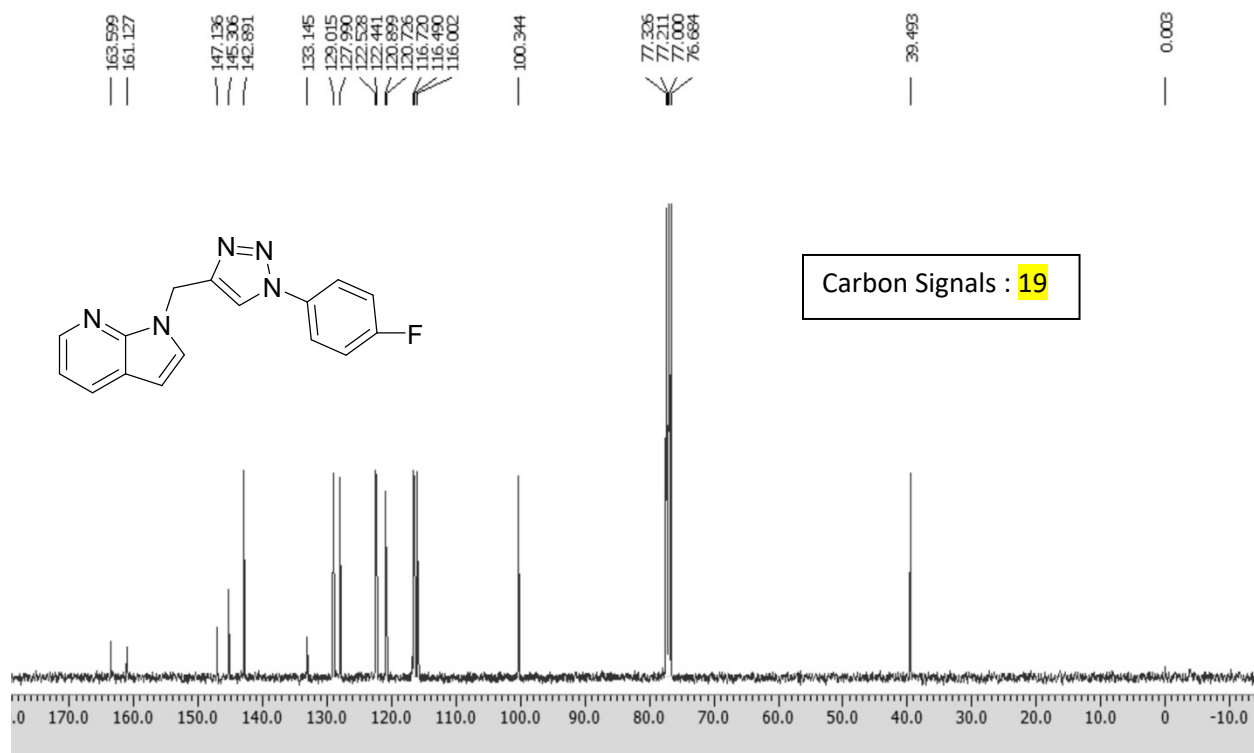


Figure SI-36. ESI-MS $[M+H]^+$: m/z for (4j) $C_{16}H_{13}N_5$: 276.12

Figure SI-37. ¹H-NMR (4k)Figure SI-38. ¹³C-NMR (4k)

Sample Name : KS_18
Test Name :
200722_KS_18 37 (0.643)

IITRPR

XEVO G2-XS QTOF

1: TOF MS ES+
2.50e7

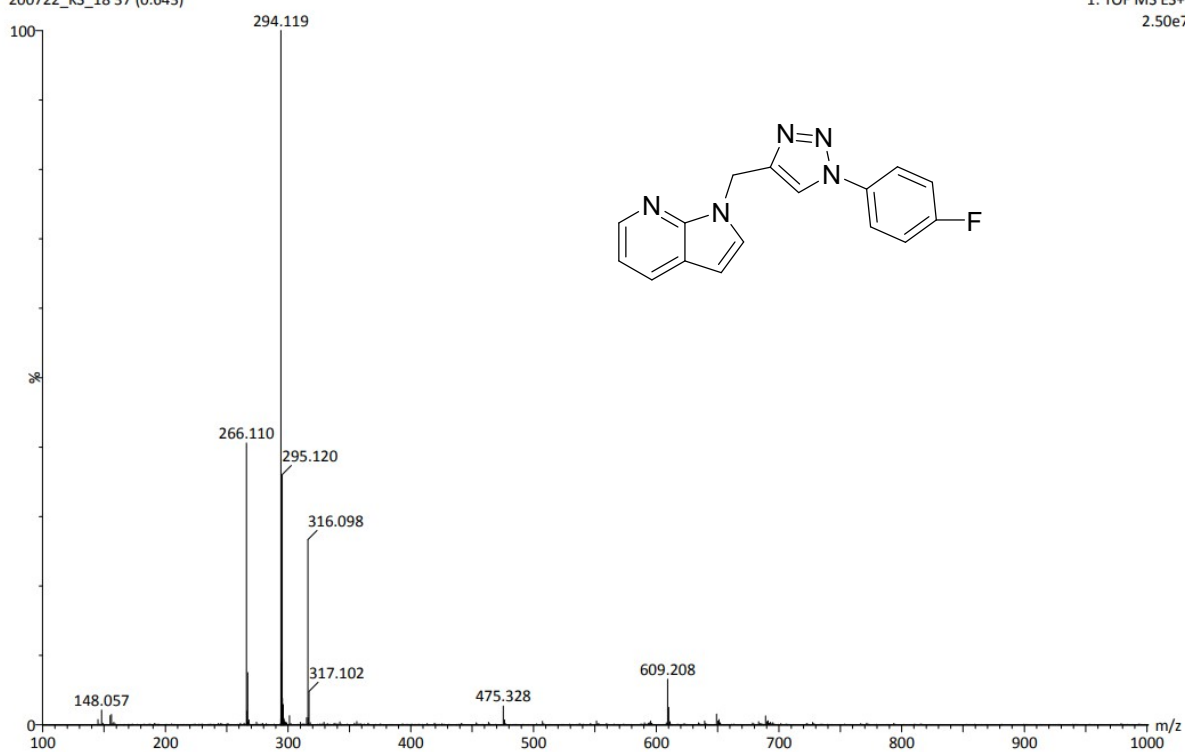
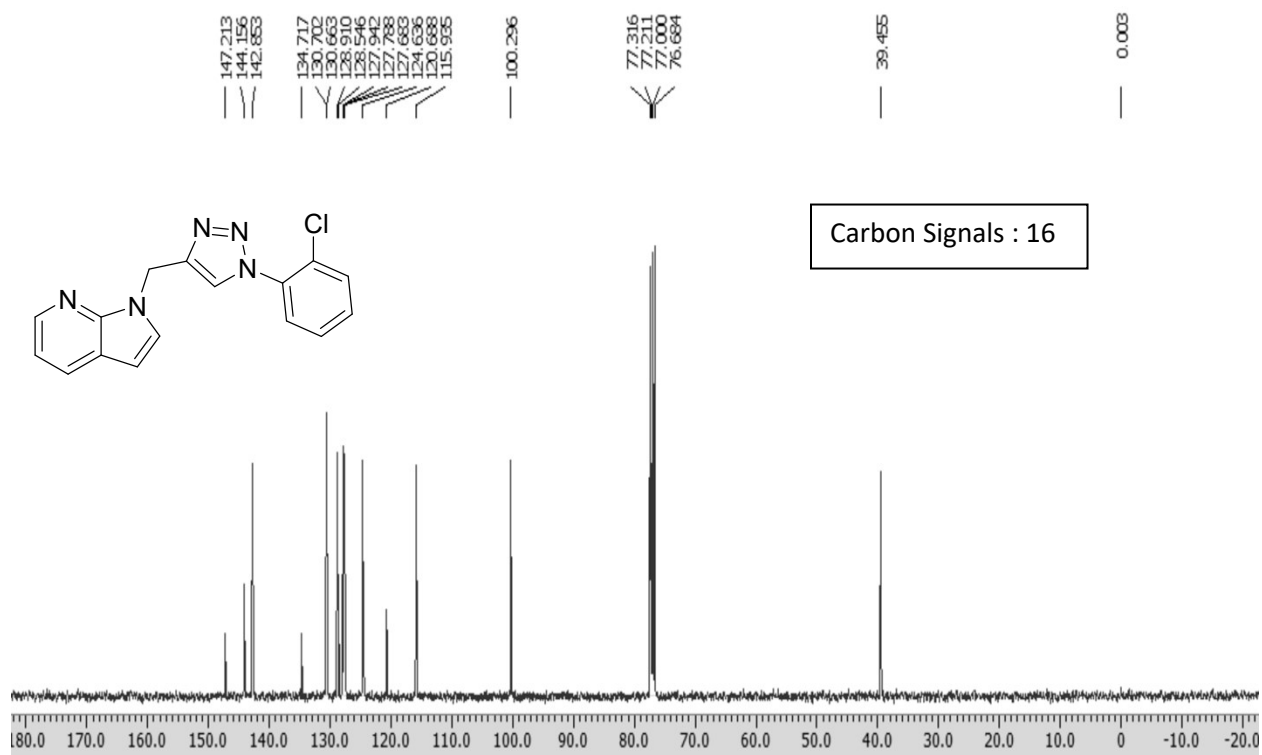
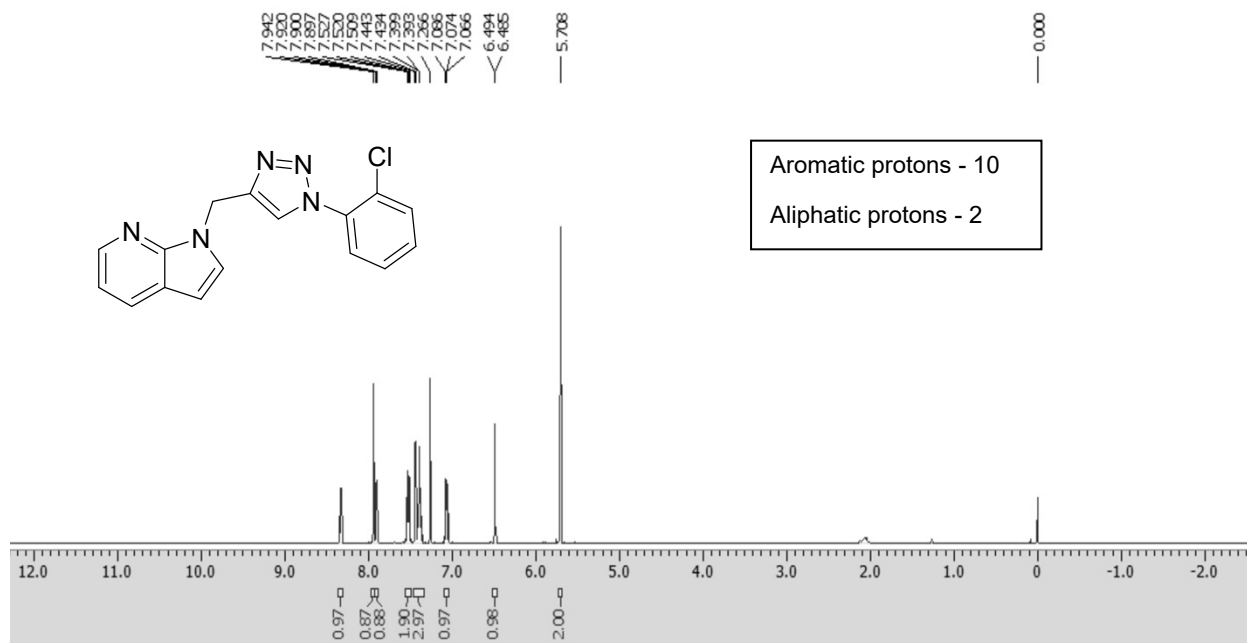


Figure SI-39. ESI-MS $[M+H]^+$: m/z for (4k) $C_{16}H_{12}N_5F$: 294.119



Sample Name : KS_15
Test Name :
200722_KS_15_23 (0.406)

HTRPR

XEVO G2-XS QTOF

1: TOF MS ES+
1.95e7

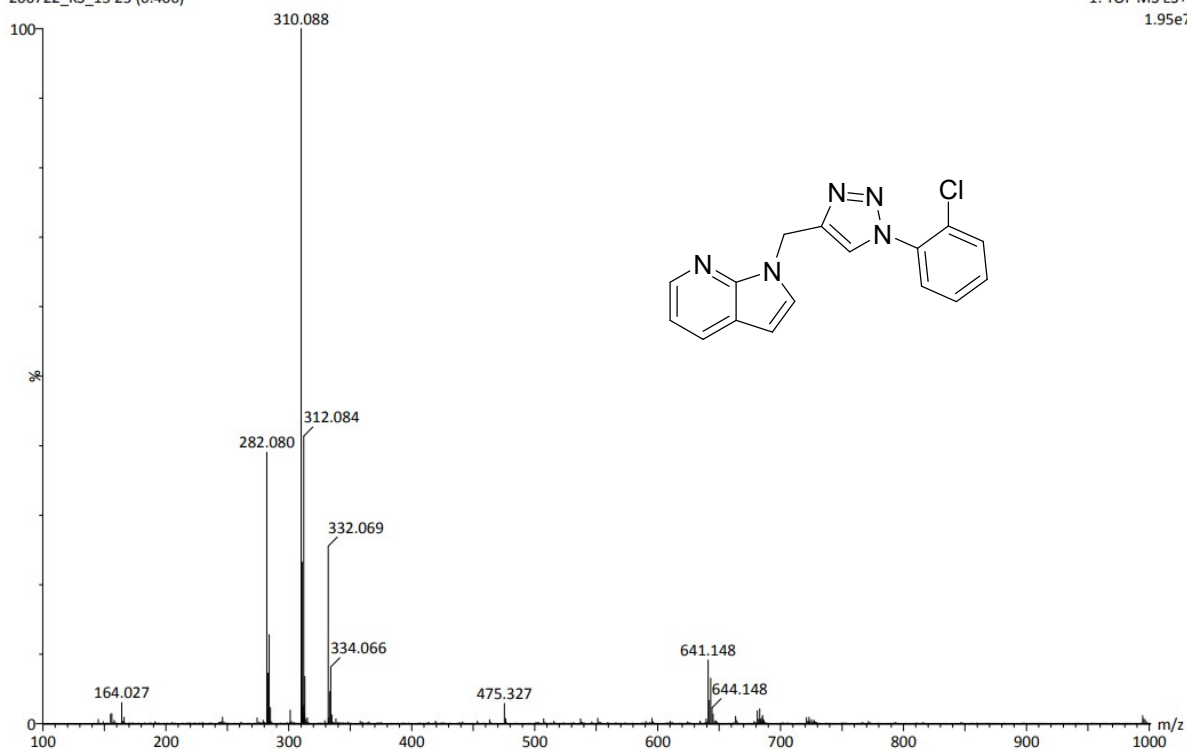
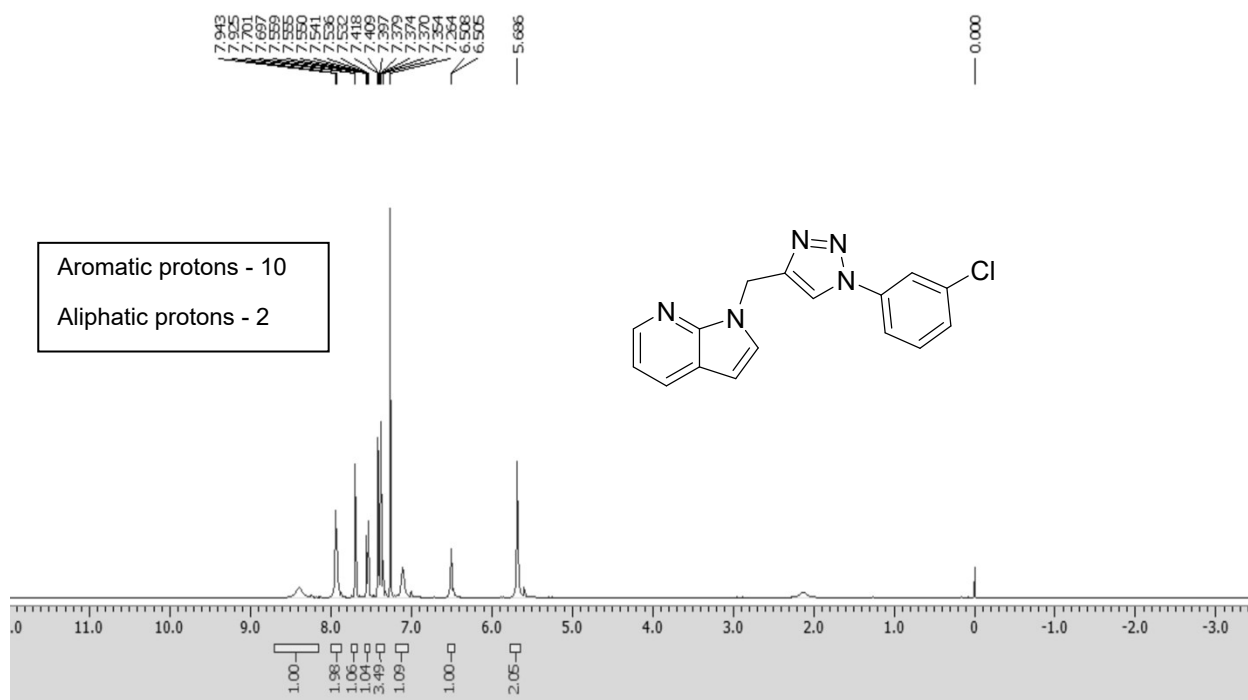
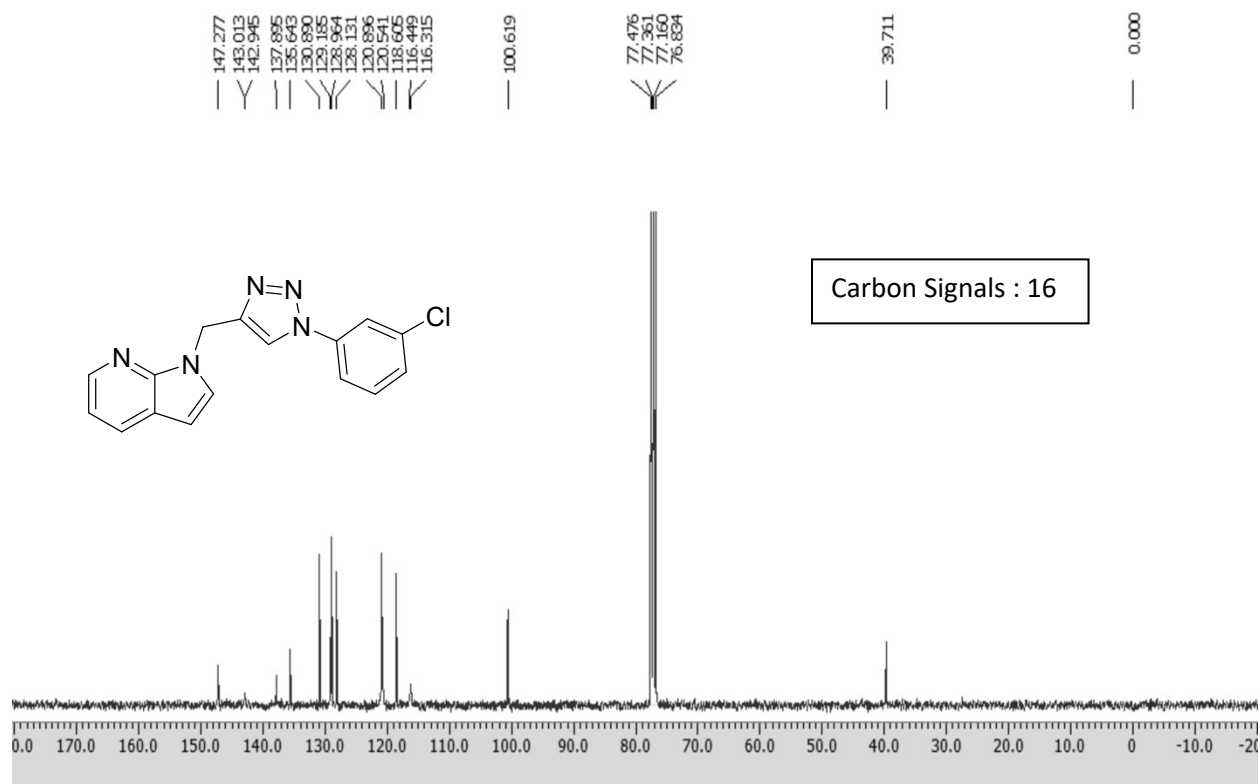


Figure SI-42. ESI-MS $[M+H]^+$: m/z for (4) $C_{16}H_{12}ClN_5$: 310.08

Figure SI-43. ¹H-NMR (4m)Figure SI-44. ¹³C-NMR (4m)

Sample Name : KS_14
Test Name :
200722_KS_14 27 (0.473)

IITRPR

XEVO G2-XS QTOF

1: TOF MS ES+
1.20e7

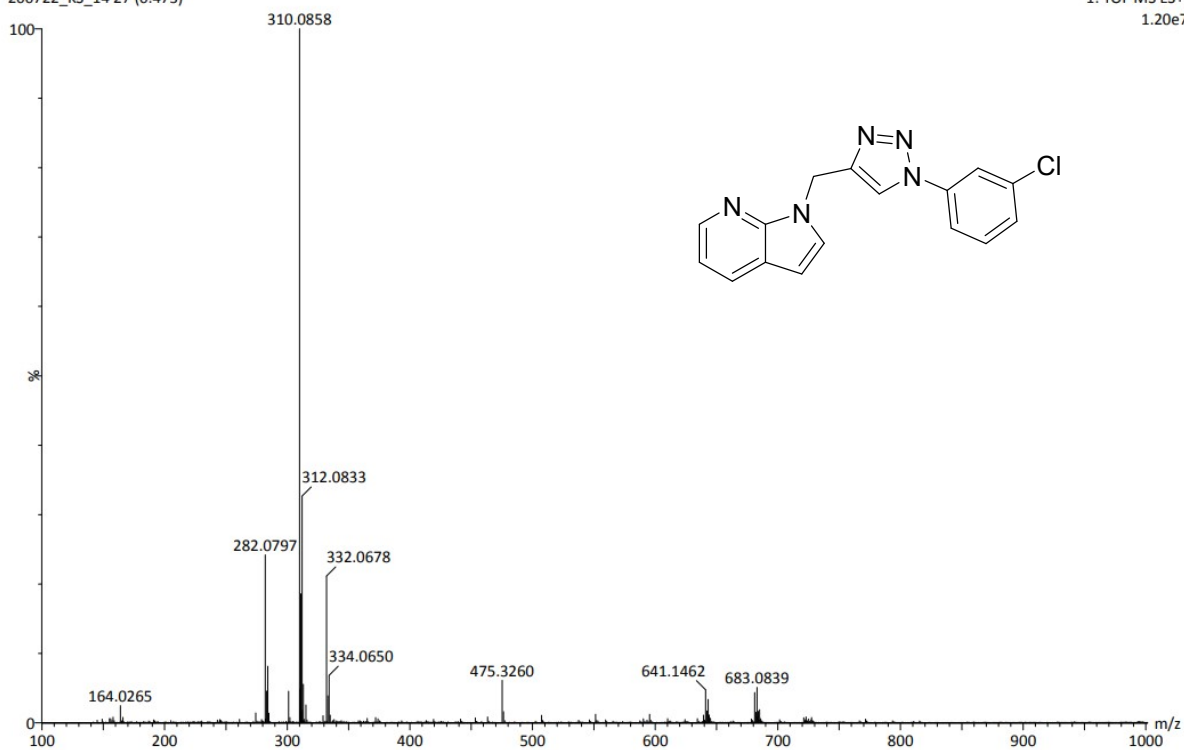
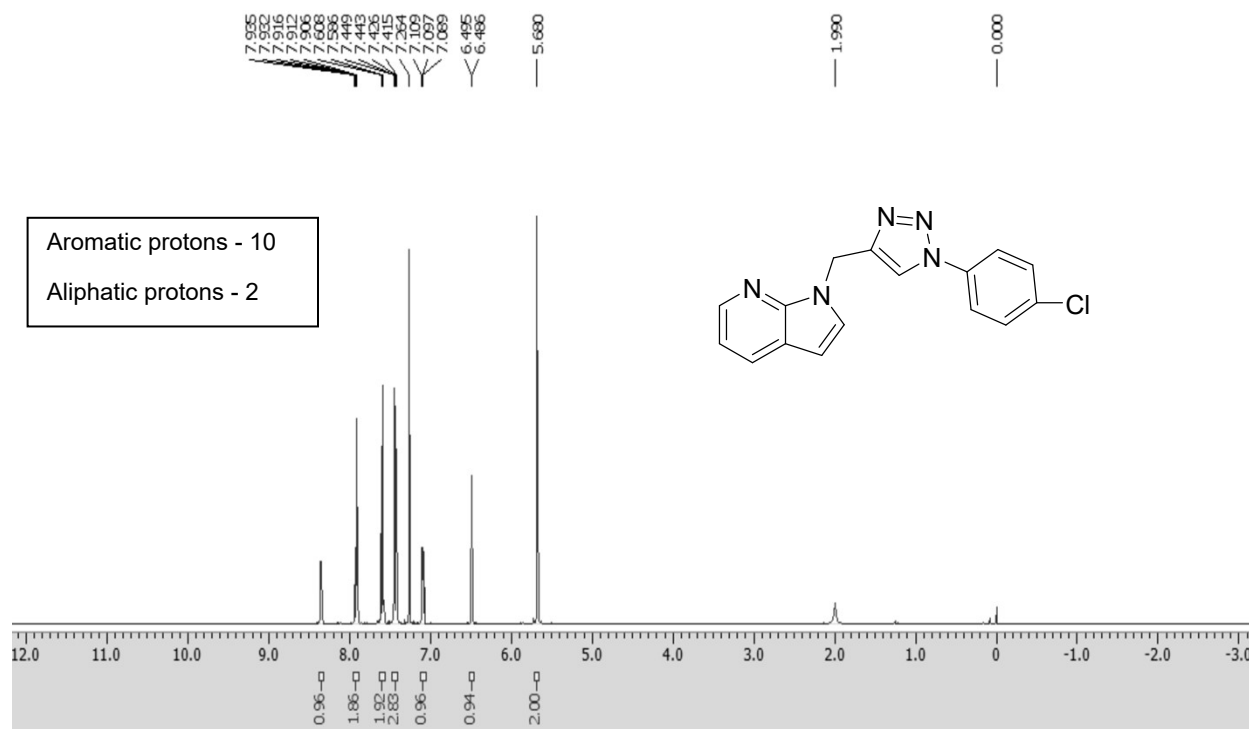
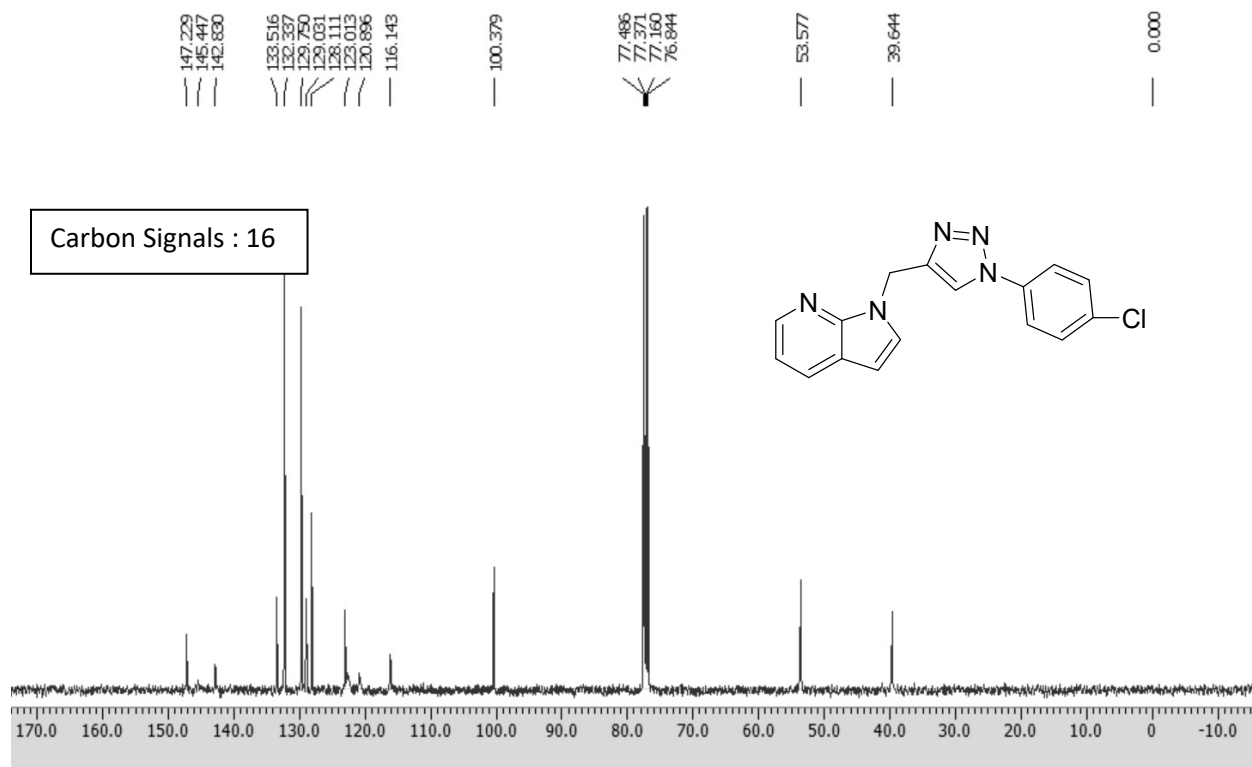


Figure SI-45. ESI-MS $[M+H]^+$: m/z for (**4m**) $C_{16}H_{12}N_5Cl$: 310.08

Figure SI-46. ¹H-NMR (4n)Figure SI-47. ¹³C-NMR (4n)

Sample Name : KS_16
Test Name :
200722_KS_16 17 (0.304)

IITRPR

XEVO G2-XS QTOF

1: TOF MS ES+
2.42e7

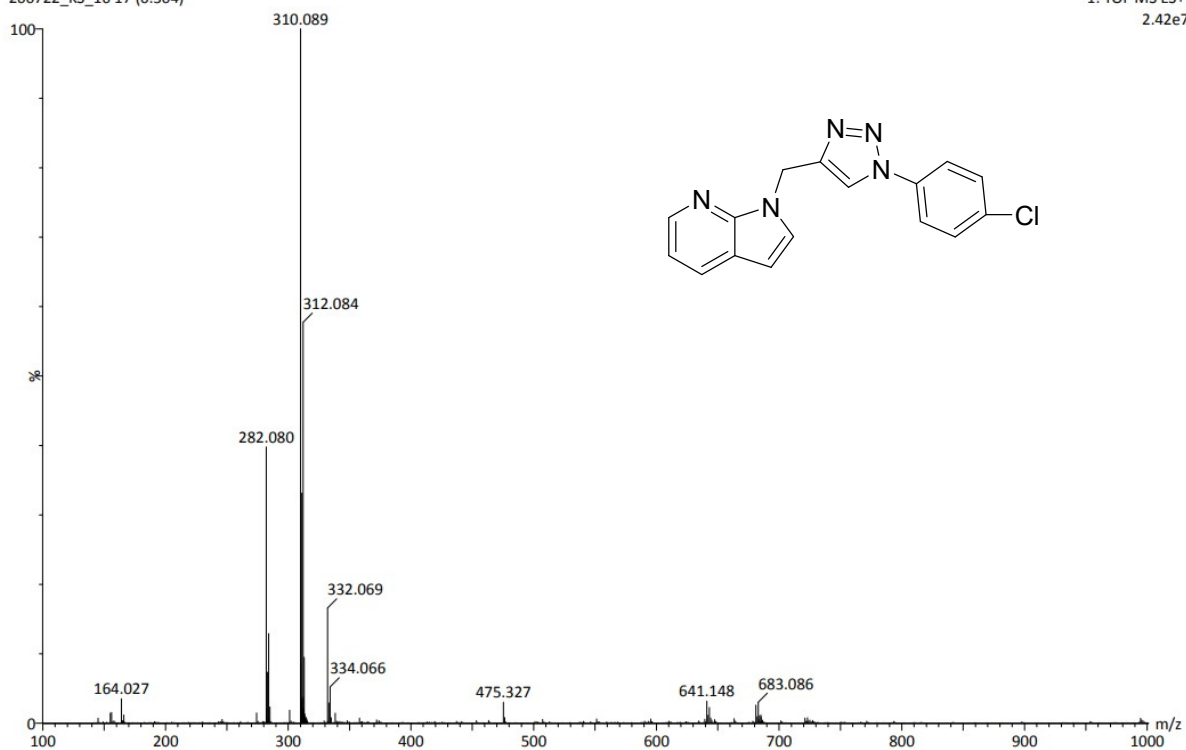
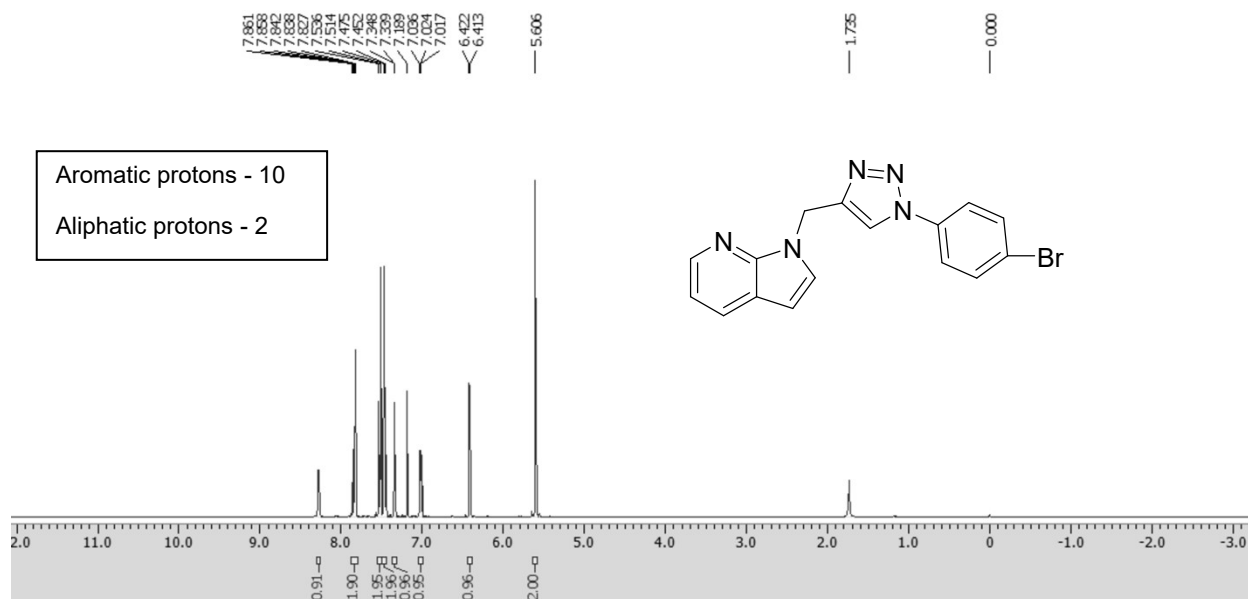
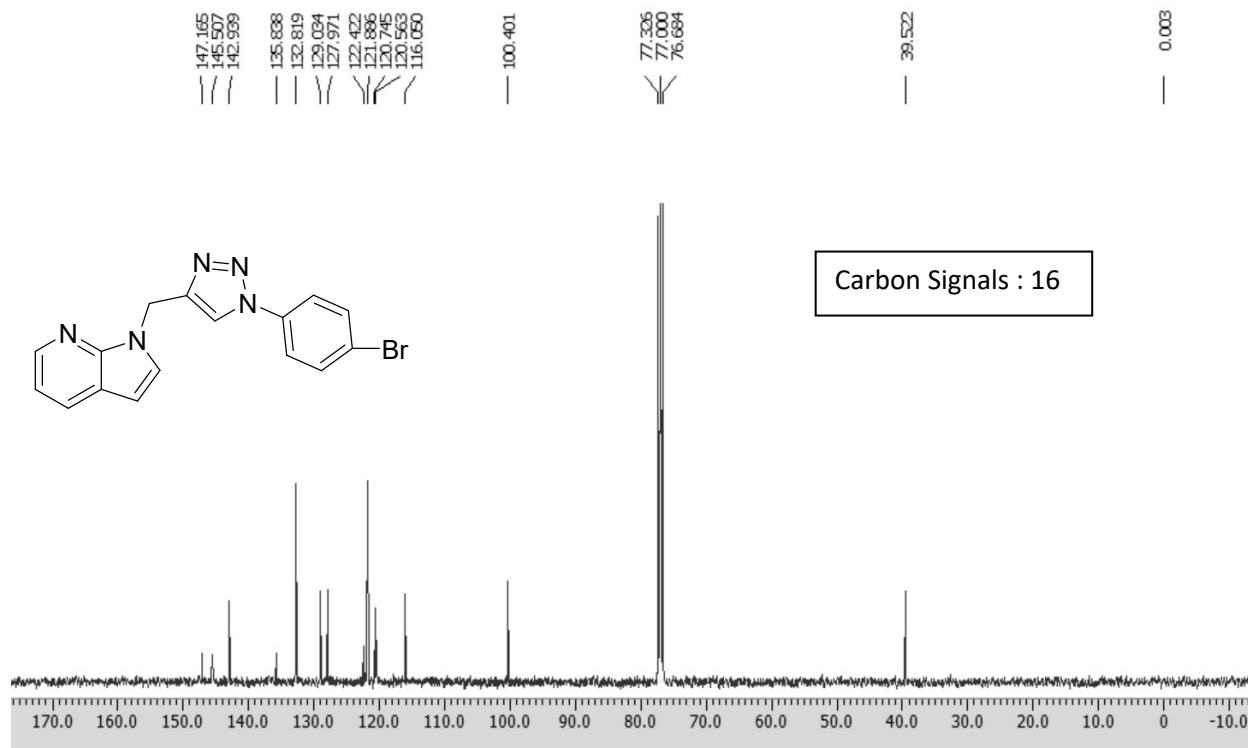


Figure SI-48. ESI-MS $[M+H]^+$: m/z for (4n) $C_{16}H_{12}N_5Cl$: 310.089

Figure SI-49. ¹H-NMR (4o)Figure SI-50. ¹³C-NMR (4o)

Sample Name : KS_17
Test Name :
200722_KS_17 12 (0.220)

HTRPR

XEVO G2-XS QTOF

1: TOF MS ES+
2.95e7

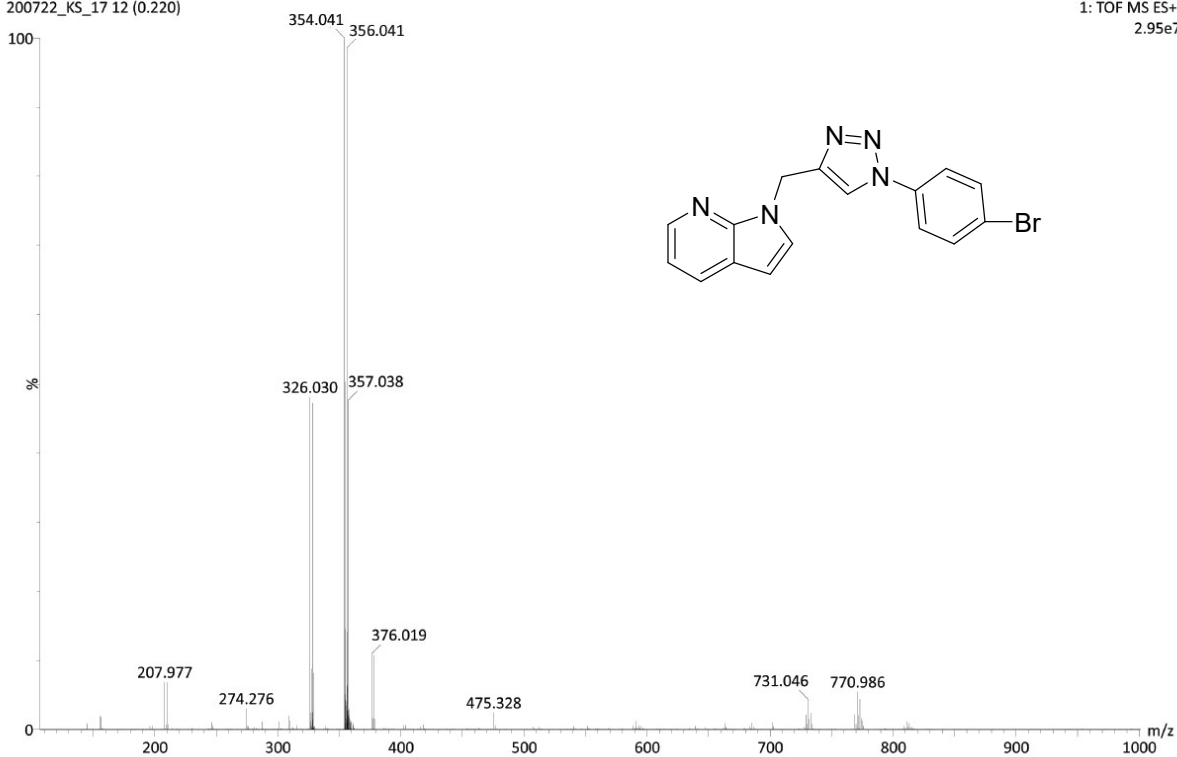
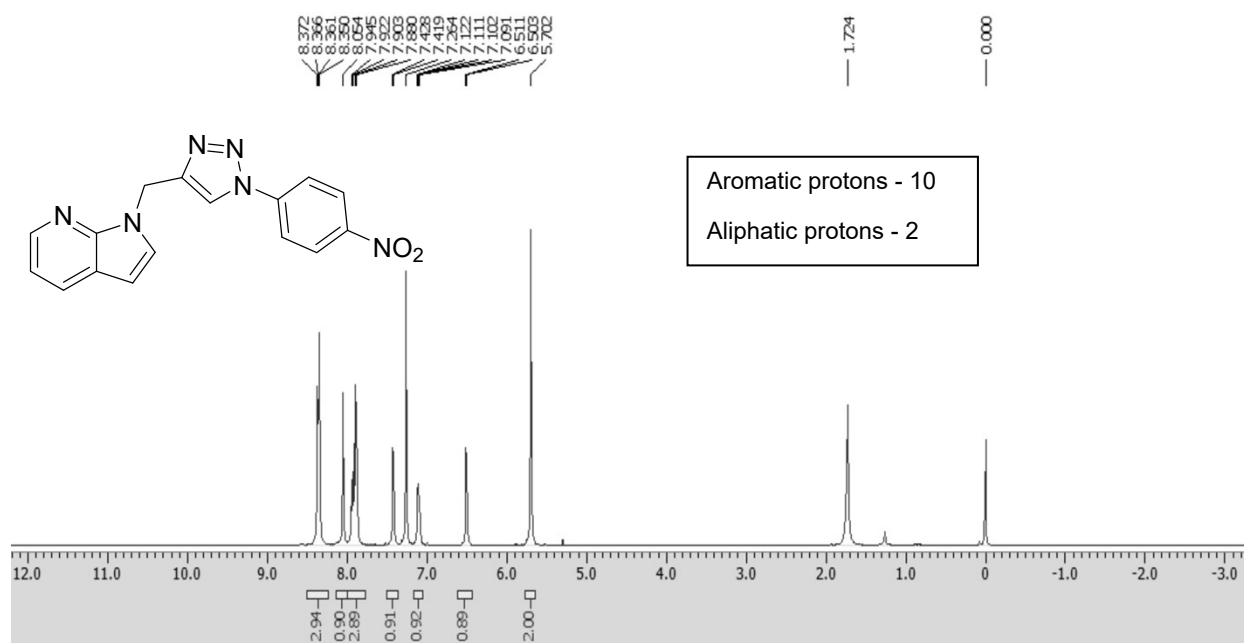
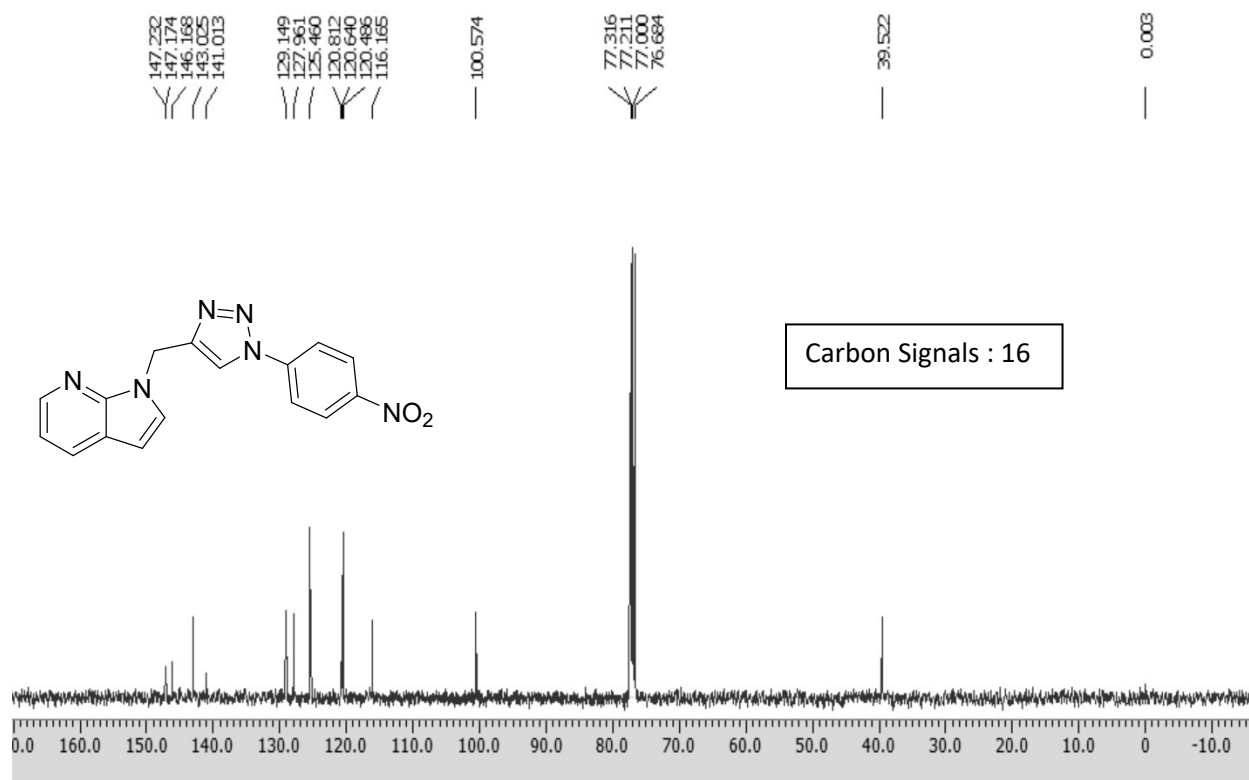


Figure SI-51. ESI-MS $[M+H]^+$: m/z for (4o) $C_{16}H_{12}N_3Br$: 354.041

Figure SI-52. ¹H-NMR (4p)Figure SI-53. ¹³C-NMR (4p)

Sample Name : KS_11
Test Name :
010622_KS_11 17 (0.304)

IITRPR

XEVO G2-XS QTOF

1: TOF MS ES+
1.14e8

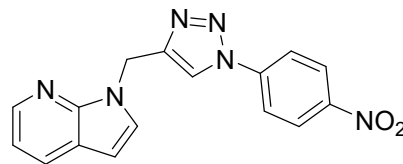
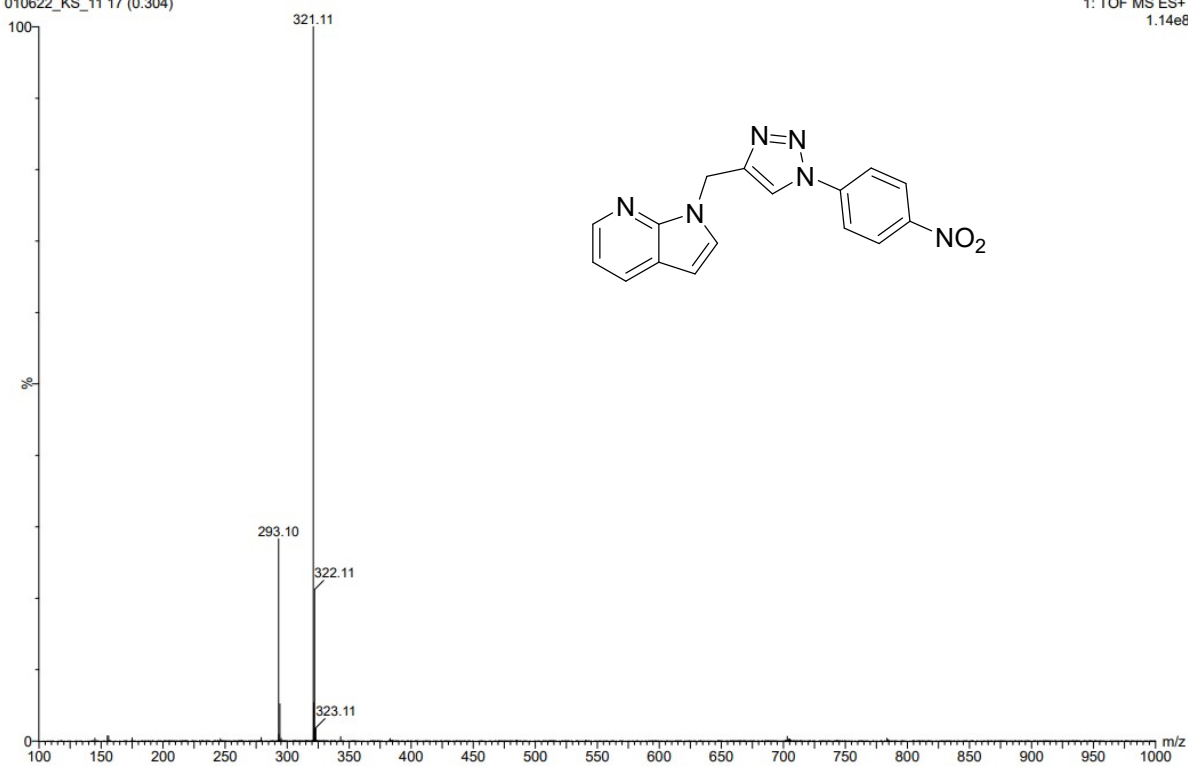
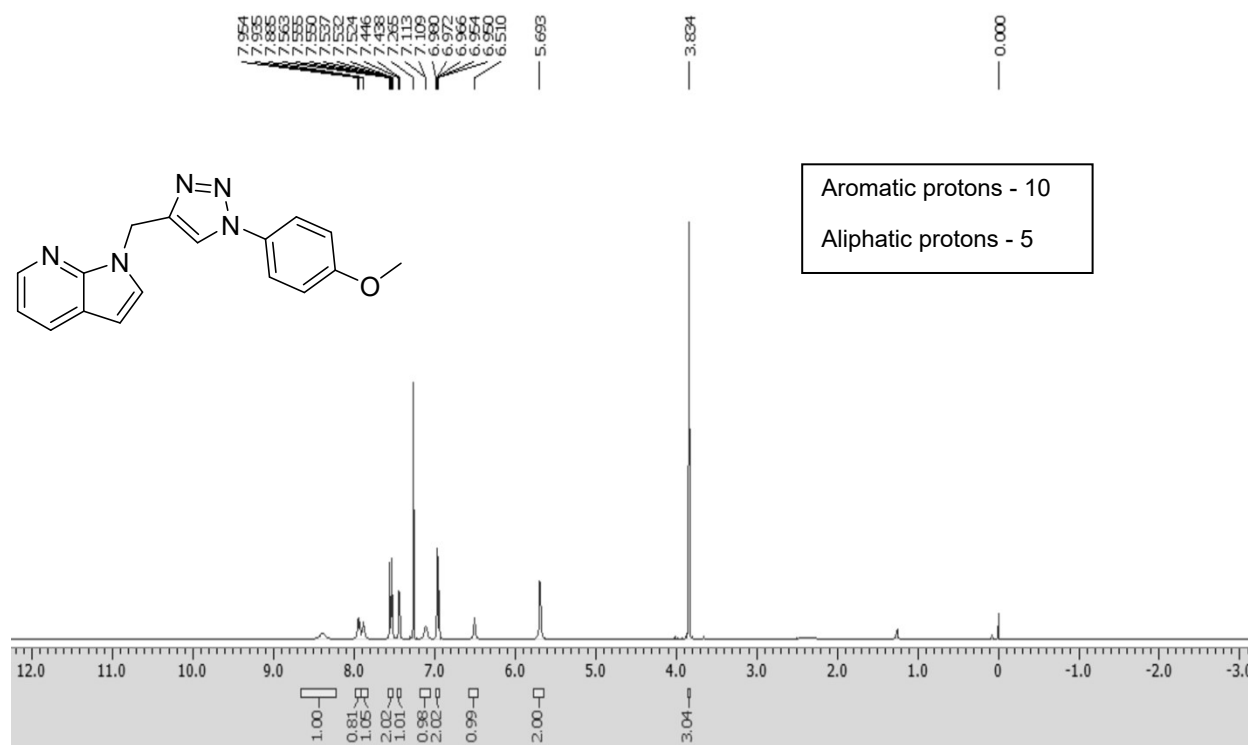
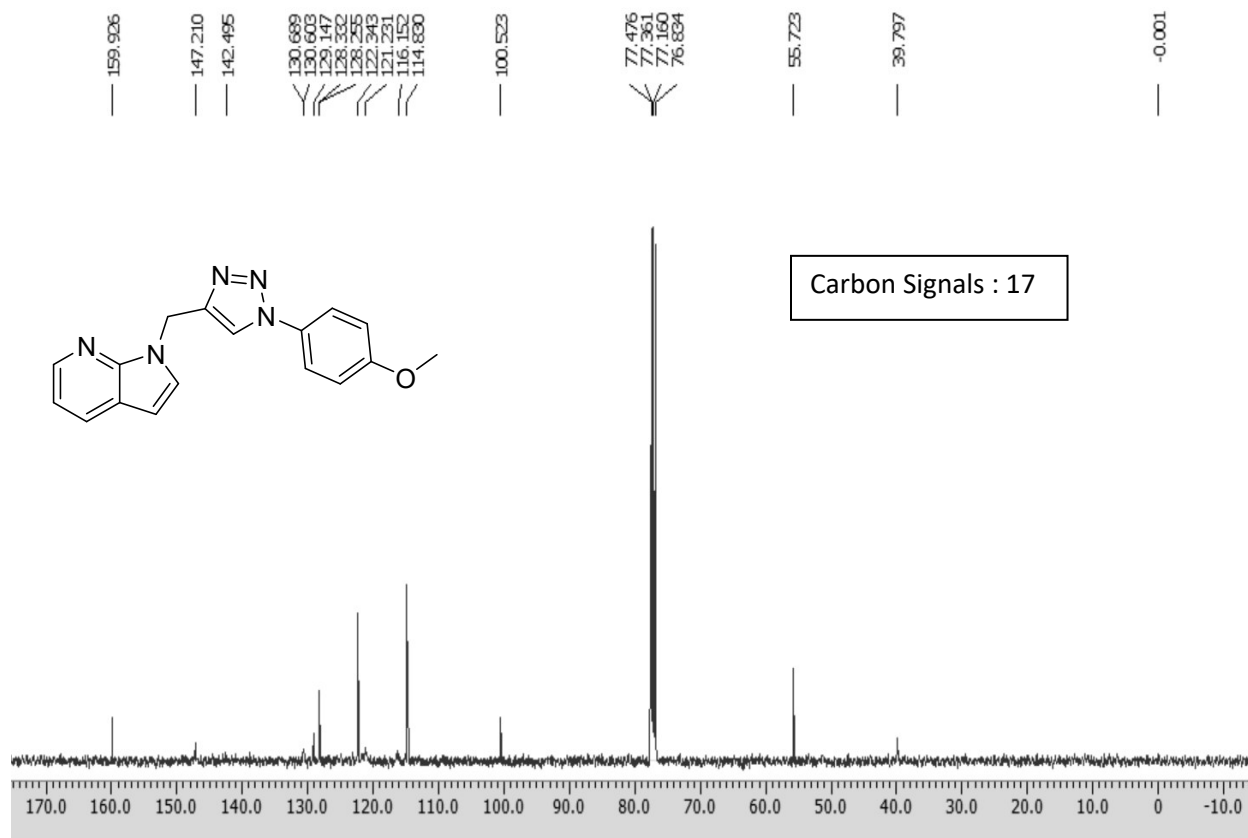


Figure SI-54. ESI-MS $[M+H]^+$: m/z for (**4p**) $C_{16}H_{12}N_6O_2$: 321.11

Figure SI-55. ¹H-NMR (4q)Figure SI-56. ¹³C-NMR (4q)

Sample Name : KS_13
Test Name :
010622_KS_13 23 (0.406)

IITRPR

XEVO G2-XS QTOF

1: TOF MS ES+
1.24e8

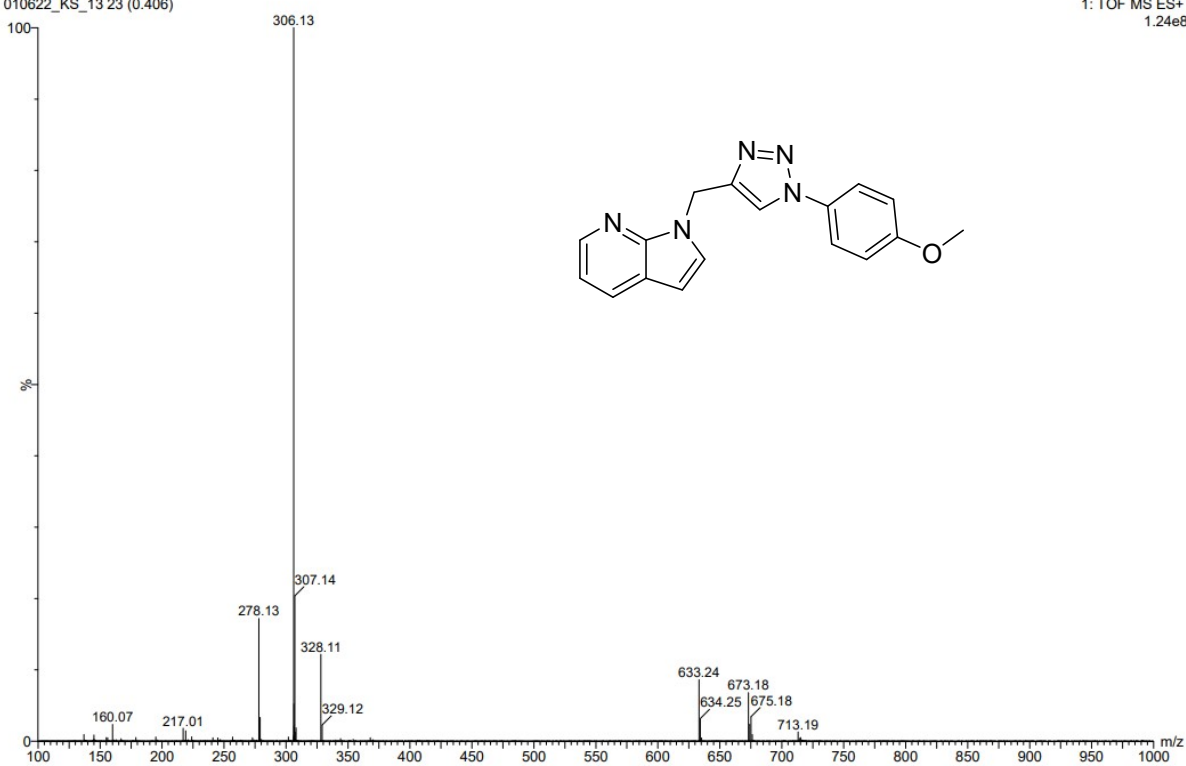


Figure SI-57. ESI-MS $[M+H]^+$: m/z for (4q) $C_{17}H_{15}N_5O$: 306.13